TRC2201

Update to ARDOT Superpave Gyratory Compaction (SGC) Specification to Increase Pavement Durability

Andrew Braham, Principal Investigator
Kevin Hall, Co-Principal Investigator
M. Tahir Ansari
Amarjeet Tiwari

University of Arkansas - Fayetteville
College of Engineering, Department of Civil Engineering

Final Report

June 2025

TRC2201

Update to ARDOT Superpave Gyratory Compaction (SGC) Specification to Increase Pavement Durability

Andrew Braham, Principal Investigator
Kevin Hall, Co-Principal Investigator
M. Tahir Ansari
Amarjeet Tiwari

University of Arkansas - Fayetteville
College of Engineering, Department of Civil Engineering

Final Report

June 2025

Arkansas Department of Transportation

Notice of Nondiscrimination

The Arkansas Department of Transportation (ARDOT) complies with all civil rights provisions of federal statutes and related authorities that prohibit discrimination in programs and activities receiving federal financial assistance. Therefore, ARDOT does not discriminate on the basis of race, sex, color, age, national origin, religion (not applicable as a protected group under the FMCSA Title VI Program), or disability in the admission, access to and treatment in ARDOT's programs and activities, as well as ARDOT's hiring or employment practices. Complaints of alleged discrimination and inquiries regarding ARDOT's nondiscrimination policies may be directed to Civil Rights Officer Joanna P. McFadden (ADA/504/Title VI Coordinator), P. O. Box 2261, Little Rock, AR 72203, (501) 569-2298, (Voice/TTY 711), or the following email address: joanna.mcfadden@ardot.gov

Free language assistance may be available upon request.

This notice is available from the ADA/504/Title VI Coordinator in large print, on audiotape, and in Braille.

Disclaimer:

The contents of this report reflect the views of the authors, who are responsible for the facts and the accuracy of the data presented herein. The contents do not necessarily reflect the official views or policies of ARDOT and they assume no liability for the contents or use thereof. This report does not constitute a standard, specification, or regulation. Comments contained in this report related to specific testing equipment and materials should not be considered an endorsement of any commercial product or service; no such endorsement is intended or implied.

TECHNICAL REPORT DOCUMENTATION PAGE

1. Report No. TRC2201	2. Government Accession No.	3. Recipient's Catalog No.		
4. Title and Subtitle Update to ARDOT Superpave Gyratory Compaction (SGC) Specification to Increase Pavement Durability		5. Report Date June 2025		
		6. Performing Organization Code:		
7. Author(s) Andrew Braham, Principal Investigator Kevin Hall, Co-Principal Investigator M. Tahir Ansari Amarjeet Tiwari		8. Performing Organization Report No.		
9. Performing Organization Name and Address University of Arkansas – Fayetteville 4190 Bell Engineering Center Fayetteville, AR 72701		10. Work Unit No.		
		11. Contract or Grant No. Project TRC2201		
12. Sponsoring Agency Name and Address Arkansas Department of Transportation (SPR) 10324 Interstate 30 Little Rock, AR 72209		13. Type of Report and Period Final Report, March 28, 2022 - June 30, 2025		
		14. Sponsoring Agency Code		
15. Supplementary Notes				

16. Abstract
The primary goal of TRC2201 was to enhance the durability of asphalt pavements in Arkansas. This was accomplished through two steps: exploring extreme scenarios with lab mixtures and comparing eight field sites. Further analysis was conducted using Pavement ME and a life-cycle cost analysis. In the extreme scenario, air voids decreased as Pb and N levels increased; CTIndex increased with rising Pb levels, but APA rut depth results were inconsistent. Additional testing with moisture damage indicated that mixtures that performed well in IDEAL-CT and APA tests still showed poor resistance to moisture damage. For the eight field projects, lab-mixed samples exhibited slightly better crack resistance at lower values, while plant-mixed samples performed slightly better at higher values. No consistent trend in APA rut depth was observed between lab- and field-produced samples. Additional performance tests indicated that some of the BMD mixtures could be susceptible to rutting with the additional asphalt binder content, and field validation of APA minimum values should be conducted for these eight projects. Pavement ME analysis revealed that, except for thermal cracking, standard Superpave mixtures performed similarly to the BMD mixtures, with thermal cracking occurring after only 5 years. Using this criterion, adding an extra 0.5% asphalt binder would result in approximately 61% savings over a 20-year period.

17. Key Words BMD, Pavement ME, IDEAL-CT, APA, life-cycle cost analysis, Superpave, Rutting	18. Distribution Statement No restrictions. This document is available to the public through the National Technical Information Service, Springfield, VA 22161. http://www.ntis.gov		
19. Security Classif. (of this report) Unclassified	20. Security Classif. (of this page) Unclassified	21. No. of Pages 168 pages	22. Price

Form DOT F 1700.7 (8-72)   Reproduction of completed page authorized.

SI* (MODERN METRIC) CONVERSION FACTORS

APPROXIMATE CONVERSIONS TO SI UNITS

Symbol	When You Know	Multiply By	To Find	Symbol
LENGTH				
in	inches	25.4	millimeters	mm
ft	feet	0.305	meters	m
yd	yards	0.914	meters	m
mi	miles	1.61	kilometers	km
AREA				
in^2	square inches	645.2	square millimeters	mm^2
ft^2	square feet	0.093	square meters	m^2
yd^2	square yard	0.836	square meters	m^2
ac	acres	0.405	hectares	ha
mi^2	square miles	2.59	square kilometers	km^2
VOLUME				
fl oz	fluid ounces	29.57	milliliters	mL
gal	gallons	3.785	liters	L
ft^3	cubic feet	0.028	cubic meters	m^3
yd^3	cubic yards	0.765	cubic meters	m^3
NOTE: volumes greater than 1000 L shall be shown in m^3				
MASS				
oz	ounces	28.35	grams	g
lb	pounds	0.454	kilograms	kg
T	short tons (2000 lb)	0.907	megagrams (or "metric ton")	Mg (or "t")
TEMPERATURE (exact degrees)				
°F	Fahrenheit	5 (F-32)/9 or (F-32)/1.8	Celsius	°C
ILLUMINATION				
fc	foot-candles	10.76	lux	lx
fl	foot-Lamberts	3.426	candela/m^2	cd/m^2
FORCE and PRESSURE or STRESS				
lbf	poundforce	4.45	newtons	N
lbf/in^2	poundforce per square inch	6.89	kilopascals	kPa

APPROXIMATE CONVERSIONS FROM SI UNITS

Symbol	When You Know	Multiply By	To Find	Symbol
LENGTH				
mm	millimeters	0.039	inches	in
m	meters	3.28	feet	ft
m	meters	1.09	yards	yd
km	kilometers	0.621	miles	mi
AREA				
mm^2	square millimeters	0.0016	square inches	in^2
m^2	square meters	10.764	square feet	ft^2
m^2	square meters	1.195	square yards	yd^2
ha	hectares	2.47	acres	ac
km^2	square kilometers	0.386	square miles	mi^2
VOLUME				
mL	milliliters	0.034	fluid ounces	fl oz
L	liters	0.264	gallons	gal
m^3	cubic meters	35.314	cubic feet	ft^3
m^3	cubic meters	1.307	cubic yards	yd^3
MASS				
g	grams	0.035	ounces	oz
kg	kilograms	2.202	pounds	lb
Mg (or "t")	megagrams (or "metric ton")	1.103	short tons (2000 lb)	T
TEMPERATURE (exact degrees)				
°C	Celsius	1.8C+32	Fahrenheit	°F
ILLUMINATION				
lx	lux	0.0929	foot-candles	fc
cd/m^2	candela/m^2	0.2919	foot-Lamberts	fl
FORCE and PRESSURE or STRESS				
N	newtons	0.225	poundforce	lbf
kPa	kilopascals	0.145	poundforce per square inch	lbf/in^2

*SI is the symbol for the International System of Units. Appropriate rounding should be made to comply with Section 4 of ASTM E380.
(Revised March 2003)

Table of Contents

8

List of Tables

List of Figures

15

Executive Summary

The Arkansas Department of Transportation (ARDOT) moved forward in the direction of BMD with the implementation of the results obtained from the research project TRC 1802. The study recommended the use of the Asphalt Pavement Analyzer (APA) to capture rutting and the IDEAL-CT to capture cracking. The primary goal of TRC2201 was to enhance the durability of asphalt pavements in Arkansas. This was accomplished through two steps. First, extreme scenarios within the BMD Approach D for rutting and cracking were explored, which established boundaries for implementation and identified optimal performance zones using both ARDOT's selected and additional performance tests. Second, the performance of ARDOT's BMD was assessed using IDEAL-CT and APA tests across three specimen fabrication methods: Laboratory-Produced and Laboratory-Compacted (LMLC), Plant-Produced and Laboratory-Compacted (PMLC), and Reheated Plant-Produced and Laboratory-Compacted (RPMLC) on eight field studies. This work was supplemented by an exploration of Pavement ME and a Life Cycle Cost Analysis (LCCA).

The analysis of extreme scenarios was conducted by examining three gradations and identifying optimal performance zones. The three gradations were a coarse gradation with no reclaimed asphalt pavement (RAP), a fine gradation with no RAP, and a fine gradation with 15% RAP. As expected, air voids decreased as Pb and N levels increased. In addition, the CTIndex increased with rising Pb levels across all three gradations. However, a clear relationship between Pb and APA rut depth was not observed for the coarse gradation, but a consistent increase in rut depth was observed with an increase in binder content in fine gradations with 0 and 15% RAP. Additionally, APA rut depth consistently decreased with increasing N across all three gradations. Mixtures from the initially identified optimal performance zones were evaluated for moisture susceptibility using HWTT and TSR tests, and they exhibited significant moisture-related distress. They did not contain any anti-strip agents, so further work should be explored with mixtures including anti-strip agents. Regardless, these findings emphasized the need for supplementary testing to validate the results obtained from standard performance

tests used by state agencies. As demonstrated in this study, mixtures that performed well in IDEAL-CT and APA tests still showed poor resistance to moisture damage.

The second step focused on eight field projects approved by ARDOT in 2023 and 2024 and compared three fabrication methods: LMLC, PMLC, and RPMLC. Initial assessments of rutting and cracking performance were conducted using the APA and IDEAL-CT tests, ARDOT's preferred evaluation methods. The CTIndex results for the eight BMD projects show that LMLC has slightly better crack resistance at lower values, while PMLC and RPMLC perform slightly better at higher values. No consistent trend was observed in APA rut depth across the three fabrication methods. Additionally, five supplementary performance tests—moisture-induced damage (tensile strength ratio, TSR), HWTT, I-FIT, dynamic modulus, and flow number (FN)— were performed to further validate the findings. First, TSR values showed no clear trend among the techniques, whereas HWTT rut depths for the eight BMD projects indicate that most results fell below the 10.0 mm limit recommended by Louisiana. Second, I-FIT flexibility index values for all eight BMD field projects fall below the minimum threshold of 8.0 recommended by Illinois and New York. Third, dynamic modulus test results indicated that RPMLC samples generally exhibited higher stiffness than LMLC samples across most projects. Finally, RPMLC samples generally have higher FN values than LMLC, indicating potentially better rutting resistance. However, these additional performance tests did indicate that some of the BMD mixtures could potentially become rutting susceptible to the additional asphalt binder content, and field validation of APA minimum values should be conducted with these eight projects.

The Pavement ME analysis showed that the IRI, top-down fatigue cracking, bottom-up fatigue cracking, total deformation, and asphalt mixture deformation all remain below the threshold after twenty years for standard Superpave designs and BMD. However, the thermal cracking of the standard Superpave mixture reached its threshold after 5 years, whereas the BMD did not reach its threshold after 20 years. This shows that the standard Superpave mixtures are predicted to be more susceptible to cracking than the BMD. Using this criterion, the LCCA of project 100959 (I-555) was estimated over a 20-year period. It is estimated that maintaining the standard Superpave mix section for 20 years would cost $ 679,724.30, while

maintaining the BMD mix section for 20 years would cost $259,215.90. Therefore, adding an extra 0.5% asphalt binder would result in a savings of approximately 61%.

Chapter 1. Introduction

1.1 Overview of the Superpave Method

The Strategic Highway Research Program (SHRP), conducted in the late 1980s and early 1990s, carried out comprehensive research in the field of asphalt binders and mixtures. The results obtained from the study led to significant changes in the design and testing of asphalt materials (1). The result of the research program led to the development of a Performance Grading (PG) system for asphalt binders and a mix design system called Superpave (SUperior PERforming Asphalt PAVEments). The volumetric analysis common to the Hveem and Marshall methods provides the basis for the Superpave mix design method for determining the optimum binder content. The Superpave system ties asphalt binder and aggregate selection into the mix design process and considers traffic and climate as well. SHRP also recommended three levels of mix design based on the level of traffic and the analysis approach – Level I, Level II, and Level III. Level I mix design was primarily based on volumetric analysis and accounted for low-traffic pavements. Level II and Level III, which were designed for moderate and high-traffic pavements, required mixture performance testing in addition to volumetric analysis for evaluating the mixture's rutting, fatigue, and low-temperature cracking resistance properties (2). However, out of the three mix design systems, only the Level 1 Superpave volumetric mix design was adopted as the latter were not found to be practically feasible.

The Superpave mix design system mainly revolves around the use of the Superpave Gyratory Compactor (SGC) to compact asphalt concrete hot mix (ACHM) specimens in the laboratory. The number of design gyrations, also called the "N_{des}" determines the design aggregate structure and governs the mixture design in the SGC. During the early 1990s, soon after the implementation of Superpave, a higher value of N_{des} was adopted to design ACHM for moderate and high traffic to improve rutting resistance. The higher N_{des} and a few other modifications in the mix design procedure virtually eliminated the rutting-related distress from the pavement, but further resulted in "dry" ACHM (3). Pavements showed premature cracking and durability-related issues due to the inadequacy of the asphalt binder content.

The term "durability" has been used in several studies to relate ACHM and pavement performance (4, 5). ACHM durability has been defined as the ability of compacted ACHM to maintain its structural integrity throughout its expected service life when exposed to the damaging effects of the environment and traffic loading. While pavement durability has been defined as the retention of a satisfactory level of performance over the structure's expected service life without major maintenance for all properties that are required for the road situation, in addition to asphalt durability (6). Several mix design and construction specification changes were implemented by the state highway agencies (SHAs) to counter the pavement durability-related concerns. The changes were primarily intended to increase the design binder content, improve the quality of asphalt binder, and increase the in-place density of ACHM (7). However, most of the SHAs believed that the lack of adequate asphalt binder was the potential reason for the ACHM to show cracking-related problems. Several adjustments to the Superpave mix design method were implemented by the SHAs to obtain higher design asphalt binder contents, but the three most common changes were lowering the design gyration level, increasing the minimum voids in mineral aggregate (VMA) requirement, and lowering design air voids. The SHAs that made changes to the volumetric mix design methods to increase asphalt binder content are shown in **Figure 1**.

The number of design gyrations corresponds to the compaction effort in the field, which significantly affects the Superpave volumetric analysis results. For a fixed aggregate gradation, lowering the N_{des} increases the optimum asphalt binder content that corresponds to a specific design air void, i.e., 4.0%, while vice versa, increasing N_{des} decreases the optimum asphalt binder content. Several SHAs in the United States and Canada reported increased asphalt binder content as an outcome of reduced design gyration levels (8, 9, 10) . However, the Oregon Department of Transportation and West Virginia Division of Highways indicated that they did not observe a substantial increase in asphalt binder content over time. They observed that the asphalt binder content initially increased and then returned to earlier levels after a year or two. The adjustments in the design gradation made by the contractors were considered the primary reason for the unchanged asphalt binder content. Furthermore, a few SHAs, like

the Alabama Department of Transportation, reduced the N_{des} and fixed it for all the traffic levels based on the aggregate locking point concept.

I have made changes
I have not made changes
Not using Superpave mix design
Not responded to the survey
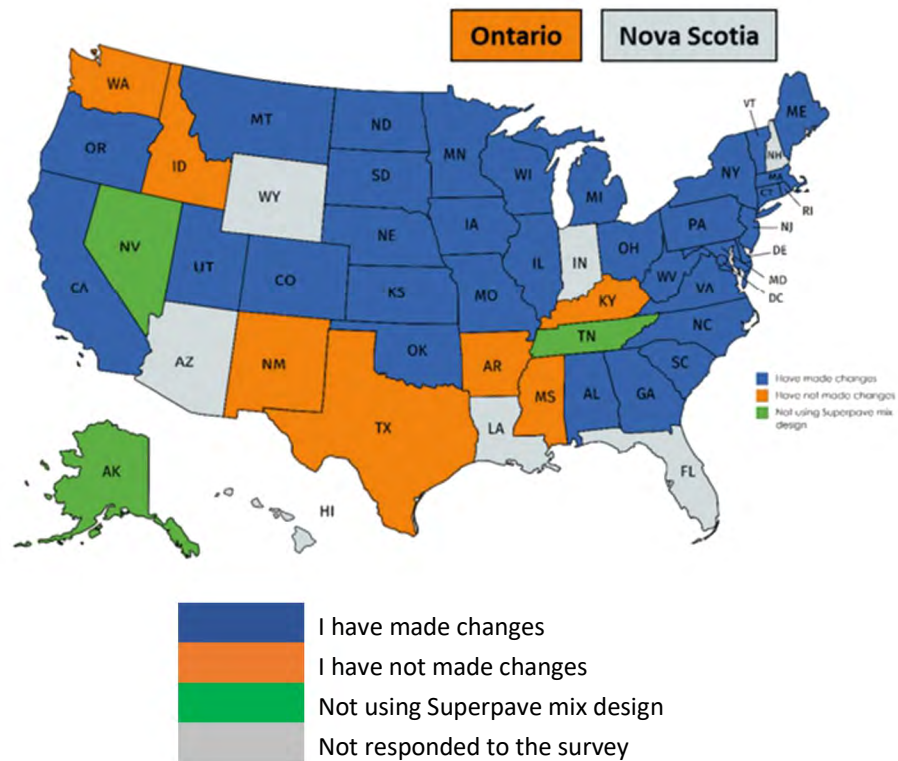
Figure 1. SHAs which made changes in volumetric mix design methods (7)

Increasing the minimum VMA requirement was also one of the major adjustments to the mix design which was implemented by the SHAs. VMA is the void space between the aggregate particles of the compacted mix which includes the air voids and the effective asphalt content. For a given design gyration level, VMA is influenced by changing the aggregate blend. As a rule of thumb, a one percent increase in VMA generally increases the design asphalt content by 0.44 percent (7). The key to achieving this increase in asphalt content was to ensure the correct aggregate specific gravity (G_{sb}) was used in the design. Any increase in asphalt binder content from increased VMA can be reduced or eliminated if G_{sb} of the aggregate was inaccurately increased. The Federal Highway Administration (FHWA) also recommended increasing the minimum VMA limits from those specified in AASHTO M 323 by 0.5% for each NMAS (11, 12).

Lowering the design air voids was also found to increase the design asphalt binder content if the VMA criteria were fixed. For a given N_{des}, lowering the design air voids requires more asphalt binder to be added to occupy the voids. As a rule of thumb, reducing the design air voids by 1% results in a 0.4% increase in the asphalt binder content, while considering a fixed VMA (7). The air voids regression approach was also adopted by the SHAs, which was a very similar approach to lowering the design air voids wherein a mix was designed using standard laboratory methods and criteria, including a target air void content of 4.0 percent. The asphalt content was then increased to achieve a "regressed" target of 3.5 percent or 3.0 percent air voids. Once the JMF and aggregate proportions were locked in, the binder content was typically increased up to 0.4 percent. Compared with the approach to lowering design air voids, the air void regression approach does not require any significant specification changes for mix design approval, although the volumetric properties at the regressed air voids content would be needed for acceptance testing (13).

1.2 The Balanced Mix Design Concept

While SHAs were adjusting their existing Superpave specifications and procedures, concerns persisted regarding the limitations of mix design methods that relied solely on volumetric properties. Key issues included the limited reliability and accuracy of VMA measurements, largely due to challenges in precisely determining the bulk specific gravity (G_{sb}) of both aggregates and Reclaimed Asphalt Pavement (RAP) materials (14,15). Additionally, these methods lacked an effective means to account for the complex interactions among virgin binders, recycled binders, and additives like recycling agents. These shortcomings in the volumetric-based design process spurred the development of a new approach known as Balanced Mix Design (BMD).

The FHWA Expert Task Group (ETG) on mixtures and construction defined BMD as the process of designing asphalt mixtures using performance tests on properly conditioned specimens to evaluate various types of pavement distress. This approach accounts for factors such as aging, traffic loads, climate conditions, and the mixture's placement within the pavement structure. The goal is to strike a balance between resistance to rutting, cracking, and

other distresses by considering the combined effects of these factors (16). According to insights gathered from the 2023 BMD Peer Exchanges (17, 18, 19), the leading motivations for SHAs to adopt BMD were to extend the service life of asphalt pavements, prevent early pavement failures, lower the environmental impact by reducing the carbon footprint, and enhance the performance of asphalt mixtures for specific applications.

Based on the degree of strictness in meeting volumetric criteria and the potential allowed for innovation in meeting the performance criteria, four BMD approaches have been identified in AASHTO PP 105-20 (20):

- Approach A: Volumetric design with performance verification
- Approach B: Volumetric design with performance optimization
- Approach C: Performance-modified volumetric design
- Approach D: Performance design

Full compliance with the existing volumetric requirements and additional performance requirements is required in Approach A, and hence is the most conservative approach with the lowest innovation potential. Approach B allows moderate changes in asphalt binder content for performance optimization based on mixture performance test results, but still requires full compliance with the existing volumetric requirements at the preliminary optimum binder content. Although Approach B is slightly more flexible than Approach A, it is still considered a conservative approach with limited innovative potential. Some of the volumetric requirements are relaxed or eliminated in Approach C, provided the performance criteria are satisfied, and thus it is less conservative than Approach A and Approach B. It also provides a medium degree of innovation potential. Finally, Approach D has no requirement on volumetric properties and relies entirely on mixture performance test results for mix design optimization, and thus, is considered the least conservative approach with the highest degree of innovation potential.

1.3 Performance Testing in BMD

Performance testing plays a vital role in BMD, as it ensures the durability of asphalt mixtures and their ability to resist key distresses such as rutting, cracking, and moisture

damage. BMD relies on laboratory testing to develop asphalt mixtures that are specifically designed to perform under actual traffic loads, climatic conditions, and pavement environments. These tests evaluate how the mixture will respond to different stresses and environmental influences. According to the National Asphalt Pavement Association (NAPA), SHAs nationwide use a variety of performance tests to assess rutting, cracking, and moisture susceptibility. **Table 1** provides an overview of these tests; however, only the tests relevant to this study are described in detail in the following section.

Table 1. Summary of performance tests under the BMD initiative

Rutting	
Test	**Specification**
Asphalt Pavement Analyzer	AASHTO T 340-10 (2019)
Flow Number Test	AASHTO T 378-17
Hamburg Wheel Tracking Test	AASHTO T 324-19
High Temperature Indirect Tension	N/A
Rapid Shear Rutting Test	WK 71466
Stress Sweep Rutting	AASHTO TP 134-19
Cracking	
Test	**Specification**
Cantabro Test	AASHTO TP 108-14 (2020)
Direct Tension Cyclic Fatigue Test	AASHTO TP 107-14 (Large Specimens), AASHTO TP 133-19 (Small Specimens)
Disc Shaped Compact Tension Test	ASTM D7313-13
Flexural Bending Beam Fatigue	AASHTO T 321-17 / ASTM D8273-18
IDT Creep Compliance and Strength Test	AASHTO T 322-07 (2020)
Illinois Flexibility Index Test	AASHTO T 393-21
Indirect Tensile Asphalt Cracking Test	ASTM D8225-19
NFLEX Factor	AASHTO TP 141-20
Overlay Test	NJDOT B-10 / Tex-248-F
Semi-Circular Bend Test	LADOTD TR 330-14/ASTM D8044-16
Moisture Damage	
Test	**Specification**
Hamburg Wheel Tracking Test	AASHTO T 324-19
Tensile Strength Ratio Test	AASHTO T 283-14 (2018)

1.3.1 Overview of BMD Adoption Across Different U.S. States

BMD is a relatively recent yet increasingly adopted approach within the U.S. asphalt industry. According to the most recent data from the NAPA website, updated as of June 7, 2025, eight SHAs have adopted Approach A, four have implemented Approach B, and two have chosen Approach C. Additionally, 22 states are currently in the pre-implementation phase, while one state has adopted a hybrid of Approaches A and B. Altogether, 37 states are actively working toward implementing the BMD concept in some form. The BMD implementation effort across the U.S. has been shown in **Figure 2**.
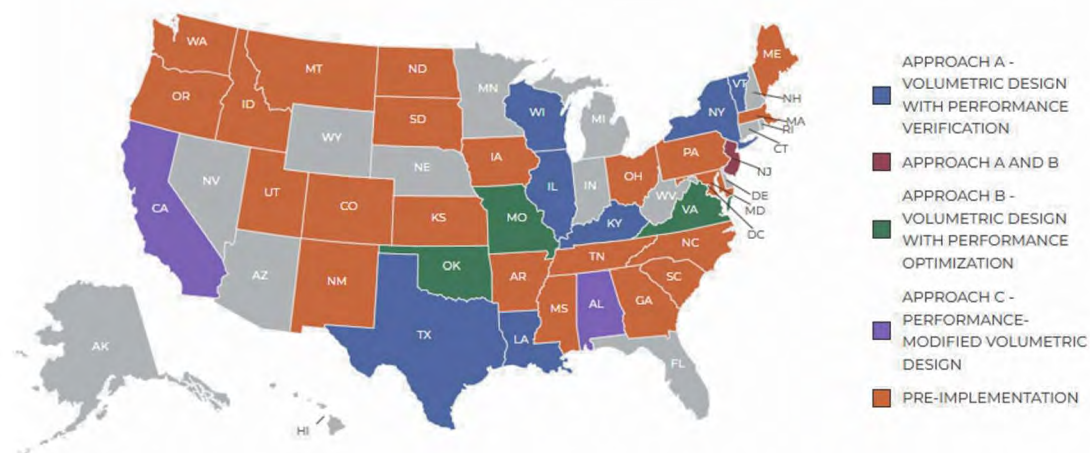
Figure 2. **BMD implementation across the SHAs in the U.S. (As of June 6th, 2025)**

In addition to SHAs, several other organizations are also advancing the adoption of the BMD approach. These include the City of Janesville in Wisconsin, the Illinois Tollway, and the Kentucky Department of Aviation, all of which have implemented Approach A. The New York City Department of Design and Construction has adopted Approach C, while St. Clair County in Alabama has chosen Approach D for its Superpave mixtures. This supplementary information is illustrated in **Figure 3**.

Figure 3. **BMD implementation effort by other agencies. (As of June 6th, 2025)**

As outlined in **Table 1.** Summary of performance tests under the BMD initiative SHAs across the U.S. have selected various performance tests to assess the rutting and cracking susceptibility of their asphalt mixtures. **Figure 4** and **Figure 5** provide a visual summary of the tests adopted by different agencies for each type of distress. The Hamburg Wheel Tracking Test emerges as the most used method for evaluating rutting potential, while the Indirect Tensile Asphalt Cracking Test, also known as the IDEAL-CT, is the preferred choice among SHAs for assessing cracking resistance.

Figure 4. **Rutting tests adopted by different SHAs. (As of June 6th, 2025)**

Figure 5. **Cracking tests adopted by different SHAs. (As of June 6th, 2025)**

1.4 Arkansas's BMD Approach

Like many other SHAs, the Arkansas Department of Transportation (ARDOT) moved forward in the direction of BMD with the implementation of the results obtained from the research project TRC 1802 (21). The study recommended the use of the Asphalt Pavement Analyzer (APA) to capture rutting and the IDEAL-CT to capture cracking. As shown in **Figure 6,** the study also suggested producing maximum and minimum guidelines for the asphalt binder content to balance rutting and cracking performance.

Figure 6. Balance between rutting and cracking (22)

The two tests, especially the IDEAL-CT test was chosen by ARDOT due to the ease of sample preparation and ability to run on a simple load frame at ambient temperature. However, other performance tests could potentially provide similar insights as the IDEAL-CT and APA tests but are not currently utilized by ARDOT. These alternative performance tests could help assess ARDOT's chosen methods and potentially lead to updates in their specifications. Additionally, these tests focus more on fundamental analysis rather than empirical approaches. By incorporating these fundamental tests, there would be a deeper understanding of ARDOT's performance test selections. **Table 2** lists the additional performance tests considered in this study.

Table 2. Additional performance tests considered in the study

Name of the test	Specification
Dynamic Modulus and Flow Number	AASHTO T 378
Illinois Flexibility Index test	AASHTO T 393
Hamburg Wheel Tracking Test	AASHTO T 324
Moisture-Induced Damage	AASHTO T 283

The test procedures are described in detail below.

APA

        The APA is a second-generation device that was originally developed as the Georgia Loaded Wheel Tester. The APA test is performed in compliance with ARDOT Test Method 480 (23), and it tracks a loaded wheel back and forth across a pressurized linear hose over an ACHM sample. A temperature chamber is used to control the test temperature. Rut depths along the wheel path are measured for each wheel pass. The sample is typically loaded for 8,000 wheel passes. ACHM specimens are conditioned and fabricated to 150 mm in diameter and 75 mm in height, with 7.0±1.0 percent air voids. The final test result is the average APA rut depth calculated from two sets of two asphalt samples. According to ARDOT Test Method 480, acceptable rut depths are set at 8.0 mm for mixtures using PG 64-22 and PG 67-22 binders, and 5.0 mm for those using PG 70-22 and PG 76-22 binders.

IDEAL-CT

        The IDEAL-CT is an indirect tension test following ASTM D8225 (24), that determines the cracking potential of ACHM with a fracture mechanics-based parameter, CT_{Index}. ACHM specimens are conditioned and fabricated to 150 mm in diameter and 62 mm in height, with 7.0±0.5 percent air voids. The test is run at room temperature with a monotonic loading rate of 50 mm/minute of cross-headed displacement. In this study, the CT_{Index} value is reported as the average of three replicates for both the field projects approved in 2023 and the lab calibration study. However, for the field projects approved in 2024, the number of replicates was increased to five. Initially, ARDOT set a minimum CT_{Index} requirement of 50 based on findings from the research project TRC 1802. This threshold was later raised to 65 for 2024 field projects and further increased to 75 for those approved in 2025.

Dynamic Modulus and Flow Number

        The dynamic modulus and flow number tests were conducted in accordance with AASHTO T 378 (25). In the dynamic modulus test, a specimen is exposed to a controlled sinusoidal (haversine) compressive stress at various frequencies while maintaining a specific temperature. This test can be performed with or without confining pressure. The applied stresses and the resulting axial strains are recorded over time, allowing for the calculation of

30

both the dynamic modulus and the phase angle. In the flow number test, a specimen is subjected to a repeated haversine axial compressive load pulse, applied for 0.1 seconds every 1.0 seconds, also at a specific temperature. This test may also be conducted with or without confining pressure. The permanent axial strains produced by the load cycles are measured and numerically differentiated to determine the flow number, which is defined as the load cycle number corresponding to the minimum rate of change in permanent axial strain. Both tests are carried out on the same asphalt specimen, which is cored from a larger specimen with a diameter of 150 mm and a height of 170 mm. The test specimen's diameter and height should be between 100 and 104 mm, and 147.5 and 152.5 mm, respectively. Specimens with air voids not within the range of 7.0±0.5 percent are rejected. The dynamic modulus test is performed before the flow number test because the latter is more destructive. The dynamic modulus and flow number values reported in this study represent the average results from two test replicates.

Illinois Flexibility Index Test

The Illinois Flexibility Index Test (I-FIT) is used to determine the fracture resistance parameters of an ACHM at an intermediate temperature. The test method is in agreement with AASHTO T 393 (26) covers the determination of Mode I (tensile opening mode during crack propagation) cracking resistance properties of ACHM at intermediate test temperatures. The data analysis procedure associated with this test determines the fracture energy (G_f) and post peak slope (m) of the load–load line displacement curve. These parameters are used to develop a Flexibility Index (FI) to predict the fracture resistance of an ACHM at intermediate temperatures. The FI can be used as part of the ACHM approval process. The test specimen, which has a thickness of 50 mm and is semi-circular, is extracted from the center of a 160 mm high gyratory compacted specimen. The air void tolerance for this circular disc is 7.0±1.0%. The FI reported in this study is the average of three test replicates.

Hamburg Wheel Tracking Test

The Hamburg Wheel Tracking Test (HWTT) is used to test the rutting and moisture-susceptibility of ACHM. The test method following AASHTO T 324 (27) describes the testing of a

submerged, compacted ACHM in a reciprocating rolling-wheel device. This test provides

information about the rate of permanent deformation from a moving, concentrated load. The

deformation of the specimen, caused by the wheel loading, is measured. ACHM specimens are

conditioned and fabricated to 150 mm in diameter and 60 mm in height, with 7.0±0.5 percent

air voids. Like the APA test, the final test result in HWTT is also the average rut depth calculated

from two sets of two asphalt samples.

Moisture-Induced Damage

The test method in accordance with AASHTO T 283 (28), is intended to evaluate the

effects of saturation and accelerated water conditioning, with a freeze–thaw cycle, of

compacted ACHM. The specimens are then tested for indirect tensile strength (ITS) by loading

the specimens at a constant rate and measuring the force required to fail the specimen. The ITS

of the conditioned specimens, which has been denoted as moisture-conditioned tensile

strength (MCTS) in the study, is compared to the control specimens to determine the tensile

strength ratio (TSR). The test specimens are conditioned and fabricated to 150 mm in diameter

and 100 mm in height, with 7.0±0.5 percent air voids. In total, the test utilizes six specimens,

three are controlled and three are conditioned

The information found in the preliminary literature review highlighted the fact that

many changes have been made in the current mix design method to improve pavement

durability, but there is still some sort of discrepancy and reluctance among the SHAs in moving

forward with the modifications, particularly with the concept of BMD. The study proposes to

change the current volumetric-based mix design strategies for surface ACHM used around the

state of Arkansas by implementing the concept of BMD using Approach D. The blend of

performance testing with no gyration requirements is anticipated to increase the durability of

asphalt pavements.

1.5 Objectives of the Study

The primary goal of the current study is to enhance the durability of asphalt pavements in Arkansas. This will be accomplished through a two-step approach:

1. **Laboratory Research: Concept Calibration** - The first step involves exploring extreme scenarios within the BMD Approach D for rutting and cracking by simultaneously adjusting asphalt binder content and the number of gyrations. This phase will establish boundaries for implementation and identify optimal performance zones using both ARDOT's selected and additional performance tests.

2. **Contractor Involvement: Practical Application** - Building on existing research, this phase will incorporate contractor expertise and their familiarity with local materials to support project advancement. The performance of ARDOT's BMD will be assessed using IDEAL-CT and APA tests across three specimen fabrication methods: Laboratory-Produced and Laboratory-Compacted (LMLC), Plant-Produced and Laboratory-Compacted (PMLC), and Reheated Plant-Produced and Laboratory-Compacted (RPMLC). Further validation of ARDOT's BMD will be conducted using additional testing applied to specimens prepared using LMLC and RPMLC techniques. Additionally, the study will evaluate how different sample fabrication methods influence predicted rutting and cracking performance using AASHTOWare Pavement ME.

The following chapters of the report cover the methodology and findings related to the objectives of the study. Chapter two details the laboratory calibration phase, while chapter three concentrates on the BMD field projects. Chapter four presents and discusses the results obtained from the AASHTOWare Pavement ME software. Lastly, chapter five provides a summary of the practical application of these results.

Chapter 2. Lab Calibration Stage

This section discusses in detail the approach being adopted in the laboratory for exploring the extreme scenarios of the BMD Approach D. The main objectives of the study are to provide boundaries for implementation and to identify optimal zones from both the rutting and cracking perspectives.

The lab calibration stage of the current research began with identifying one existing mix design. For the sake of convenience and proximity to the lab, a 12.5 mm NMAS surface course, with a PG 64-22 asphalt binder grade, from APAC-Central in Northwest Arkansas, has been considered as the base mix design. Both aggregates and asphalt binder were collected, representing the base mix design. **Table 3** shows the aggregates used in the base mix design, while **Table 4** depicts the combined aggregate gradation with different cold-feed percentages. The graphical representation of the combined aggregate gradation has been shown in **Figure 7**.

Table 3. Aggregates used in the base mix design

Serial no.	Aggregate name	Type of rock
1	3/4"	Limestone and chert
2	1/2" Chips	Sandstone
3	Manufactured Sand	Limestone and chert
4	Screenings	Limestone and chert
5	Asphalt Grit	Limestone
6	RAP	N/A

Three mix design variables- aggregate gradation, asphalt binder content (P_b), and number of gyrations (N) were considered in the study. The subsequent sections discuss in detail each of the variables.

Table 4. Combined aggregate gradation for the base mix design

Sieve size (mm)	1	2	3	4	5	6	Job Mix	Control Points
50	100	100	100	100	100	100	**100**	100%
37.5	100	100	100	100	100	100	**100**	100%
25	100	100	100	100	100	100	**100**	100%
19	100	100	100	100	100	100	**100**	100%
12.5	68	100	100	100	100	100	**96**	90-100%
9.5	42	89	100	100	100	96	**90**	90% Max
4.75	4	29	97	100	93	75	**62**	
2.36	2	5	65	74	48	56	**36**	28-58%
1.18	1	5	41	53	19	43	**24**	
0.6	1	5	26	40	9	35	**17**	
0.3	1	5	16	31	6	27	**13**	
0.15	1	4	9	23	5	18	**9**	
0.075	1.0	3.6	4.1	16.2	4.5	12.4	**6.4**	2-10%
Cold feed%	**11**	**31**	**15**	**12**	**16**	**15**		
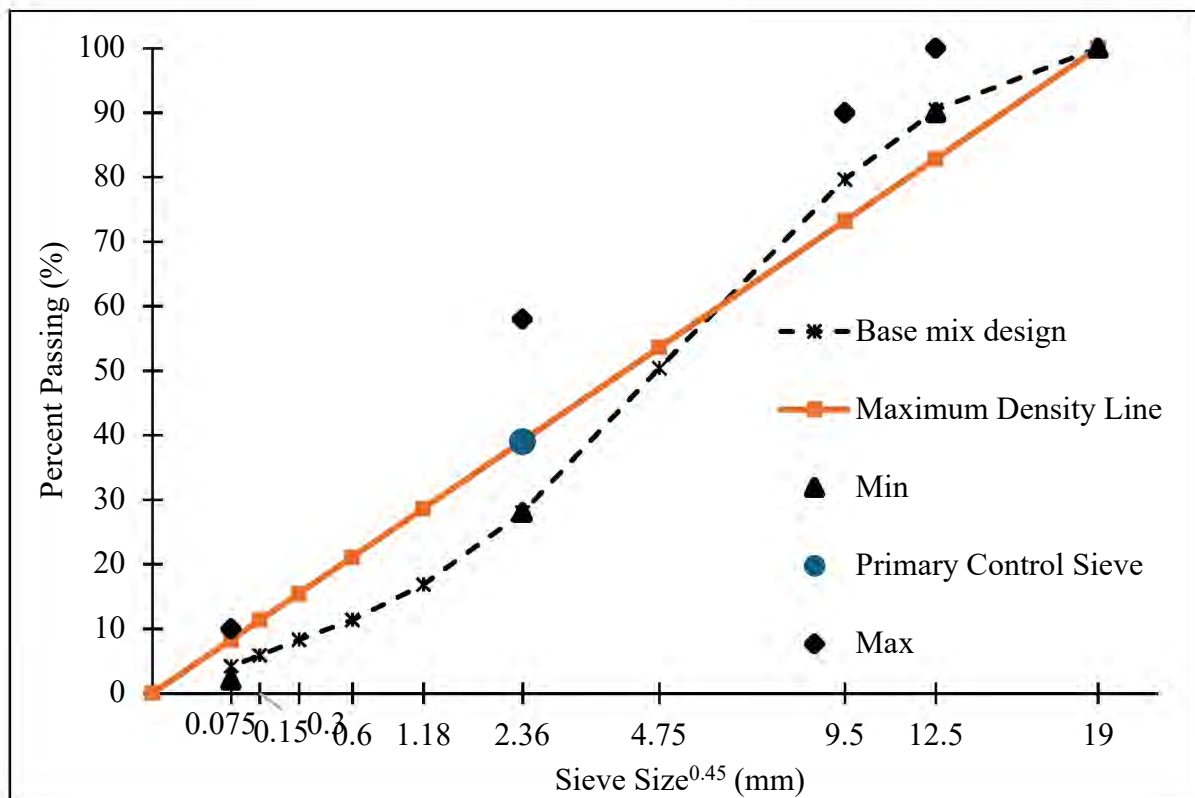
Figure 7. Combined aggregate gradation for the base mix design

35

2.1 Aggregate Gradation

Using the aggregate sources in the base mix design, three aggregate blends were created using AASHTO M 323 (11) and AASHTO R 35 (29). Two of the aggregate blends were fine gradation (passing well over the primary control sieve), and the third aggregate blend was a coarse gradation (passing well under the primary control sieve). One of the fine aggregate blends had 15% reclaimed asphalt pavement (RAP), while the other fine aggregate blend and coarse aggregate blend were devoid of any RAP. The three aggregate blends have been named as coarse gradation with 0% RAP, fine gradation with 0% RAP, and fine gradation with 15% RAP in the study.

2.2 Asphalt Binder Content

The initial trial binder content (P_{bi}) for the aggregate blends was determined following the procedure outlined in AASHTO R 35 (Appendix X1) (29), using the properties of the asphalt binder and aggregates as input, as shown in **Equation 1** . Each aggregate blend was mixed at four different asphalt binder contents: P_{bi} minus 0.5%, P_{bi}, P_{bi} plus 0.5%, and P_{bi} plus 1.0%.

$$P_{bi} = 100 * \left(\frac{G_b(V_{be} + V_{ba})}{G_b(V_{be} + V_{ba}) + W_s} \right)$$

Equation 1

where, G_b = specific gravity of asphalt binder

V_{be} = volume of effective binder, cm^3

V_{ba} = volume of binder absorbed into the aggregate, cm^3

W_s = mass of aggregate in 1 cm^3 of mix, g

2.3 Number Of Gyrations

The NCHRP report 9-9 (30) established four gyration levels (50, 75, 100, and 125) corresponding to different traffic conditions. However, recent studies (31, 32, 33) propose decreasing these gyrations during mixture design to ensure that the laboratory compaction mimics the effect of traffic loads on in-place density of ACHM. Baker's research (34) conducted for the Arkansas Asphalt Pavement Association, also recommended lowering the design

36

gyratory levels to enhance the durability of ACHM in Arkansas. Consequently, this study adopted gyratory levels of 40, 55, 70, and 85 based on these insights.

2.4 Experimental Matrix for the Lab Calibration Stage

A total of 48 ACHM produced using three aggregate gradations, four asphalt binder contents, and four gyration levels have been explored in the study. The experimental matrix has been summarized in **Table 5**. A pictorial depiction of the experimental matrix has been shown in **Figure 8** and has been designated as the "Cube" throughout the study.

Table 5. Experimental matrix for the lab calibration stage

Aggregate gradation	Asphalt binder content (P_b)	Number of gyrations (N)
Coarse 0% RAP	-0.5% P_{bi}	40
Fine 0% RAP	P_{bi}	55
Fine 15% RAP	+0.5% P_{bi}	70
	+1.0% Pbi	85

The "Cube" is a very convenient tool to visualize the power of the experimental matrix. This is because in some regions of the "Cube", there are optimum rutting and cracking performance zones. In addition, as we move away from these zones, either the rutting or the cracking performance decreases. By exploring all these scenarios, it will be possible to understand what happens at the extremes of each parameter. The thorough examination will allow for a very good understanding of the impact of aggregate gradation, asphalt binder contents, and the number of gyrations on the performance of ACHM on both rutting and cracking performance, and how the parameters interact with each other.

The study has been divided into three phases based on the aggregate gradations considered. The study started by evaluating the performance of coarse gradation (0% RAP),

followed by fine gradation (0% RAP) and fine gradation (15% RAP). The pictorial depiction of each phase of the study has been shown in **Figure 9**.
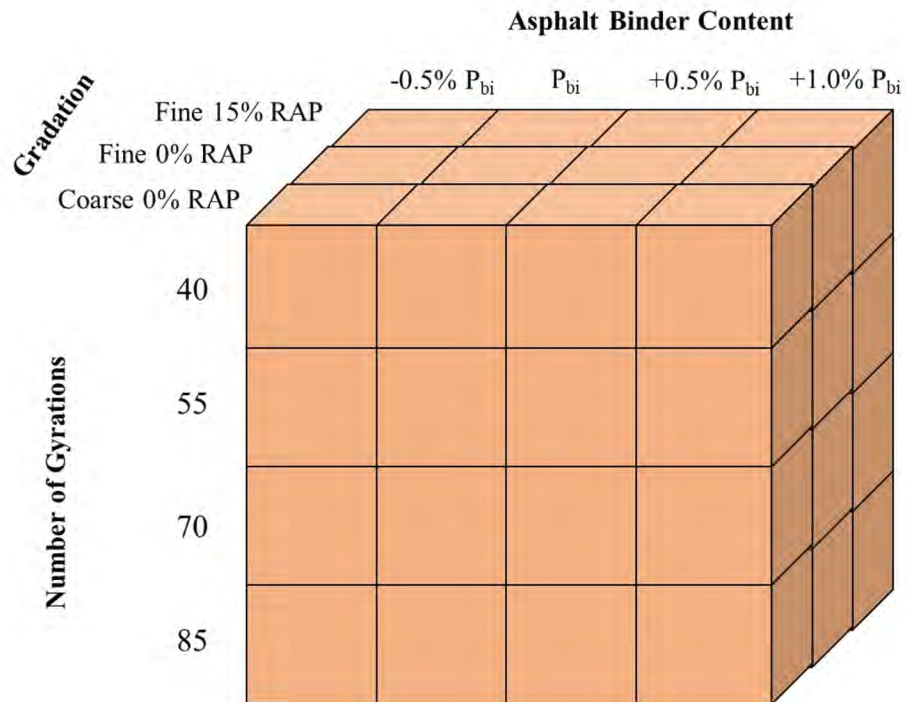
Figure 8. Pictorial depiction of the "Cube"
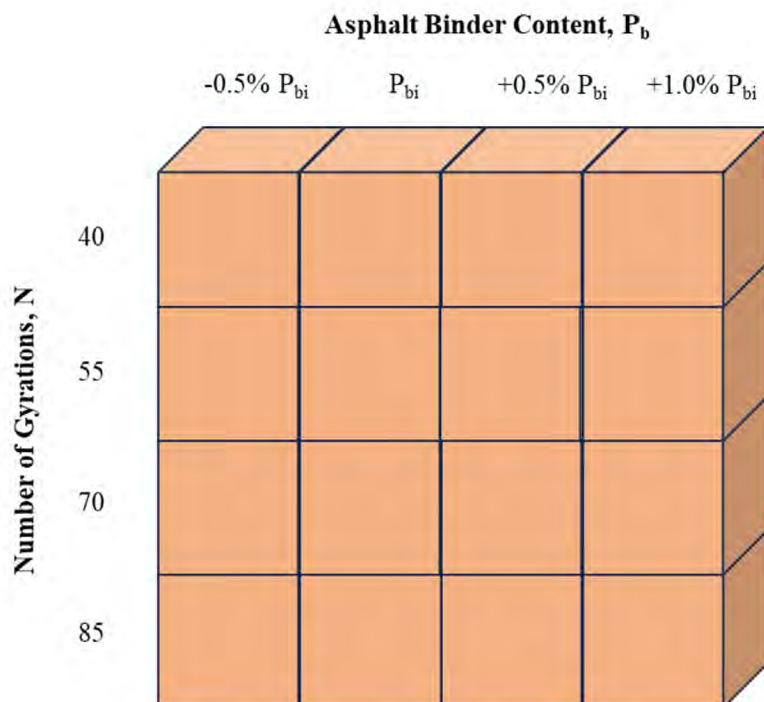
Figure 9. Pictorial illustration of one phase of the study

2.5 Determination Of Volumetric Properties

The next step in the study was the determination of volumetric properties for the 16 combinations of ACHM corresponding to each aggregate gradation. Volumetrics has been reported for each combination, as it is anticipated that volumetrics would still be used for quality control during production and construction in the field. The volumetric properties considered in the study were the volume of air voids (V_a), VMA, and voids filled with asphalt (VFA). The maximum specific gravity (G_{mm}) and bulk specific gravity (G_{mb}) data were used for calculating V_a as per ARDOT 464 (35).

Twelve loose ACHM samples, each weighing 2500 grams, were prepared for each aggregate gradation, with three samples corresponding to each binder content. The weight of the loose mixture for each G_{mm} specimen was determined based on an NMAS of 12.5 mm, as recommended by AASHTO T 209 (36). The G_{mm} value was reported as the average of three measurements for each binder content. In addition, forty-eight G_{mb} samples were prepared for each aggregate gradation, each weighing 5000 grams, with three samples corresponding to each of the sixteen ACHM combinations per gradation. The weight of the loose mix for fabricating G_{mb} specimen was determined such that the compacted specimen should have a dimension of 150 mm in diameter and 115±5 mm in height at the desired N, as specified by AASHTO T 312 (37). The G_{mb} value, measured as per AASHTO T 331 (38), was reported as the average of three measurements for each combination. The VMA and VFA were calculated following the procedures outlined in ARDOT 464 (35).

The V_a data collected for each mixture combination were used to prepare samples for performance evaluation. The initial testing included the APA and IDEAL-CT, which were recommended in Arkansas to measure rutting and cracking, respectively. For each of the forty-eight combinations, samples for the APA and the IDEAL-CT tests were compacted at V_a±1.0% and V_a±0.5%, respectively. Based on the results from the two performance tests, "initial optimal performance zones" were determined by identifying the optimal P_b and N values. Additional performance tests, including HWTT and TSR, were carried out within the identified zones to establish the "final optimal performance zones." Notably, the performance tests for both IDEAL-CT and APA, as well as the additional tests, were not performed at the conventional

average target air void content of 7.0%. The results from these additional tests will be used to evaluate ARDOT's choice of performance tests, which could lead to modifications in the current specifications. A sequential approach, as shown in **Figure 10** was employed in the study.
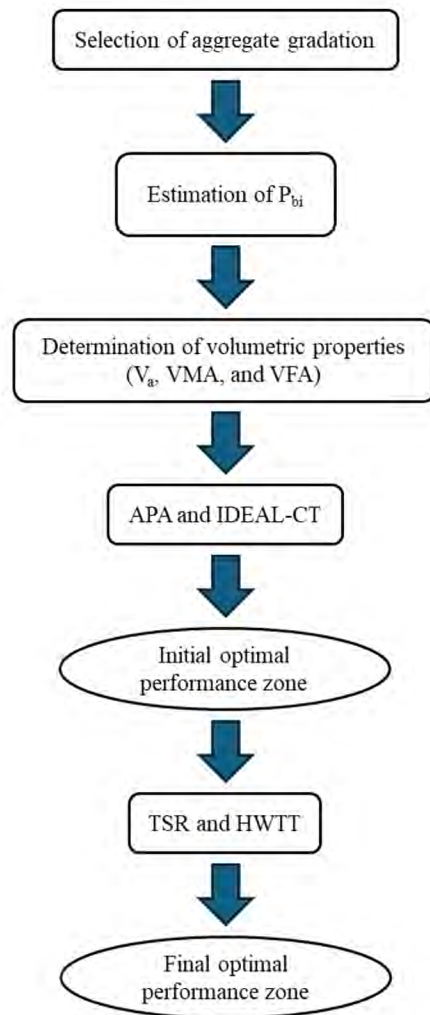
Figure 10. Step-by-step procedure adopted in the study

2.6 Coarse Gradation (0% RAP)

The present section discusses in detail the results obtained from the volumetric and performance tests for the sixteen ACHM produced using a coarse graded aggregate blend by varying two mix design variables – P_b and N. The combined aggregate gradation has been shown in **Table 6** and **Figure 11**, respectively.

Table 6. Combined aggregate gradation

Sieve size (mm)	1	2	3	4	5	Job Mix	Control Points
50	100	100	100	100	100	**100**	100%
37.5	100	100	100	100	100	**100**	100%
25	100	100	100	100	100	**100**	100%
19	100	100	100	100	100	**100**	100%
12.5	68	100	100	100	100	**90**	90-100%
9.5	42	89	100	100	100	**80**	90% Max
4.75	4	29	97	100	93	**50**	
2.36	2	5	65	74	48	**28**	28-58%
1.18	1	5	41	53	19	**17**	
0.6	1	5	26	40	9	**11**	
0.3	1	5	16	31	6	**8**	
0.15	1	4	9	23	5	**6**	
0.075	1.0	3.6	4.1	16.2	4.5	**4.2**	2-10%
Cold feed%	**30**	**27**	**18**	**9**	**16**		
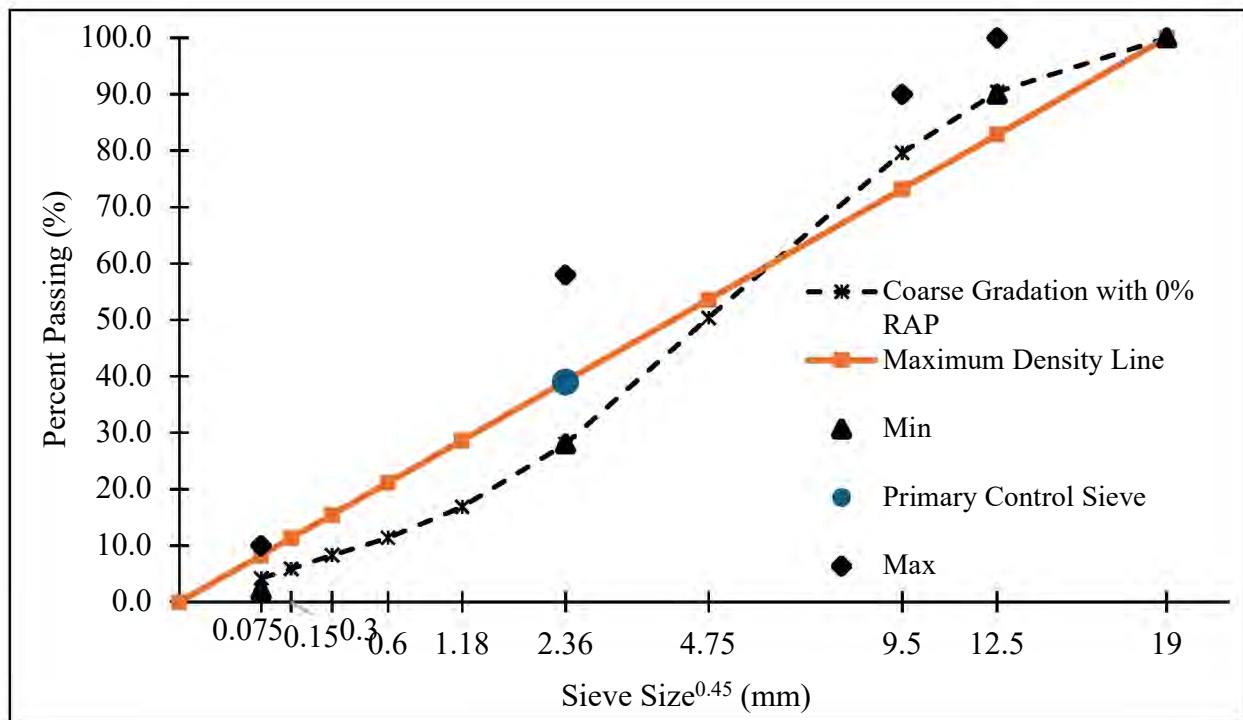
Figure 11. Combined aggregate gradation

2.7 Volumetric Properties

2.7.1 Estimation of P_{bi}

Using the aggregate and binder properties as inputs in **Equation 1**, the P_{bi} value was calculated. According to **Table 7**, the P_{bi} for the coarse aggregate gradation was found to be 5.1%. Based on this P_{bi} value, four levels of binder contents were determined: 4.6%, 5.1%, 5.6%, and 6.1%.

Table 7. Estimation of P_{bi} value

Bulk specific gravity for the combined aggregate, G_{sb}	2.557
Apparent specific gravity for the combined aggregate, G_{sa}	2.656
Effective specific gravity for the combined aggregate, G_{se}	2.636
Mass of aggregate in 1 cm^3 of mix, W_{s}, g	2.23
Volume of binder absorbed into the aggregate, V_{ba}, cm^3	0.03
Volume of effective binder, V_{be}, cm^3	0.09
Estimated initial trial binder content, P_{bi}, % by wt. of total mix	**5.1**

* Reference: AASHTO R 35 (Appendix X)

The G_{mm} values for the loose mix at each binder content were calculated and are shown in **Figure 12**. Using the aggregate properties from **Table 7** and a G_b value of 1.026, the percentage of absorbed binder (P_{ba}) was calculated to be 1.2%. Additionally, the effective binder content (P_{be}) for the four levels of P_b was determined as follows: for P_b = 4.6%, P_{be} = 3.5%; for P_b = 5.1%, P_{be} = 4.0%; for P_b = 5.6%, P_{be} = 4.5%; and for P_b = 6.1%, P_{be} = 5.0%.

After determining the G_{mm} values for all four binder contents, G_{mb} samples were fabricated for the sixteen mix combinations (four levels of P_b and four levels of N). These mix properties were then used to calculate V_a, forming the basis for preparing performance test samples. Additionally, VMA and VFA values were calculated. This study employed a BMD

Approach D, varying both P_b and N simultaneously. It demonstrates how altering these two variables together affects volumetric and performance properties.
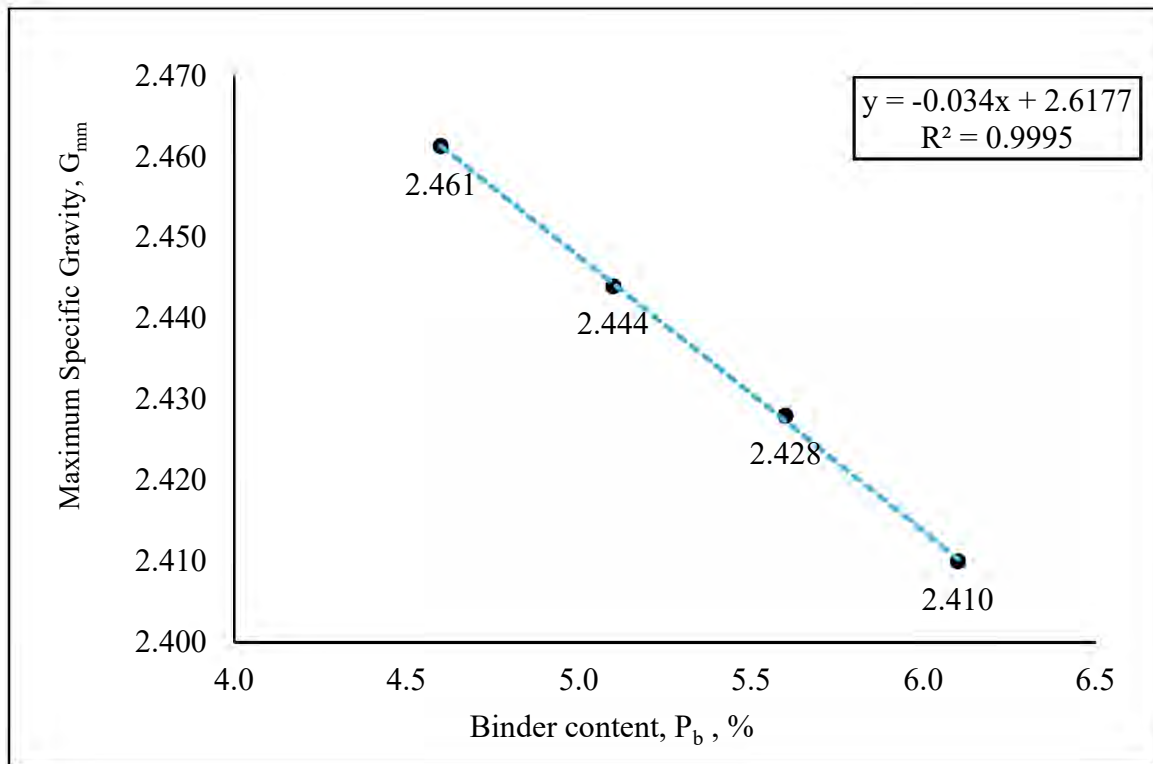
Figure 12. Relationship between G_{mm} and P_b

Figure 13 and **Figure 14** illustrate the relationship between V_a and P_b, and V_a and N, respectively. **Figure 13** shows that V_a has an inverse relationship with P_b, which is expected since increasing P_b means more binder occupies the space between aggregates. **Figure 14** depicts a linear decrease in V_a with increasing N, as higher compaction effort results in a more densely packed sample, thus reducing air voids (39). However, deviations from this trend may occur if mixtures are compacted beyond the point where aggregates begin to lock, altering aggregate gradation (40, 41, 42). It is notable that the aggregate gradation was purposely forced to be coarse-graded, however it ended up being an open-graded type. This was typically observed from the higher V_a values obtained in the study, which ranged from 5.0% to 11.6%, outside the conventional recommended range of 3.5% to 4.5%.

Table 8 presents the V_a, VMA, and VFA values for sixteen mixtures, each averaged from three readings. According to AASHTO M 323 (11), a 12.5 NMAS ACHM with a V_a of 4.0% should

ideally have a minimum VMA of 14.0% and a VFA ranging from 71.0% to 75.0%. However, in this study, these recommended VMA and VFA criteria do not apply because the mixtures have V_a ranging from 5.0% to 11.6%. It is important to note that, although we report on the VMA and VFA values, our primary focus is on evaluating the performance of the mixtures.

The chart displays the following trendline equations:

$y = -1.6937x + 19.506$, $R^2 = 0.750$

$y = -2.9211x + 24.534$, $R^2 = 0.989$

$y = -1.2597x + 13.867$, $R^2 = 0.585$

$y = -2.5394x + 20.233$, $R^2 = 0.946$

Legend: 40, 55, 70, 85

Axis labels: Air Voids, V_a (%); Binder Content, P_b (%)
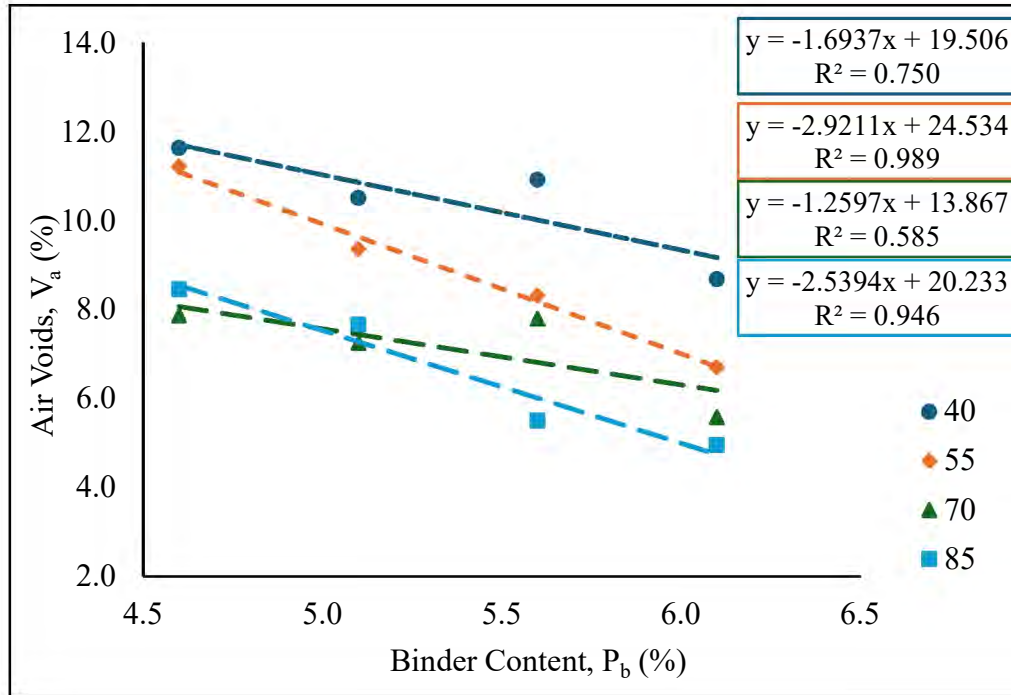
Figure 13. Relationship between V_a and P_b

Table 8 illustrates that for every 15 increments in gyration levels, there is an average decrease of 1.3% in air voids. Additionally, a 0.5% increase in binder content results in an average reduction of 1.1% in air voids. These trends can be used to predict the binder content needed to achieve the desired air voids for the aggregate gradation used in this study. For instance, the calculated binder contents for ACHM designed with 4.0% air voids at various gyration levels are: N = 40, P_b = 8.2%; N = 55, P_b = 7.3%; N = 70, P_b = 6.8%; and N = 85, P_b = 6.5%. These predicted binder contents indicate that the ACHM produced in the study is too coarse and lacks sufficient binder content. However, producing ACHM with the calculated binder contents is outside the scope of this study. There are some instances where air voids increase with an increase in gyrations, which is unintuitive. However, the overall trends are downward, and it is believed that these deviations are simply part of the variability of sample preparation and testing.
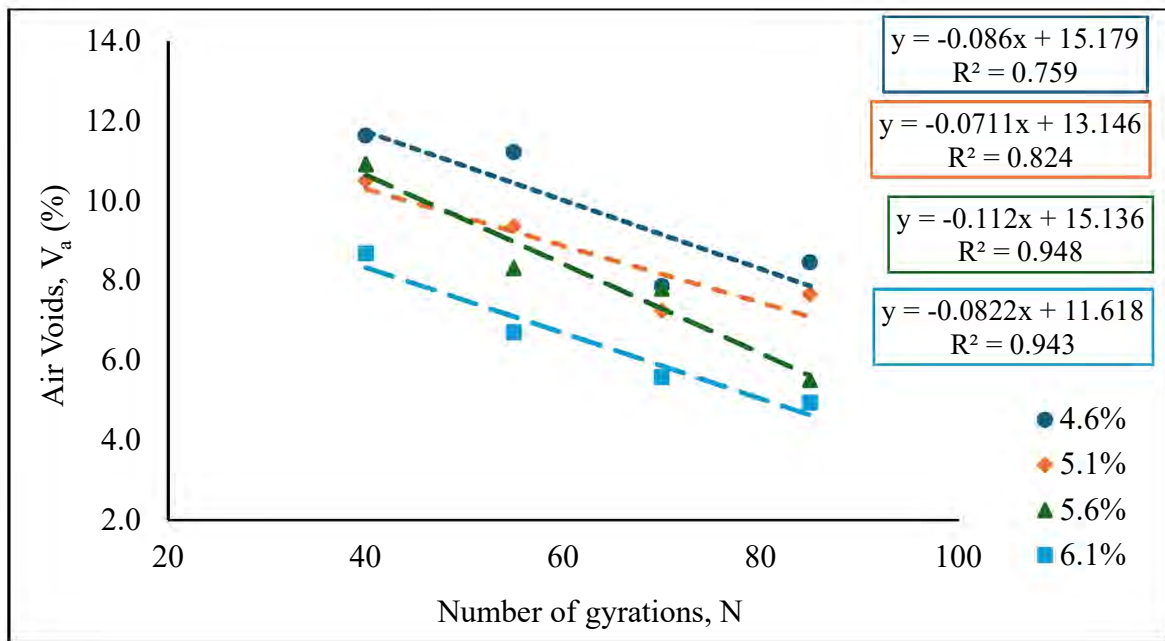
Figure 14. Relationship between V_a and N

Table 8. V_a, VMA, and VFA values

Air Voids, V_a, %				
N/ P_b	4.6%	5.1%	5.6%	6.1%
40	11.6	10.5	10.9	8.7
55	11.2	9.4	8.3	6.7
70	7.9	7.3	7.8	5.6
85	8.5	7.7	5.5	5.0
Voids in Mineral Aggregates, VMA, %				
N/ P_b	4.6%	5.1%	5.6%	6.1%
40	19.2	18.4	18.5	19.2
55	18.5	18.2	17.9	17.7
70	15.6	16.2	17.2	16.6
85	16.3	16.4	15.2	16.1
Voids Filled with Asphalt, VFA, %				
N/ P_b	4.6%	5.1%	5.6%	6.1%
40	37.6	45.3	51.1	54.7
55	39.1	46.2	52.9	60.6
70	48.2	53.3	55.6	65.5
85	45.8	52.3	64.6	67.6

2.7.2 Performance Testing

The performance test samples for each binder content and gyration level were compacted according to the air voids results detailed in the previous section. The sample thickness and air void tolerance adhered to the specifications outlined in the respective test standards.

The initial optimal performance zone was identified using the IDEAL-CT and APA tests. **Table 9** presents the results obtained from the two performance tests for the sixteen mix combinations. The CT_{Index} value ranged from 21 to 182, and the APA rut depth was reported to be between 1.511 mm and 3.252 mm, respectively.

Figure 15 illustrates the relationship between CT_{Index} and P_b, showing that CT_{Index} increases with increasing P_b. This is consistent with previous findings (39) that suggest the binder acts as a lubricant, enhancing mixture ductility and cracking resistance. **Figure 16** demonstrates that as gyratory compaction increases, CT_{Index} decreases, likely due to the increased mix stiffness resulting from greater compaction effort, thereby reducing cracking resistance.

Table 9. Summary of the performance test results

CT_{Index}				
N/ P_b	**4.6%**	**5.1%**	**5.6%**	**6.1%**
40	75	110	149	182
55	47	62	86	99
70	21	42	94	131
85	30	38	55	102
APA Rut Depth, mm				
N/ P_b	**4.6%**	**5.1%**	**5.6%**	**6.1%**
40	3.252	3.185	3.079	2.943
55	2.053	2.269	2.623	3.046
70	2.301	2.040	1.992	1.977
85	2.230	2.655	1.511	2.267
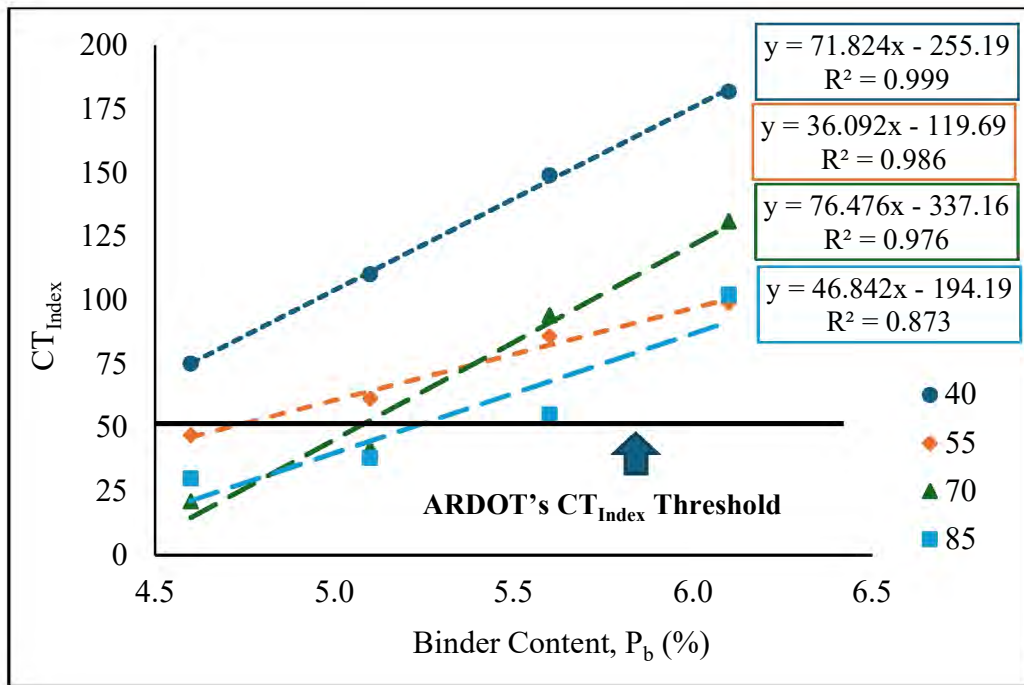
Figure 15. Relationship between CT$_{Index}$ and P$_b$
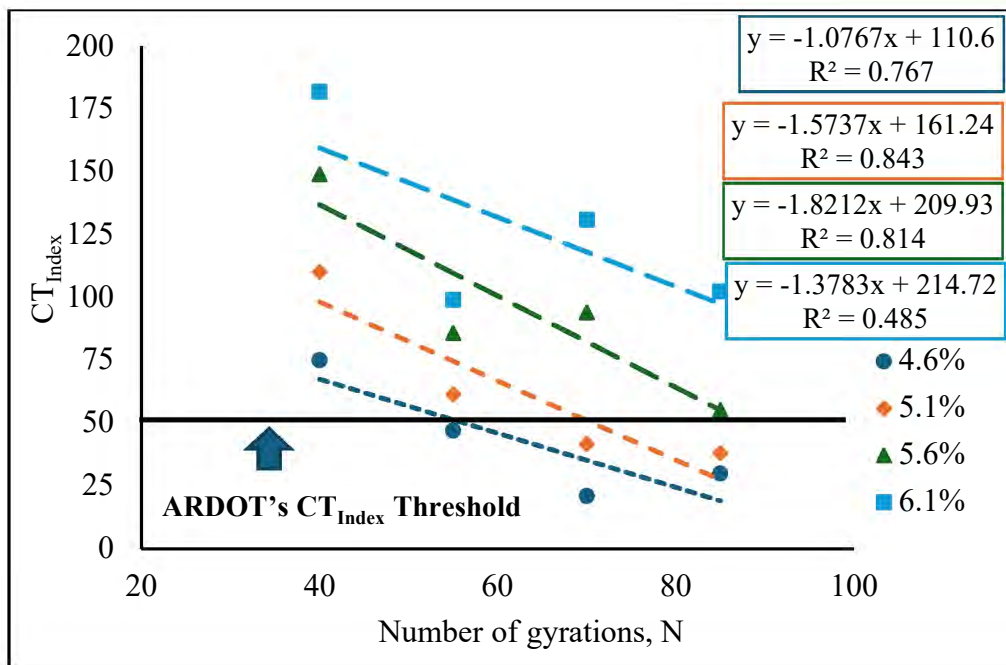
Figure 16. Relationship between CT$_{Index}$ and N

The relationship between the APA rut depth and P$_b$ is shown in **Figure 17**. The trend

between these two variables is not definitive. Previous studies (40, 41) have linked the rutting

potential of ACHM to asphalt binder properties. However, the findings of the current study highlight that aggregate gradation, or the overall aggregate skeleton, significantly influences asphalt rutting performance. The inconclusive trend in this study might be due to changes in the aggregate gradation of the mix during the compaction process. **Figure 18** illustrates the relationship between APA rut depth and N, where a decreasing trend is observed. This indicates that as the compaction level increases, the asphalt sample's stiffness also increases, enhancing rutting resistance. Additionally, it is important to note that for all samples, the APA rut depth is below the ARDOT recommended maximum value of 8.0 mm, corresponding to the PG 64-22 asphalt binder being used.

$y = -0.2066x + 4.2201$
$R^2 = 0.978$

$y = 0.6666x - 1.0686$
$R^2 = 0.980$

$y = -0.204x + 3.1689$
$R^2 = 0.756$

$y = -0.2066x + 3.2711$
$R^2 = 0.078$
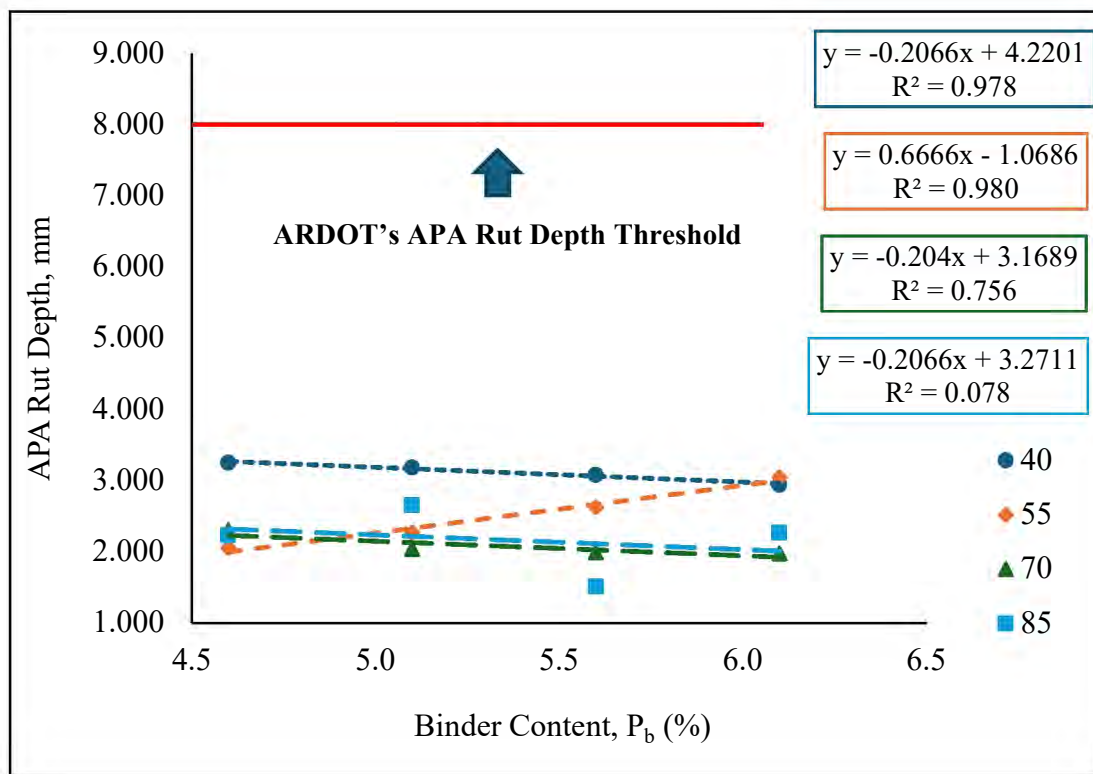
Figure 17. Relationship between APA rut depth and P_b

The findings from the IDEAL-CT and APA tests are depicted in **Figure 19**, where each data point represents the average CT_{Index} and APA rut depth for each mix type. It is evident that five out of the sixteen mixtures fail in terms of cracking, with CT_{Index} values falling below the minimum recommended threshold of 50. However, rutting does not pose a concern, as all mixtures exhibit rut depths below the recommended maximum of 8.0 mm. These results

emphasize that, in the current study, the overall performance of the coarse-graded mix is largely governed by its cracking performance.
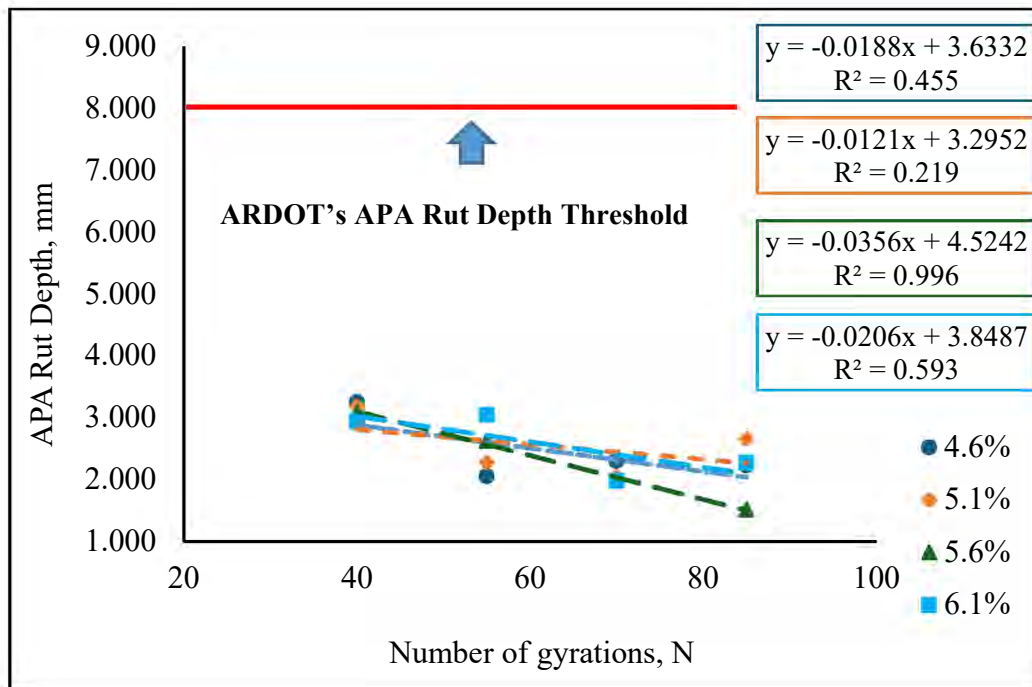
Figure 18. Relationship between APA rut depth and N
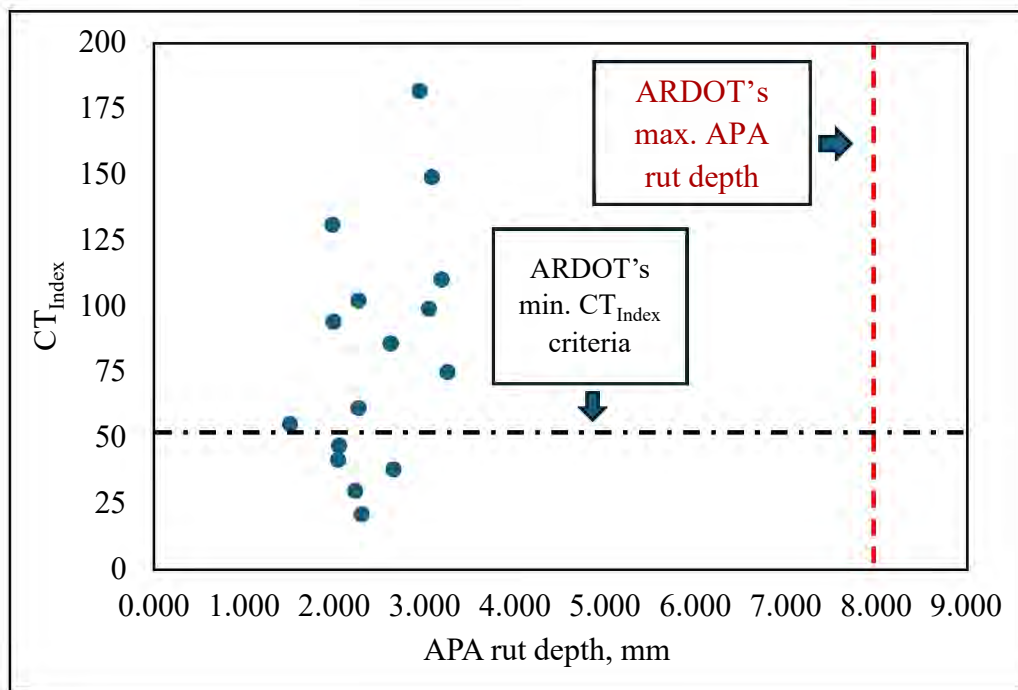
Figure 19. Summary of the performance test results

Based on CT_{Index} as the primary criterion, performance zones were identified and are illustrated in **Figure 20**. These zones are categorized as 'Poor' (CT_{Index} less than 50), 'Moderate' (CT_{Index} between 50 and 75), 'Good' (CT_{Index} between 75 and 100), and 'Excellent' (CT_{Index} above 100).

Figure 20 illustrates that ACHM in the zone with lower P_b, and higher N have a CT_{Index} less than 50, categorizing them as "Poor" in terms of performance. However, the zones designated as "Excellent" are found in regions with both higher and lower P_b, compacted to both higher and lower N. For this study, zones rated as "Good" and "Excellent" were identified as the initial optimal performance regions.
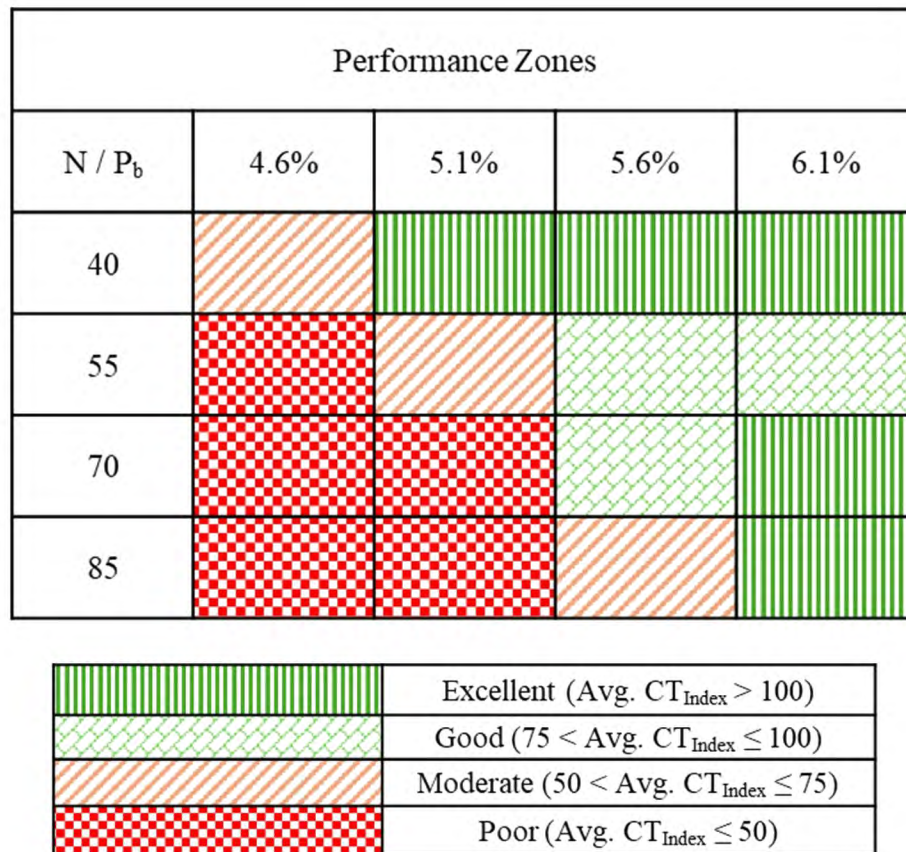
Figure 20. Performance zones obtained in the study

Following IDEAL-CT and APA testing, HWTT and TSR were chosen as the next performance tests to further refine or validate the identified zones. Eight out of sixteen zones, which exhibited "Excellent" or "Good" performance, were selected for these additional evaluations, as shown in **Figure 21**. These specific zones were selected because they already

showed strong resistance to both cracking and rutting, allowing the study to focus on promising candidates while minimizing the number of samples tested.

N / P_b	4.6%	5.1%	5.6%	6.1%
40		🟩	🟩	🟩
55			🟩	🟩
70			🟩	🟩
85				🟩

Figure 21. Performance zones considered for HWTT and TSR testing

Table 10 presents the HWTT results, which indicate that most of the asphalt mixtures demonstrated poor resistance to moisture damage, as reflected by their high rut depths. Specifically, in seven out of the eight zones, the rut depths exceeded 12.5 mm, the maximum threshold recommended by neighboring states such as Texas and Oklahoma. Since Arkansas does not currently have a specified maximum rut depth limit for HWTT, these neighboring standards were used for reference in this study. Although no distinct relationship was observed between rut depth and either binder content or compaction level, both the stripping inflection point (SIP) passes and the number of passes to failure increased consistently with higher gyration levels across all binder contents. This trend indicates that higher compaction levels result in stiffer mixtures, which are capable of withstanding more loading cycles before failing.

Table 11 presents the results from the moisture-induced damage testing. It is important to note that, in this study, the saturation time for the conditioned samples was standardized at 20 minutes, and the reported degree of saturation reflects this fixed duration. The TSR values obtained aligned with the HWTT results, as all samples recorded TSR values below the

recommended threshold of 0.80. This outcome indicates that mixtures located in zones initially identified as optimal based on IDEAL-CT and APA test results experienced significant moisture-related damage, as confirmed by both high HWTT rut depths and low TSR values. Another important consideration is that the binder used in this study did not contain an anti-stripping agent (ASA). While the inclusion of ASA could potentially improve moisture resistance, evaluating its effect falls outside the scope of this study.

Table 10. Summary of the HWTT test results

HWTT rut depth (mm)				
N / P_b	4.6%	5.1%	5.6%	6.1%
40	-	15.3	20.0	20.0
55	-	-	20.0	14.7
70	-	-	6.6	20.0
85	-	-	-	14.6
SIP passes				
N / P_b	4.6%	5.1%	5.6%	6.1%
40	-	15090	9865	10270
55	-	-	13969	13793
70	-	-	17477	12343
85	-	-	-	13938
HWTT fail passes				
N / P_b	4.6%	5.1%	5.6%	6.1%
40	-	18604	12513	12477
55	-	-	17056	18080
70	-	-	20000	16610
85	-	-	-	19004

Table 11. Summary of the moisture-induced damage test

Degree of saturation (%)				
N / P_b	4.6%	5.1%	5.6%	6.1%
40	-	68	70	72
55	-	-	69	68
70	-	-	68	66
85	-		-	66
Moisture conditioned strength (kPa)				
N / P_b	4.6%	5.1%	5.6%	6.1%
40	-	366	457	344
55	-	-	515	694
70	-	-	626	764
85	-		-	624
TSR				
N / P_b	4.6%	5.1%	5.6%	6.1%
40	-	0.45	0.53	0.41
55	-	-	0.58	0.72
70	-	-	0.53	0.63
85	-		-	0.63

2.8 Fine Gradation (0% RAP)

This section provides a detailed analysis of the results from the volumetric and performance tests conducted on sixteen ACHM, which were produced using a fine graded aggregate blend with variations in two mix design variables, P_b and N. The aggregate gradation used is illustrated in **Table 12** and **Figure 22**, respectively.

Table 12. Combined aggregate gradation

Sieve size (mm)	1	2	3	4	5	Job Mix	Control Points
50	100	100	100	100	100	**100**	100%
37.5	100	100	100	100	100	**100**	100%
25	100	100	100	100	100	**100**	100%
19	100	100	100	100	100	**100**	100%
12.5	68	100	100	100	100	**96**	90-100%
9.5	42	89	100	100	100	**90**	90% Max
4.75	4	29	97	100	93	**67**	
2.36	2	5	65	74	48	**43**	28-58%
1.18	1	5	41	53	19	**30**	
0.6	1	5	26	40	9	**22**	
0.3	1	5	16	31	6	**17**	
0.15	1	4	9	23	5	**12**	
0.075	1.0	3.6	4.1	16.2	4.5	**8.5**	2-10%
Cold feed%	**11**	**31**	**15**	**40**	**3**		

Using the aggregate and binder properties as inputs in **Equation 1**, the P_{bi} value was calculated. According to **Table 13**, the P_{bi} for the fine aggregate gradation (0% RAP) was found to be 6.5%. Based on this P_{bi} value, four levels of binder contents were determined: 6.0%, 6.5%, 7.0%, and 7.5%.
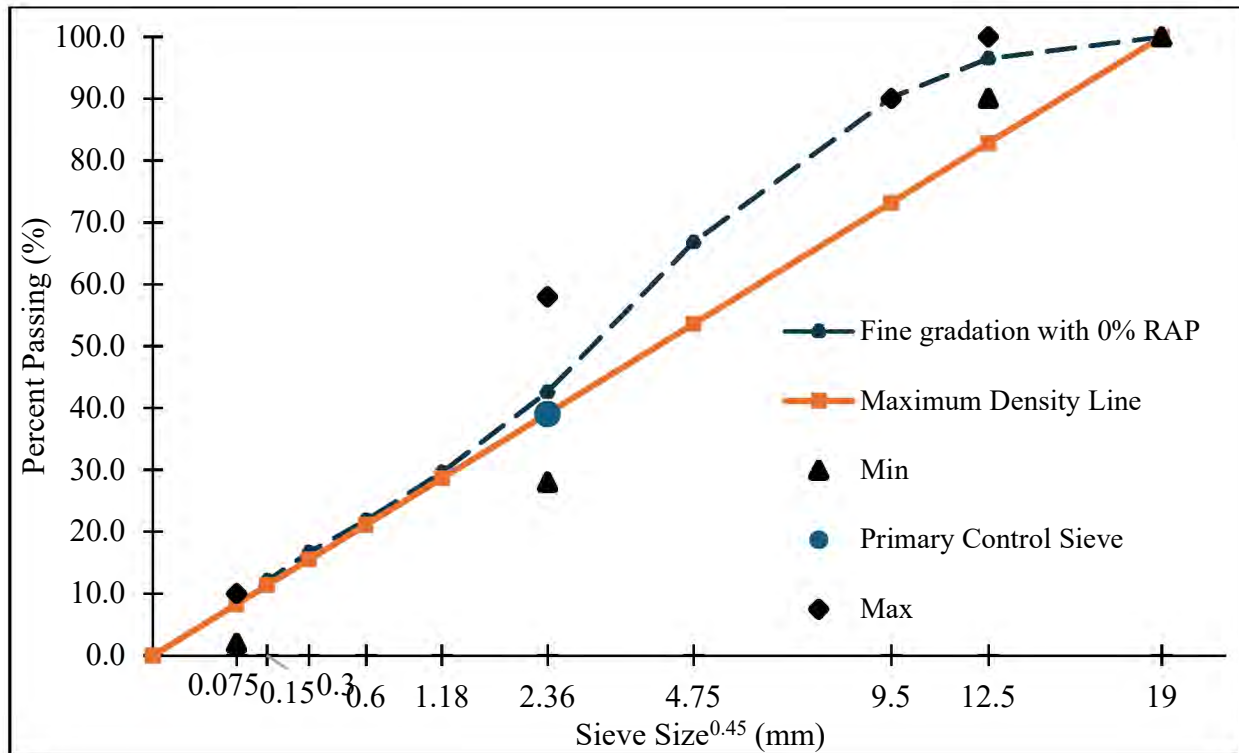
Figure 22. Combined aggregate gradation

Table 13. Estimation of P_{bi}

Bulk specific gravity for the combined aggregate, G_{sb}	2.496
Apparent specific gravity for the combined aggregate, G_{sa}	2.681
Effective specific gravity for the combined aggregate, G_{se}	2.644
Mass of aggregate in 1 cm^3 of mix, W_s, g	2.24
Volume of binder absorbed into the aggregate, V_{ba}, cm^3	0.05
Volume of effective binder, V_{be}, cm^3	0.10
Estimated initial trial binder content, P_{bi}, % by weight of total mix	**6.5**

* Reference: AASHTO R 35 (Appendix X)

The G_{mm} values for the loose mix at each binder content were calculated and are shown in **Figure 23**. Using the aggregate properties from **Table 13** and a G_b value of 1.026, the

percentage of absorbed binder (P_{ba}) was calculated to be 2.3%. Additionally, the effective binder content (P_{be}) for the four levels of P_b was determined as follows: for P_b = 6.0%, P_{be} = 3.8%; for P_b = 6.5%, P_{be} = 4.3%; for P_b = 7.0%, P_{be} = 4.9%; and for P_b = 7.5%, P_{be} = 5.4%.

The same procedures described in the previous section were followed to prepare G_{mb} samples for all sixteen mix combinations. Afterward, the volumetric properties — V_a, VMA, and VFA — were determined.
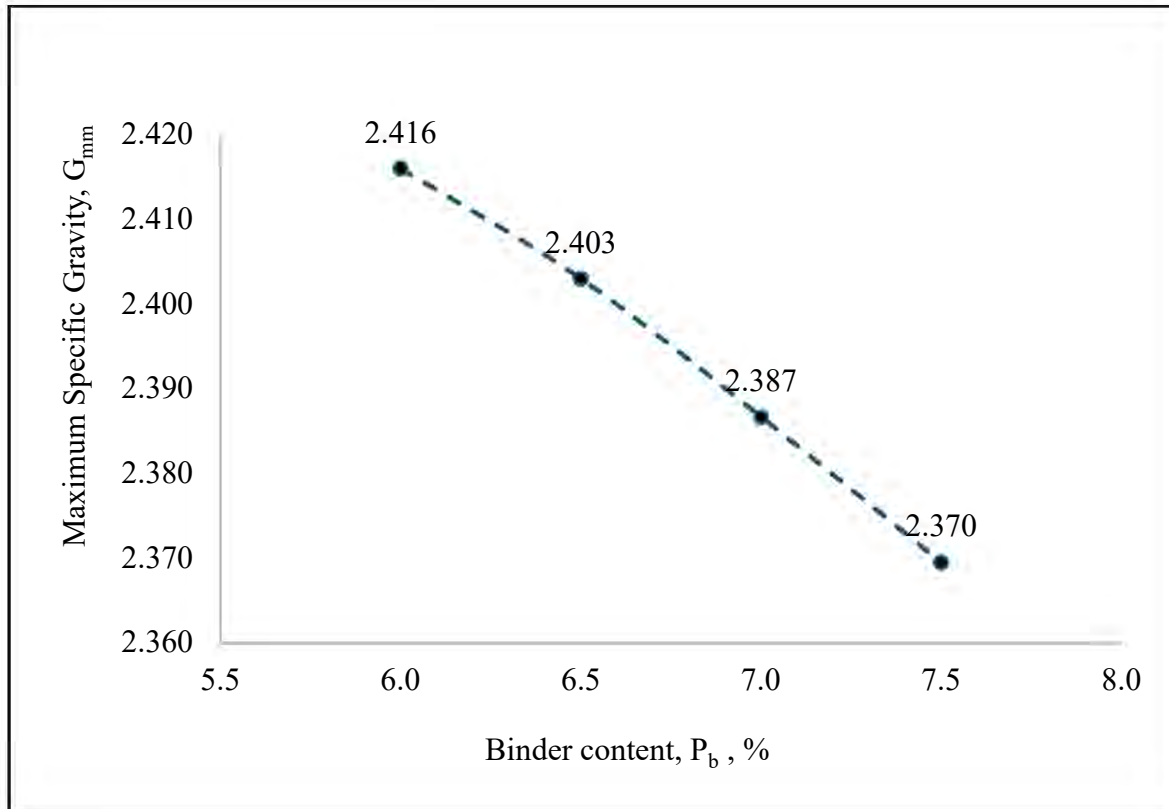
Figure 23. Relationship between G_{mm} and P_b

Figure 24 and **Figure 25** depict the correlation between V_a and P_b, and V_a and N, respectively. As with the coarse graduation (0% RAP) results, inverse relationships between V_a and both P_b and N were noted. The air voids in the present case varied between 1.0% and 5.1%. Unlike the coarse gradation scenario, some combinations of P_b and N produced ACHM with air voids within the conventional design range of 3.5% to 4.5%. It will be interesting to compare the performance of these mixtures with those having air voids outside the traditional design range.

Table 14 presents the V_a, VMA, and VFA values for sixteen mixtures, each averaged from three readings.
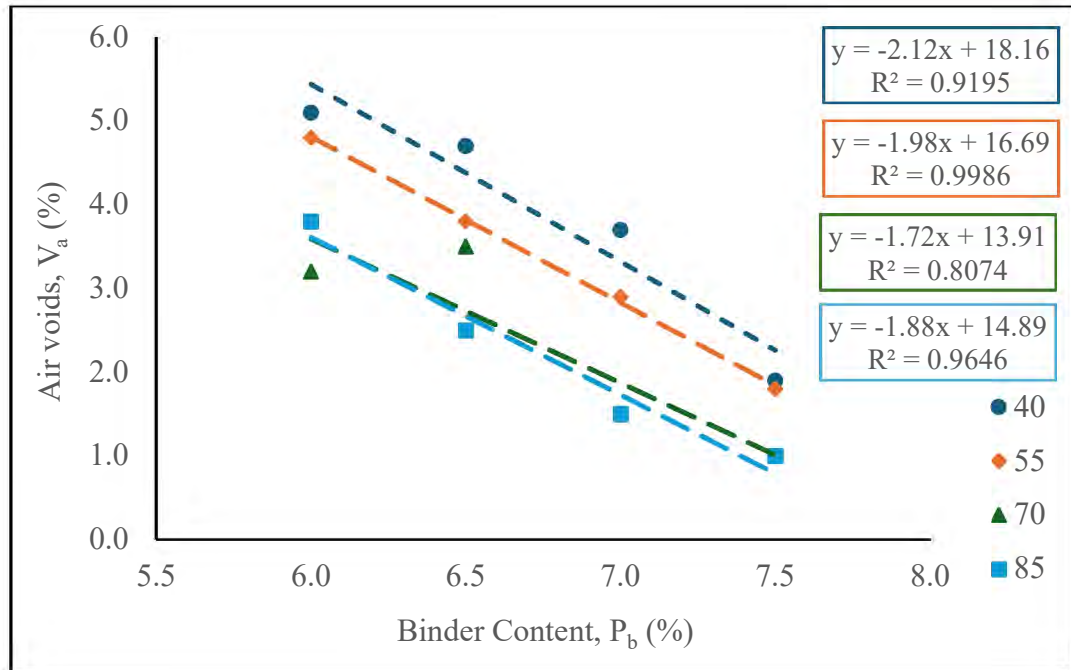
Figure 24. Relationship between V_a and P_b
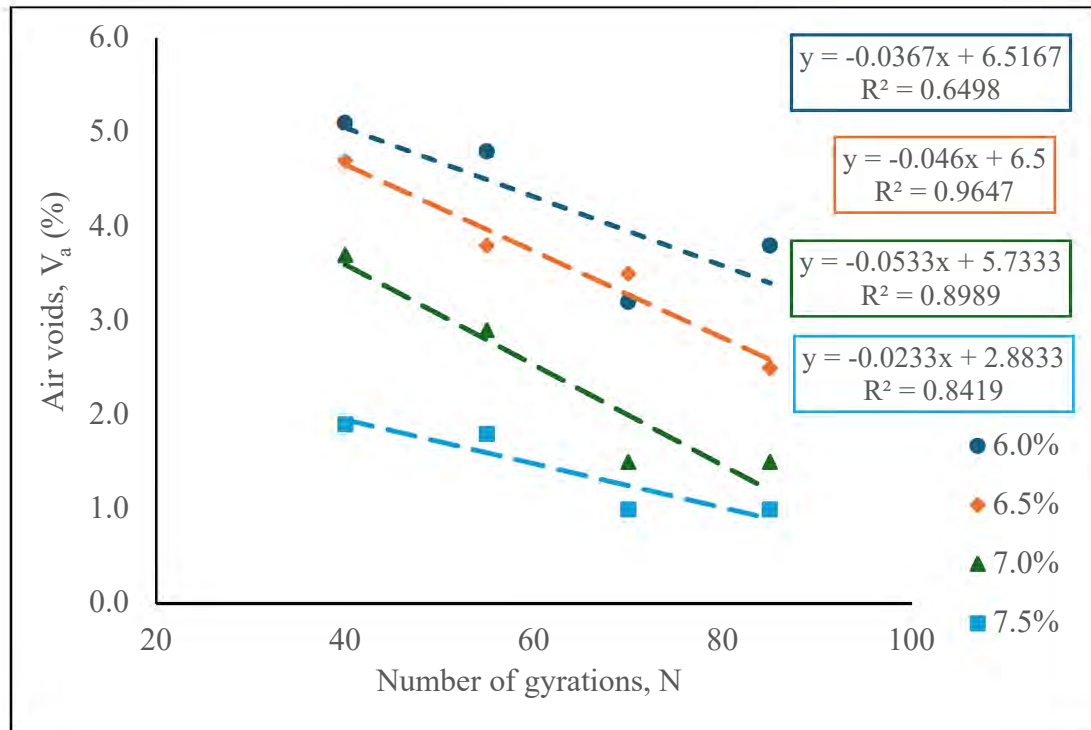
Figure 25. Relationship between V_a and N

Table 14. V_a, VMA, and VFA values

Air Voids, V_a, %				
N/ P_b	6.0%	6.5%	7.0%	7.5%
40	5.1	4.7	3.7	1.9
55	4.8	3.8	2.9	1.8
70	3.2	3.5	1.5	1.0
85	3.8	2.5	1.5	1.0
Voids in Mineral Aggregates, VMA, %				
N/ P_b	6.0%	6.5%	7.0%	7.5%
40	13.6	14.2	14.4	13.9
55	13.3	13.4	13.6	13.7
70	12.0	13.2	12.4	13.1
85	12.5	12.2	12.4	13.1
Voids Filled with Asphalt, VFA, %				
N/ P_b	6.0%	6.5%	7.0%	7.5%
40	62.8	67.2	74.2	86.2
55	64.4	71.6	79.0	87.3
70	72.9	73.2	87.9	92.3
85	69.5	79.8	87.7	92.4

2.8.1 Performance Testing

The performance test specimens for each P_b and N were prepared based on the V_a results discussed in the previous section. The sample thickness and air void tolerances complied with the requirements specified in the respective test standards.

The initial optimal performance zone was determined using results from the IDEAL-CT and APA tests. **Table 15** summarizes the outcomes of these tests for all sixteen mix

combinations. The CT_{Index} values ranged from 63 to 556, while APA rut depths varied from 1.437 mm to 4.978 mm.

      Figure 26 illustrates correlation between CT_{Index} and P_b, indicating that CT_{Index} tends to increase as P_b increases. This trend aligns with the characteristics of coarse-graded mixes and existing research, which suggests that higher binder content improves mixture ductility and cracking resistance by acting as a lubricant. The relationship between CT_{Index} and N is shown in **Figure 27**, however, no distinct pattern is observed between the two.

Table 15. Summary of the performance test results

CT_{Index}				
N/ P_b	6.0%	6.5%	7.0%	7.5%
40	63	132	257	302
55	89	136	177	255
70	76	148	228	383
85	73	158	183	556
APA Rut Depth, mm				
N/ P_b	6.0%	6.5%	7.0%	7.5%
40	2.365	4.978	3.702	4.766
55	2.774	1.437	1.945	3.307
70	2.082	4.109	3.733	4.185
85	2.086	1.977	2.401	2.679
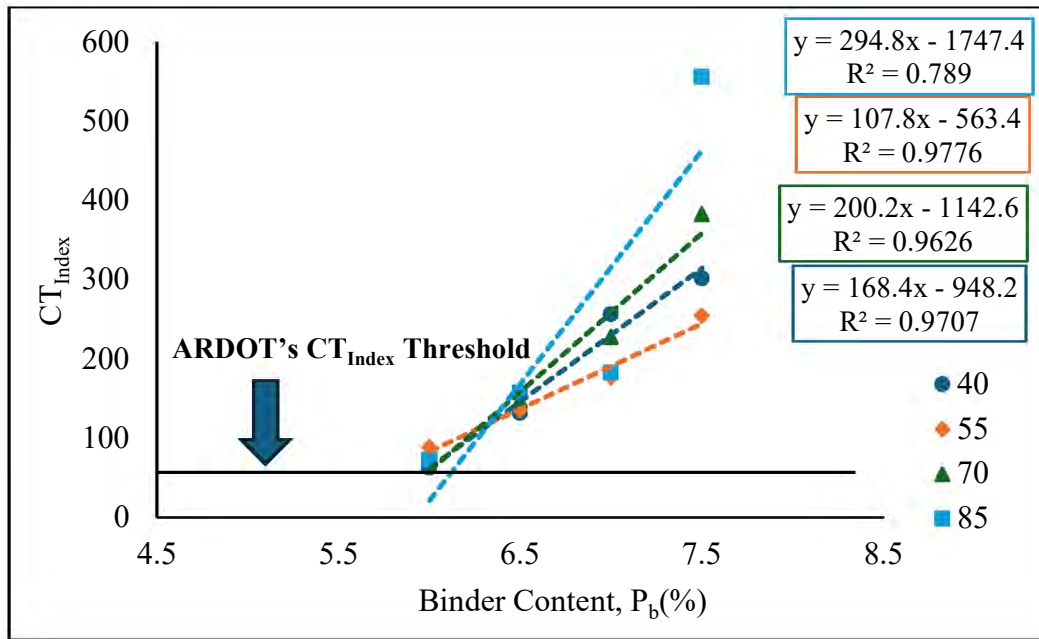
Figure 26. Relationship between CT$_{Index}$ and P$_b$
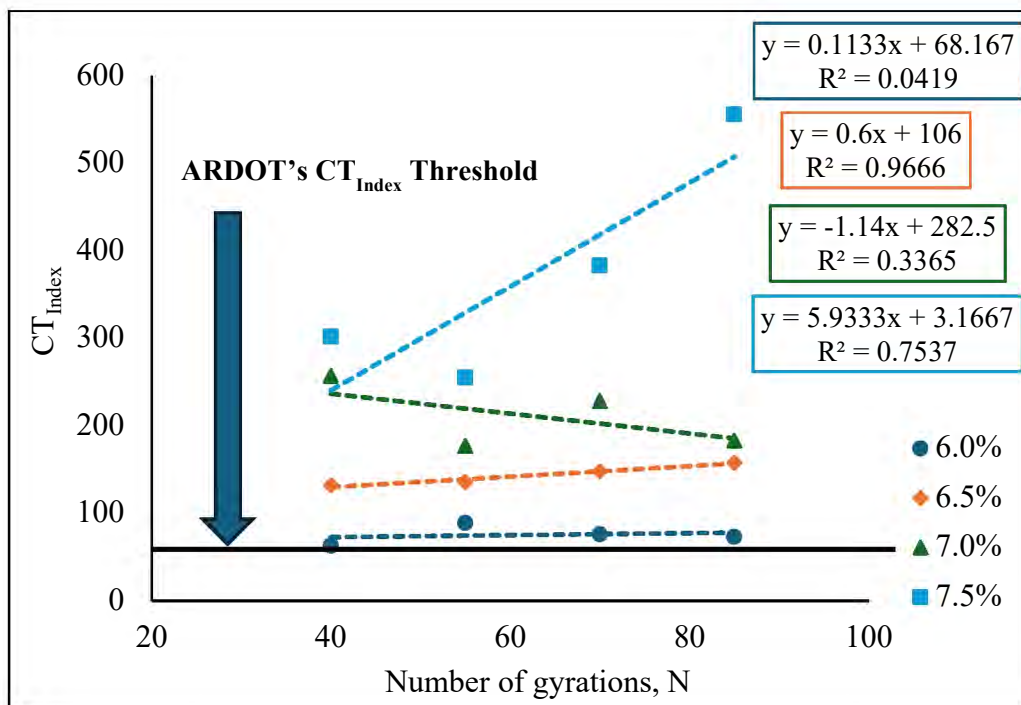
Figure 27. Relationship between CT$_{Index}$ and N

Figure 28 presents the relationship between APA rut depth and P$_b$. The results show that APA rut depth increases with higher binder content, suggesting that as binder content rises, the ACHM becomes more flexible, which is an expected outcome.
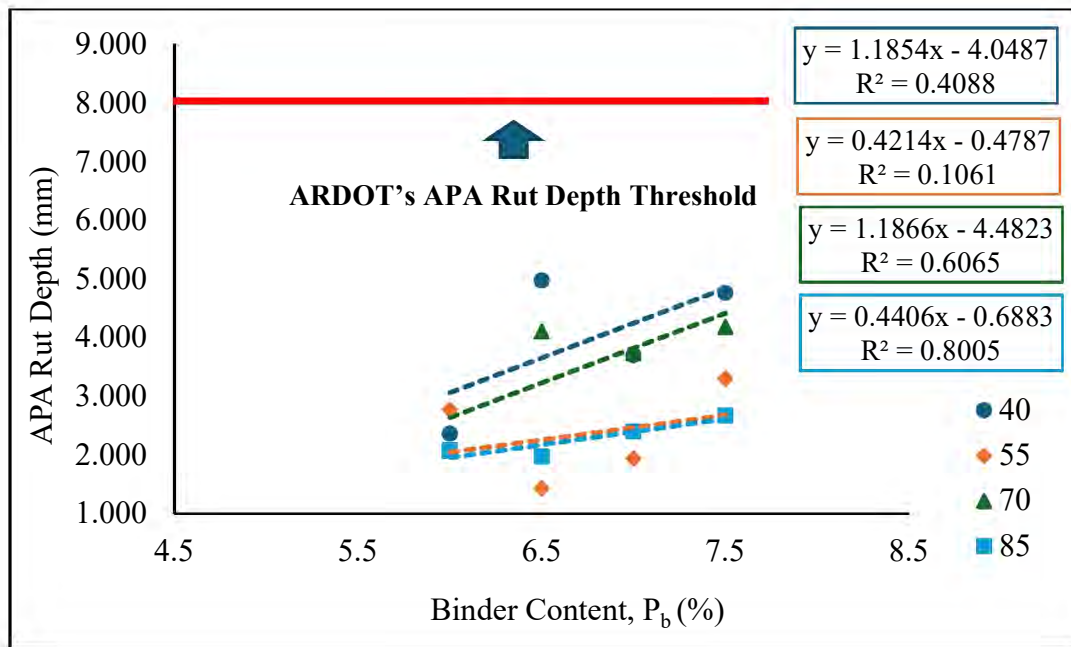
Figure 28. Relationship between APA rut depth and P$_b$

The relationship between APA rut depth and N is illustrated in **Figure *29***, showing an overall decreasing trend. This suggests that as the compaction level increases, the asphalt sample's stiffness improves, enhancing its resistance to rutting. Furthermore, it is noteworthy that the APA rut depth for all samples remains below the ARDOT-recommended maximum limit of 8.0 mm.
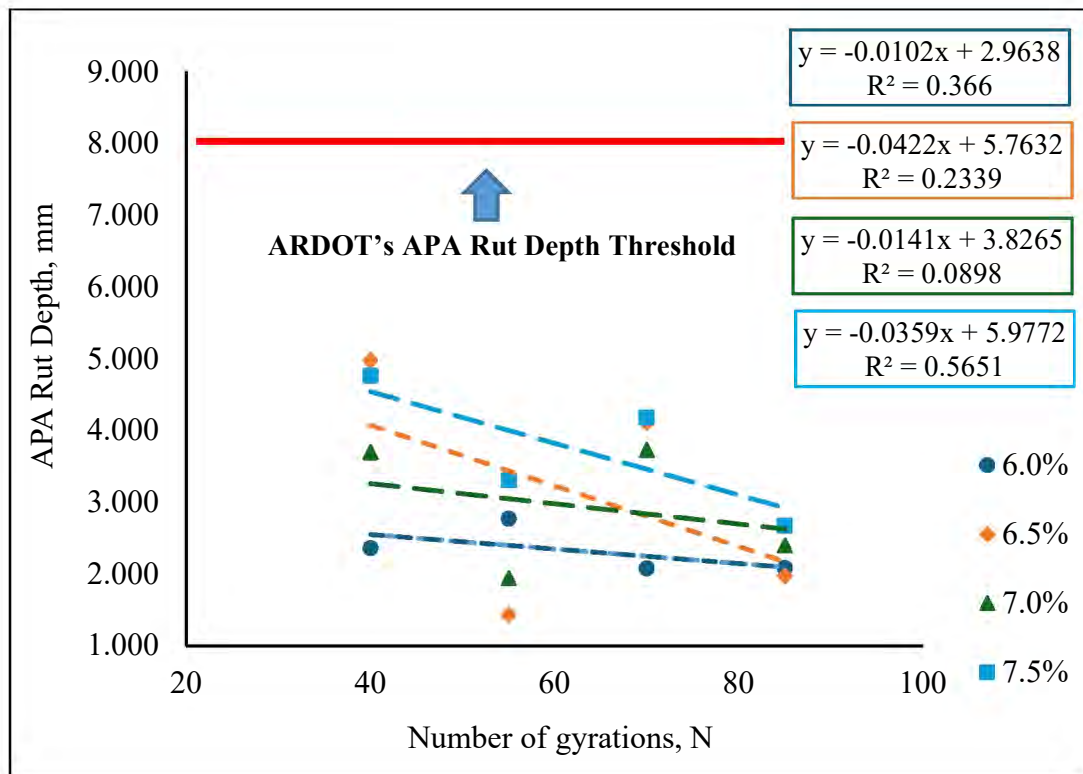
Figure 29. Relationship between APA rut depth and N

The findings from the IDEAL-CT and APA tests are depicted in **Figure 30**, with each data point representing the average CT_{Index} and APA rut depth for a given mix type. The data shows that all sixteen mixtures meet the cracking criteria, as their CT_{Index} values are above the recommended minimum threshold of 50. Similarly, rutting is not an issue, since all mixtures exhibit rut depths well below the maximum allowable limit of 8.0 mm. These results highlight that the overall performance of the fine-graded mixtures is largely influenced by their resistance to cracking.
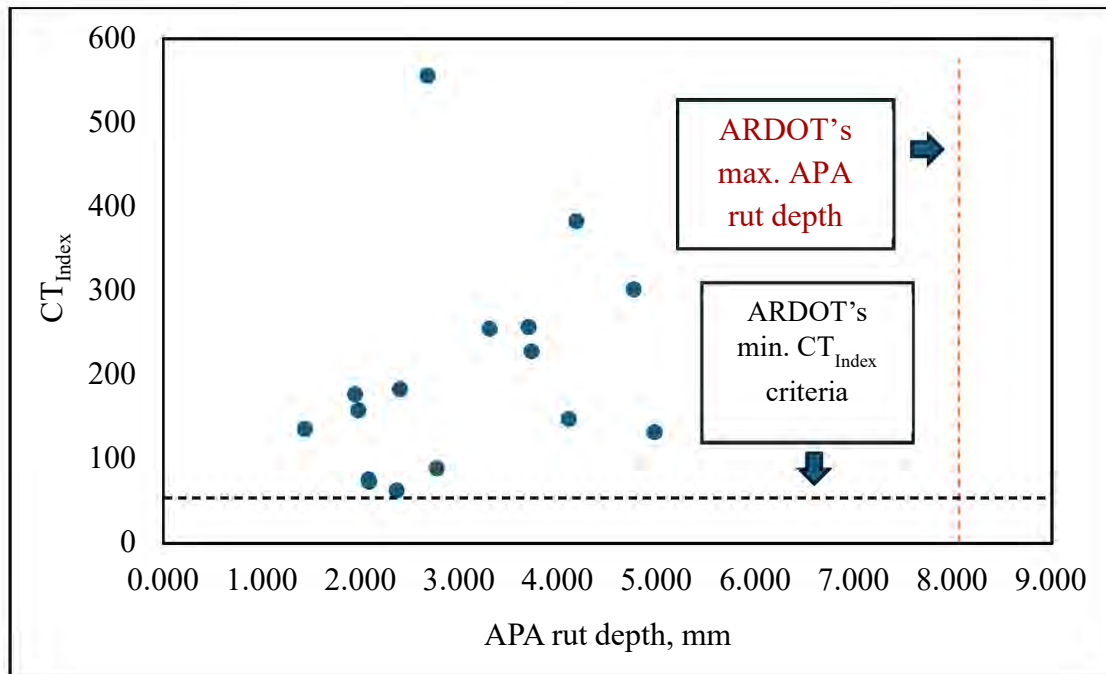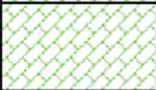
Figure 30. Summary of the performance test results

Based on CT_{Index} as the primary criterion, performance zones were identified and are illustrated in **Figure 31**. These zones are categorized as "Poor" (CT_{Index} less than 50), "Moderate" (CT_{Index} between 50 and 75), "Good" (CT_{Index} between 75 and 100), and "Excellent" (CT_{Index} above 100).

Figure 31 shows that ACHM mixtures located in zones with lower P_b combined with either lower N or higher N exhibit CT_{Index} values between 50 and 75, classifying them as having "Moderate" performance. In contrast, the zones labeled as "Excellent" are observed across a range of conditions, including both high and low P_b levels compacted at both high and low N, and are identified as the initial optimal performance zones.

Following the completion of the IDEAL-CT and APA tests, the HWTT and TSR tests were selected as additional performance evaluations to further validate or refine the identified zones. In the case of the coarse gradation, only those zones that achieved "Good" or "Excellent" ratings were considered for additional testing. For the current gradation, fourteen zones met this criterion. To streamline the selection process, zones representing both the outer edges and the central portion of the "Excellent" category were chosen for HWTT and TSR testing. This strategy aimed to evaluate whether zones at the extremes and the center

exhibited distinct performance trends, which in turn informed the selection of further test zones. From the twelve zones rated as "Excellent," six were ultimately selected for HWTT and TSR testing, as illustrated in **Figure 32**.

Performance Zones				
N / P_b	6.0%	6.5%	7.0%	7.5%
40				
55				
70				
85				

	Excellent (Avg. $CT_{Index} > 100$)
	Good ($75 < $ Avg. $CT_{Index} \leq 100$)
	Moderate ($50 < $ Avg. $CT_{Index} \leq 75$)
	Poor (Avg. $CT_{Index} \leq 50$)

Figure 31. Performance zones obtained in the study

N / P_b	6.0%	6.5%	7.0%	7.5%
40				
55				
70				
85				

Figure 32. Performance zones considered for HWTT and TSR testing in the study

Table 16 displays the HWTT results for the selected zones. As shown, the rut depths for all samples exceeded the 12.5 mm maximum threshold recommended by Texas and Oklahoma, reaching approximately 20 mm in most cases. This suggests that the asphalt mixtures exhibited

64

extremely poor resistance to moisture damage, worse than what was previously seen in the coarse-graded mix. No clear correlation was found between SIP passes or HWTT failure passes and compaction level. However, as binder content increased, both SIP passes and failure passes tended to decrease, indicating the mixtures became softer with higher binder content.

Table 16. Summary of the HWTT test results

HWTT rut depth (mm)				
N / P_b	6.0%	6.5%	7.0%	7.5%
40	-	20.4	-	20.1
55	-	-	20.0	-
70	-	-	20.0	-
85	-	19.3	-	20.0
SIP passes				
N / P_b	6.0%	6.5%	7.0%	7.5%
40	-	6171	-	6048
55	-	-	7748	-
70	-	-	7571	-
85	-	10679	-	4903
HWTT fail passes				
N / P_b	6.0%	6.5%	7.0%	7.5%
40	-	13227	-	8983
55	-	-	8491	-
70	-	-	10148	-
85	-	14950	-	7223

Table 17 shows the results from the moisture-induced damage testing. As with the coarse-graded mix, the saturation time for the conditioned samples was fixed at 20 minutes, and the reported degree of saturation corresponds to this set duration. This was particularly important given the very low air voids observed in the samples (again, a result of the Approach D to the BMD), which ranged from 1.0% to 5.1%, making it extremely difficult for water to

penetrate the specimens. Standardizing the saturation time helped conserve both time and resources. The TSR results were consistent with the HWTT findings, with almost all the samples falling below the recommended threshold of 0.80. This confirms that mixtures from zones initially deemed optimal based on IDEAL-CT and APA test results suffered considerable moisture damage, as evidenced by high HWTT rut depths and low TSR values. These findings are in line with those observed for the coarse-graded mix.

Table 17. Summary of the TSR test results

Degree of saturation (%)				
N / P_b	6.0%	6.5%	7.0%	7.5%
40	-	58	-	32
55	-	-	33	-
70	-	-	36	-
85	-	41	-	28
Moisture conditioned strength (kPa)				
N / P_b	6.0%	6.5%	7.0%	7.5%
40	-	704	-	488
55	-	-	799	-
70	-	-	930	-
85	-	940	-	563
TSR				
N / P_b	6.0%	6.5%	7.0%	7.5%
40	-	0.66	-	0.58
55	-	-	0.76	-
70	-	-	0.86	-
85	-	0.79	-	0.55

2.9 Fine Gradation (15% RAP)

This section presents a detailed analysis of the volumetric and performance test results for sixteen ACHM mixtures produced using a fine-graded aggregate blend containing 15% RAP. The mixtures varied based on two mix design parameters: P_b and N. The combined aggregate gradation used is detailed in **Table 18** and illustrated in **Figure 33**.

Using the aggregate and binder properties as inputs in **Equation 1**, the P_{bi} value was calculated. As shown in **Table 19**, the P_{bi} for the fine-graded mix containing 15% RAP was determined to be 6.6%. Based on this value, four binder content levels were selected: 6.1%, 6.6%, 7.1%, and 7.6%. The binder contribution from RAP was calculated to be 0.8%. Accordingly, the additional binder needed for each target binder content was 5.3%, 5.8%, 6.3%, and 6.8%, respectively. The G_{mm} values of the loose mixtures at each binder content were computed and are presented in **Figure 34**.

Table 18. Combined aggregate gradation

Sieve size (mm)	1	2	3	4	5	6	Job Mix	Control Points
50	100	100	100	100	100	100	**100**	100%
37.5	100	100	100	100	100	100	**100**	100%
25	100	100	100	100	100	100	**100**	100%
19	100	100	100	100	100	100	**100**	100%
12.5	68	100	100	100	100	100	**96**	90-100%
9.5	42	89	100	100	100	96	**90**	90% Max
4.75	4	29	97	100	93	75	**67**	
2.36	2	5	65	74	48	56	**43**	28-58%
1.18	1	5	41	53	19	43	**29**	
0.6	1	5	26	40	9	35	**22**	
0.3	1	5	16	31	6	27	**16**	
0.15	1	4	9	23	5	18	**12**	
0.075	1.0	3.6	4.1	16.2	4.5	12.4	**8.1**	2-10%
Cold feed%	**11**	**25**	**15**	**26**	**8**	**15**		
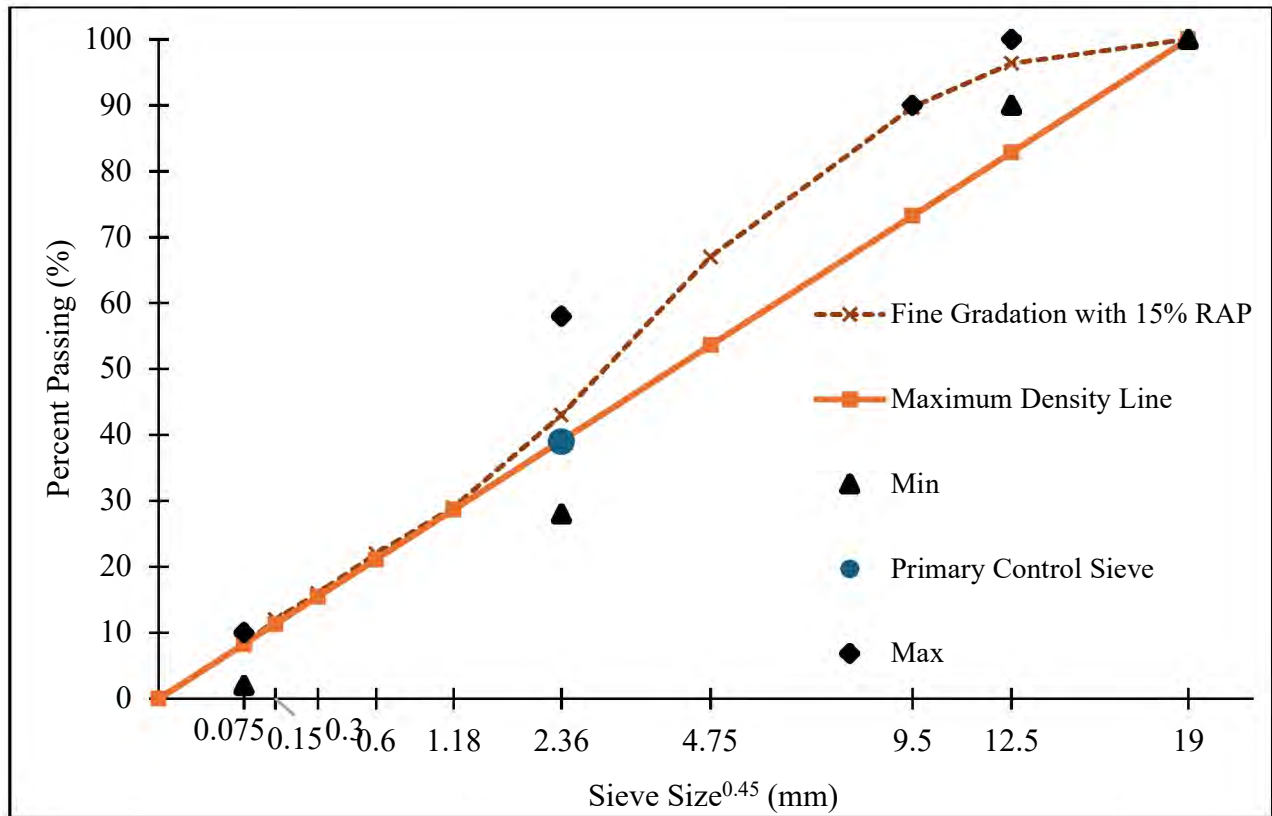
Figure 33. Combined aggregate gradation

Table 19. Estimation of P_{bi}

Bulk specific gravity for the combined aggregate, G_{sb}	2.464
Apparent specific gravity for the combined aggregate, G_{sa}	2.642
Effective specific gravity for the combined aggregate, G_{se}	2.606
Mass of aggregate in 1 cm^3 of mix, W_s, g	2.207
Volume of binder absorbed into the aggregate, V_{ba}, cm^3	0.049
Volume of effective binder, V_{be}, cm^3	0.102
Estimated initial trial binder content, P_{bi}, % by weight of total mix	**6.6**

* Reference: AASHTO R 35 (Appendix X)
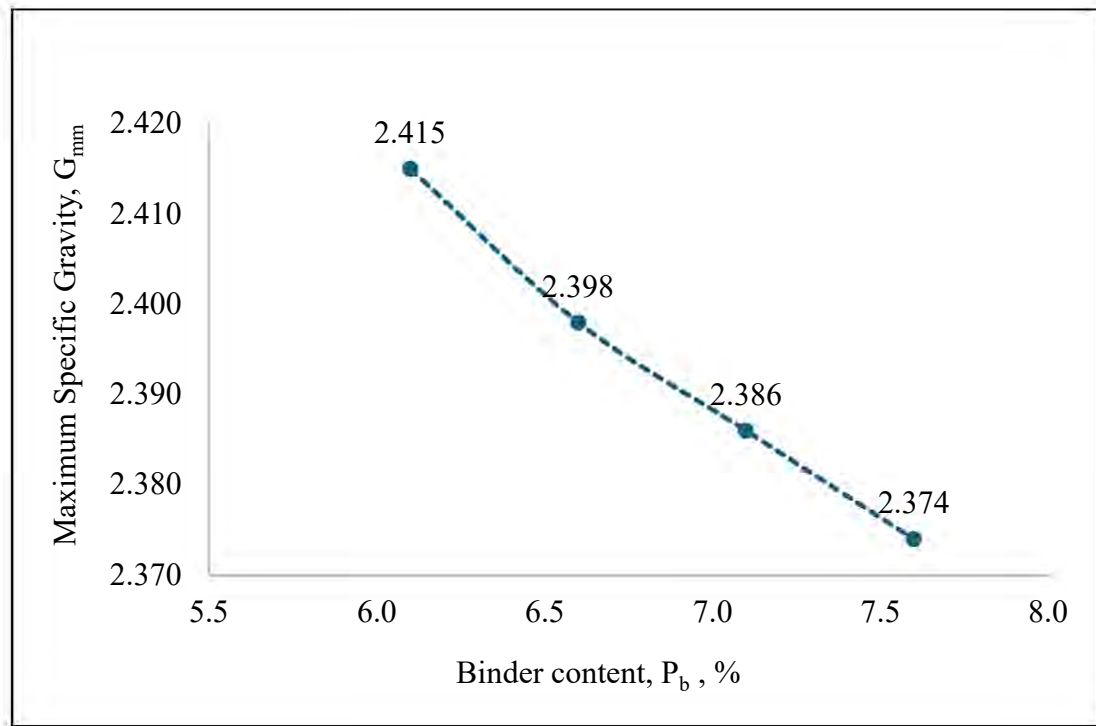
Figure 34. Relationship between G_{mm} and P_b

The same procedures described in the previous section were followed to prepare G_{mb} samples for all sixteen mix combinations. Afterward, the volumetric properties — V_a, VMA, and VFA — were determined.

Figure 35 and **Figure 36** depict the relationship between Va and Pb, and Va and N, respectively. In **Figure 35**, V_a is shown to decrease as P_b increases, which is anticipated since a higher binder content fills more of the voids between aggregate particles. Similarly, **Figure 36** demonstrates that V_a decreases with increasing N, as greater compaction effort results in a more tightly packed mixture, thereby lowering the air void content.

Table 20 presents the V_a, VMA, and VFA values for sixteen mixtures, each averaged from three readings. According to AASHTO M 323 (11), a 12.5 NMAS ACHM with V_a of 4.0% should ideally have a minimum VMA of 14.0% and a VFA ranging from 71.0% to 75.0%. However, in this study, these recommended VMA and VFA criteria do not apply because the mixtures have V_a ranging from 1.5% to 6.1%. It is important to note that, although we report on the VMA and VFA values, our primary focus is on evaluating the performance of the mixtures.

69

$y = -2.5736x + 20.809$
$R^2 = 0.6981$

$y = -1.9245x + 15.822$
$R^2 = 0.7342$

$y = -1.0219x + 8.974$
$R^2 = 0.7725$

$y = -0.6776x + 6.7008$
$R^2 = 0.9467$

40
55
70
85
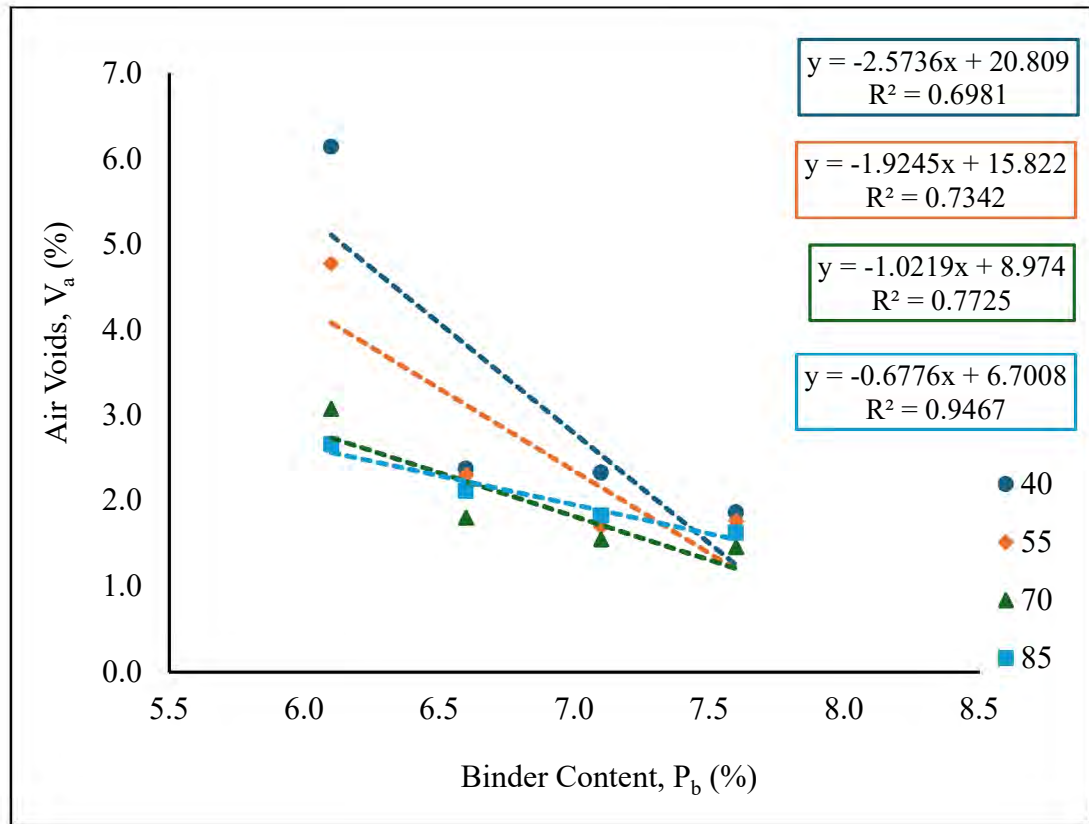
Figure 35. Relationship between V_a and P_b

$y = -0.0809x + 9.2202$
$R^2 = 0.9537$

$y = -0.0086x + 2.6897$
$R^2 = 0.4279$

$y = -0.0111x + 2.5473$
$R^2 = 0.4012$

$y = -0.0068x + 2.1085$
$R^2 = 0.5589$

6.1%
6.6%
7.1%
7.6%
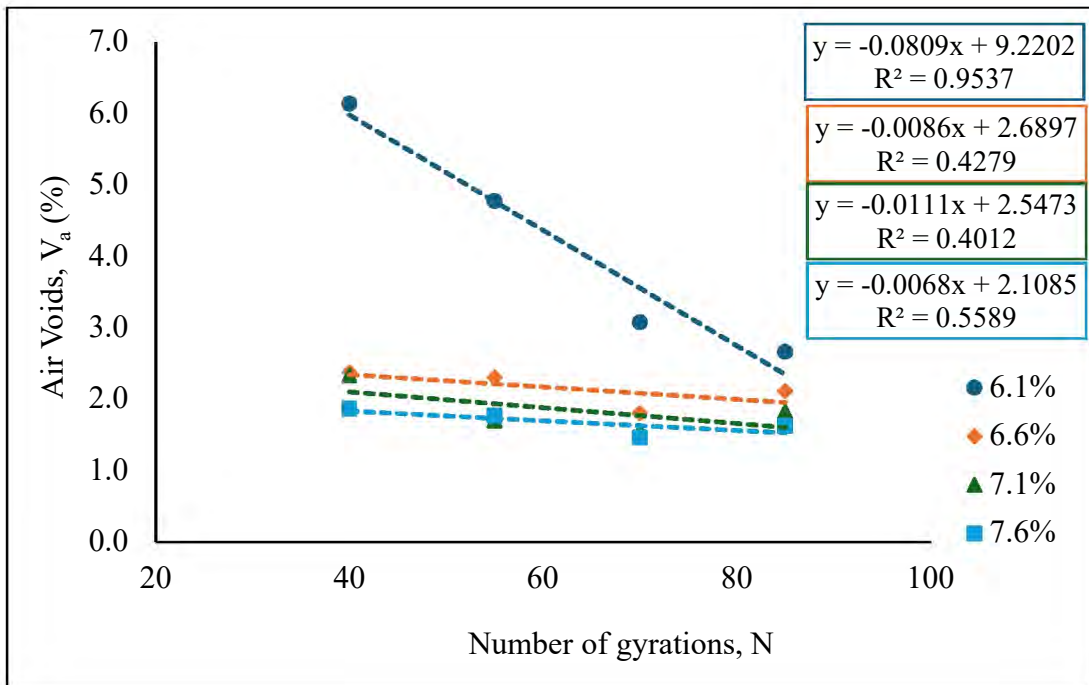
Figure 36. Relationship between V_a and N

70

Table 20. V_a, VMA, and VFA values

Air Voids, V_a, %				
N/ P_b	6.1%	6.6%	7.1%	7.6%
40	6.1	2.4	2.3	1.9
55	4.8	2.3	1.7	1.8
70	3.1	1.8	1.6	1.5
85	2.7	2.1	1.8	1.6
Voids in Mineral Aggregates, VMA, %				
N/ P_b	6.1%	6.6%	7.1%	7.6%
40	14.6	12.3	13.2	13.7
55	13.4	12.2	12.6	13.6
70	11.8	11.8	12.5	13.3
85	11.5	12.1	12.7	13.5
Voids Filled with Asphalt, VFA, %				
N/ P_b	6.1%	6.6%	7.1%	7.6%
40	58.2	80.7	82.3	86.4
55	64.5	81.2	86.6	87.0
70	74.1	84.7	87.6	89.0
85	76.9	82.5	85.6	87.9

2.9.1 Performance testing

The performance test samples for each P_b and N were compacted according to the V_a results detailed in the previous section. The sample thickness and air void tolerance adhered to the specifications outlined in the respective test standards.

The optimal performance zone was identified using the IDEAL-CT and APA tests. **Table 21** presents the results obtained from the two performance tests for the sixteen mix combinations. The CT_{Index} value ranged from 71 to 357, and the APA rut depth was reported to be between 1.841 mm and 6.247 mm, respectively.

Figure 37 depicts the relationship between CT_{Index} and P_b, revealing an increasing trend as P_b increases. This pattern aligns with both coarse gradation and fine gradation with 0% RAP, as well as previous findings, that suggest the binder acts as a lubricant, enhancing mix ductility

and cracking resistance. **Figure 38** illustrates the relationship between CT_{Index} and N, showing no clear or consistent trends.

Table 21. Summary of the performance test results

CT_{Index}				
N/ P_b	**6.1%**	**6.6%**	**7.1%**	**7.6%**
40	177	167	217	294
55	81	171	207	261
70	86	137	254	357
85	71	140	199	297
APA Rut Depth, mm				
N/ P_b	**6.1%**	**6.6%**	**7.1%**	**7.6%**
40	2.228	2.484	3.289	6.247
55	1.841	3.265	3.040	3.660
70	1.868	3.080	4.661	5.076
85	2.321	2.417	2.143	4.688
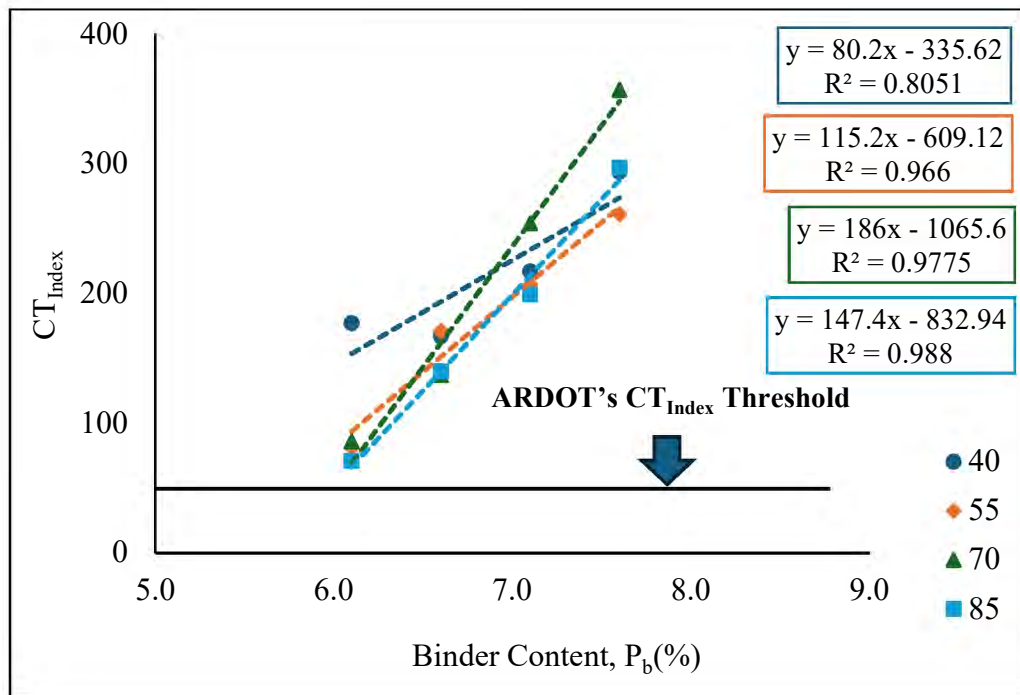
Figure 37. Relationship between CT$_{Index}$ and P$_b$
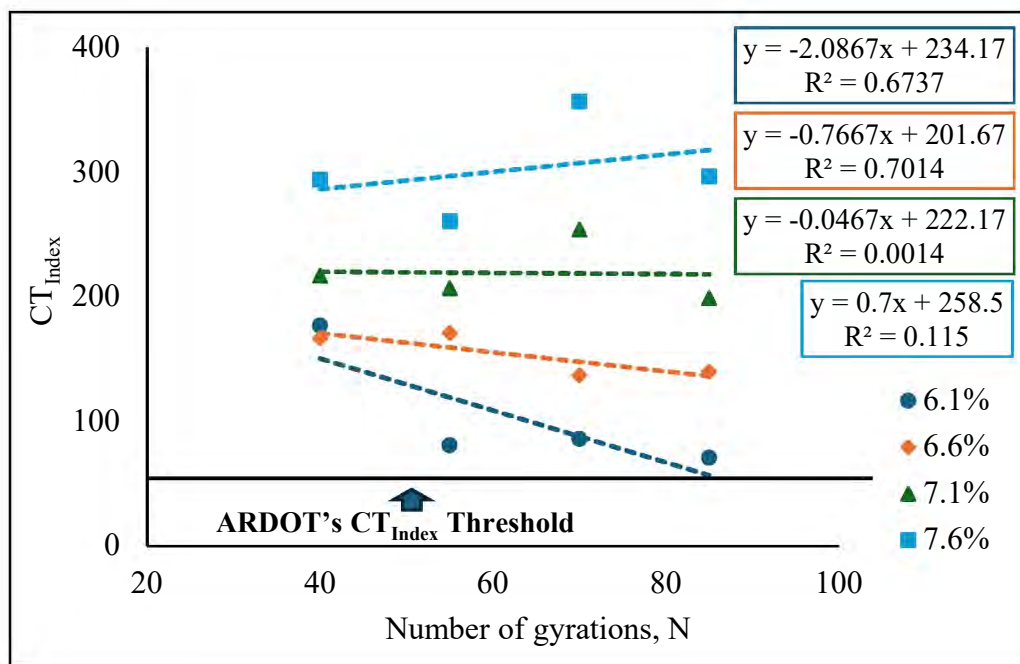
Figure 38. Relationship between CT$_{Index}$ and N

Figure 39 presents the relationship between APA rut depth and P$_b$, showing that rut depth increases with higher binder content. This fundamental trend occurs because increased binder content enhances mixture flexibility, making it more susceptible to rutting.

The chart contains the following trend line equations:
$y = 2.5724x - 14.059$, $R^2 = 0.8089$
$y = 1.0464x - 4.2163$, $R^2 = 0.7433$
$y = 2.241x - 11.68$, $R^2 = 0.9578$
$y = 1.3654x - 6.4607$, $R^2 = 0.5372$

Legend: 40, 55, 70, 85

Axis labels: APA Rut Depth (mm) vs Binder Content, P_b (%)

ARDOT's APA Rut Depth Threshold
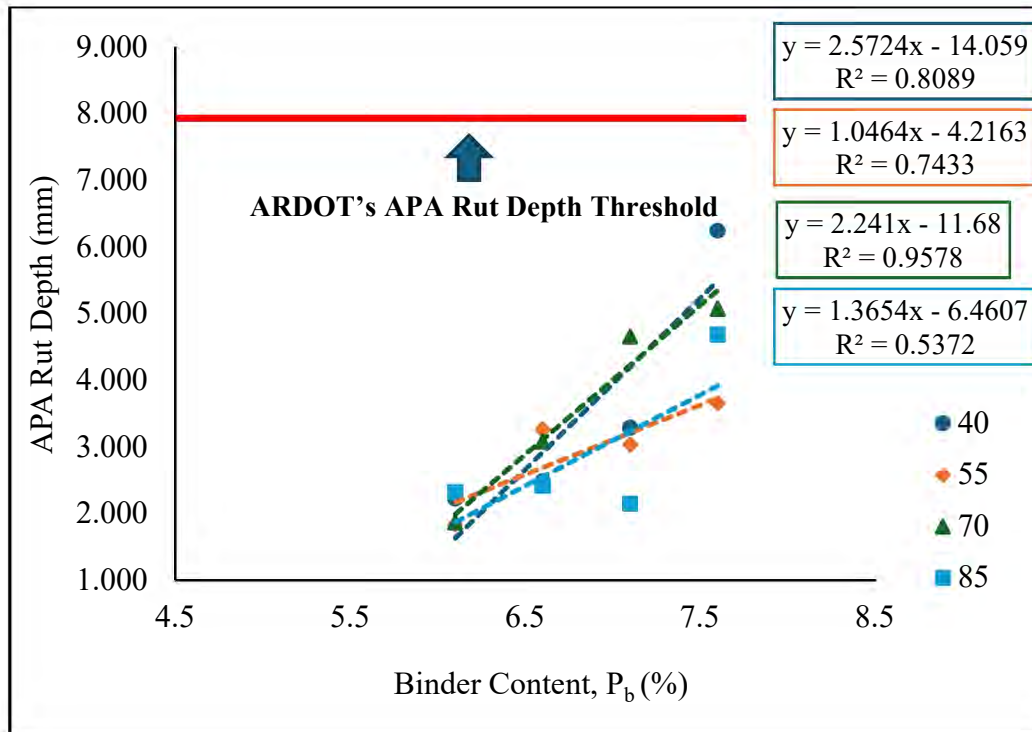
Figure 39. Relationship between APA rut depth and P_b

Figure 40 illustrates the relationship between APA rut depth and N, revealing a decreasing trend. This suggests that as compaction levels increase, the asphalt sample's stiffness improves, enhancing its resistance to rutting. Furthermore, it is important to note that for all samples, the APA rut depth remains below the recommended ARDOT maximum limit of 8.0 mm.

Figure 41 presents the results from the IDEAL-CT and APA tests, where each data point reflects the average CT_{Index} and APA rut depth for a specific mix type. Importantly, all sixteen mixtures meet the cracking criteria, with CT_{Index} values surpassing the recommended minimum of 50. Rutting is also not an issue, as all rut depths remain below the maximum allowable limit of 8.0 mm. These findings highlight that, for the fine-graded mix containing 15% RAP, cracking resistance is the key factor governing overall mixture performance.
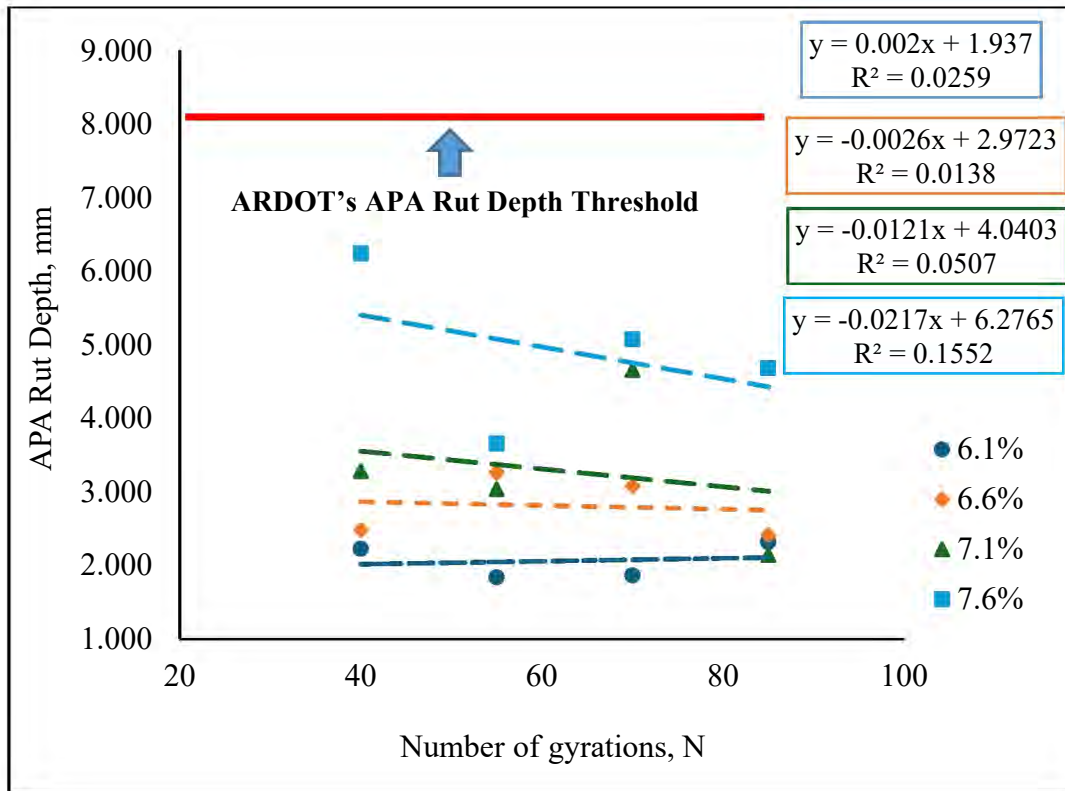
Figure 40. Relationship between APA rut depth and N
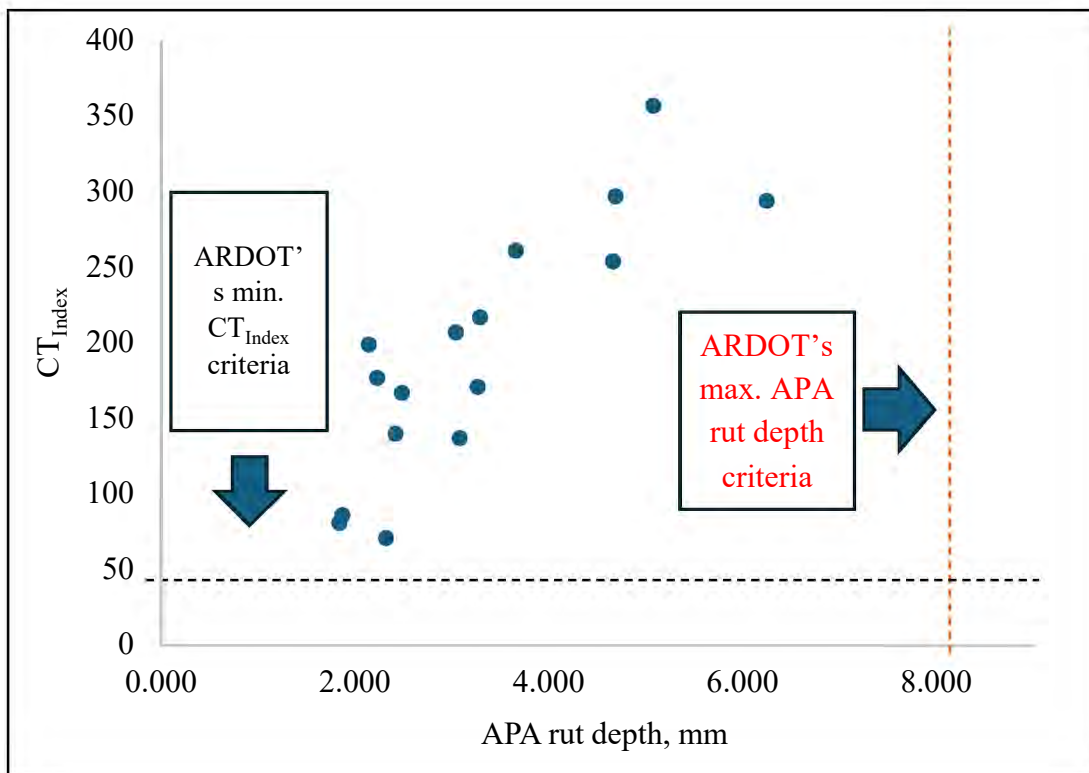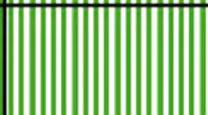
Figure 41. Summary of the performance test results

Based on CT_{Index} as the primary criterion, performance zones were identified and are illustrated in **Figure 42**. These zones are categorized as "Poor" (CT_{Index} less than 50), "Moderate" (CT_{Index} between 50 and 75), "Good" (CT_{Index} between 75 and 100), and "Excellent" (CT_{Index} above 100).

Figure 42 illustrates that ACHM in the zone with lower P_b, and higher N have a CT_{Index} less than 75 but more than 50, categorizing them as "Moderate" in terms of performance. Zones with lower P_b, and medium N have a CT_{Index} less than 100 but more than 75, classifying them as "Good" in terms of performance. However, the zones designated as "Excellent" are found in regions with both higher and lower P_b, compacted to both higher and lower N, and are considered the initial optimal performance zones.

Figure 42. Performance zones obtained in the study

Following the IDEAL-CT and APA tests, the HWTT and TSR tests were selected as additional evaluations to further validate or refine the identified zones. Six of the thirteen zones that exhibited "Excellent" performance were chosen for HWTT and TSR testing, as shown in **Figure 43**. This selection was guided by the same criteria used for fine gradation with 0% RAP.

N / P_b	6.1%	6.6%	7.1%	7.6%
40		🟩		🟩
55			🟩	
70			🟩	
85		🟩		🟩

Figure 43. Performance zones considered for HWTT and TSR testing

Table 22 summarizes the HWTT results for the selected zones. The data show that rut depths for all samples exceeded the 12.5 mm limit set by Texas and Oklahoma, with most values approaching 20 mm. This indicates very poor moisture damage resistance in the asphalt mixtures, worse than what was seen in the coarse-graded mix and comparable to the fine-graded mix without RAP. Furthermore, an increase in compaction effort was associated with a reduction in both SIP passes and HWTT failure passes, implying the development of stiffer mixtures. In contrast, increasing binder content led to a decrease in these passes, indicating that the mixtures became softer and more flexible.

Table 22. Summary of the HWTT test results

HWTT rut depth (mm)

N / P_b	6.1%	6.6%	7.1%	7.6%
40	-	17.3	-	20.0
55	-	-	20.0	-
70	-	-	14.8	-
85	-	20.1	-	20.1

SIP passes

N / P_b	6.1%	6.6%	7.1%	7.6%
40	-	14925	-	10855
55	-	-	10356	-
70	-	-	13187	-
85	-	7848	-	7215

HWTT fail passes

N / P_b	6.1%	6.6%	7.1%	7.6%
40	-	17686	-	13977
55	-	-	14261	-
70	-	-	17309	-
85	-	12303	-	9111

Table 23 presents the results from the moisture-induced damage testing. Similar to the coarse-graded and fine-graded mixes without RAP, the saturation time for the conditioned samples was set at 20 minutes, and the reported degree of saturation reflects this fixed duration. This was especially necessary due to the low air voids in the samples, which ranged from 1.5% to 6.1% (again, a result of the Approach D to the BMD), making water infiltration difficult. Except for the mixtures compacted at the lowest gyration level (N = 40), the TSR results did not correspond with the findings from the HWTT, as TSR values remained above the recommended 0.80 threshold. These patterns differ from those observed in the other two gradation types.

Table 23. Summary of the TSR test results

% Saturation				
N / P_b	**6.1%**	**6.6%**	**7.1%**	**7.6%**
40	-	34	-	28
55	-	-	24	-
70	-	-	17	-
85	-	40	-	28
Moisture conditioned strength (kPa)				
N / P_b	**6.1%**	**6.6%**	**7.1%**	**7.6%**
40	-	994	-	781
55	-	-	962	-
70	-	-	963	-
85	-	986	-	768
TSR				
N / P_b	**6.1%**	**6.6%**	**7.1%**	**7.6%**
40	-	0.75	-	0.69
55	-	-	0.90	-
70	-	-	0.89	-
85	-	0.89	-	0.97

2.10   Limitations of the Study

This study aimed to evaluate extreme rutting and cracking conditions in coarse-graded, fine-graded (0% RAP), and fine-graded (15% RAP) ACHM by simultaneously adjusting P_b and N. The main goal was to produce a broad range of CT_{Index} values and APA rut depths while keeping the aggregate structure constant. However, as shown in **Table 8** for the coarse gradation, the air voids ranged from 5.0% to 11.6%, well above the recommended range of 3.5% to 4.5%, indicating an overly coarse aggregate blend. An analysis of the combined gradation also revealed a deficiency in fine aggregates within the ACHM.

For the fine gradation with 0% RAP (**Table 14**) and 15% RAP (**Table 20**), the air voids ranged from 1.0% to 5.1% and 1.5% to 6.1%, respectively—values that fall outside the recommended range. These lower air voids can be attributed to a higher proportion of fine particles or binder content in both gradations. Overall, none of the three gradation types consistently achieved the target air void range across the full spectrum of binder contents and compaction levels.

The performance test results and the optimal zones identified in this study could shift with changes in aggregate gradation. Designing ACHM to consistently meet the recommended air void range could also help clarify the influence of APA rut depth on identifying optimal performance zones. In such cases, both IDEAL-CT and APA tests would contribute to a more comprehensive assessment of mixture performance.

2.11 Optimal Performance Zone

In this study, the initial optimal performance zones for all three gradations were determined using results from the IDEAL-CT and APA tests. To validate these zones, additional testing was conducted using the HWTT and TSR methods. However, for all three gradations, the mixtures initially identified as optimal exhibited poor moisture resistance, as indicated by high HWTT rut depths and low TSR values. Consequently, the final determination of optimal performance zones was based solely on the IDEAL-CT and APA test outcomes, with particular emphasis on the CT_{Index} from the IDEAL-CT test, as cracking was identified as the primary distress mechanism affecting mixture performance across all gradations.

For each gradation, mixtures with lower P_b and higher N levels generally showed "Poor" to "Moderate" cracking performance. In contrast, zones with moderate to high P_b, regardless of compaction level, consistently fell within the "Excellent" category, demonstrating strong resistance to cracking. From an economic standpoint, ACHM mixtures with both high P_b and high N are the least favorable due to elevated material and production costs, while those with lower P_b and N are the most cost-effective. However, these lower-cost mixes may compromise

long-term durability due to higher air voids. Therefore, mixtures with higher P_b and lower N are considered the most advantageous for achieving durable, long-term pavement performance.

2.12   Conclusions

The shortcomings of the Superpave method in producing durable ACHM led to several adjustments in the mix design procedure. These changes included lowering the N_{design} levels, reducing the minimum VMA requirements, and decreasing the V_a to increase the binder content in the mix. A significant amount of work has also been done towards implementing the concept of BMD for producing ACHM, performing well in terms of both rutting and cracking. The state of Arkansas is also working towards implementing BMD based on the findings from the research project TRC 1802.

For one portion of this study, the combined effects of varying P_b and N on the performance were explored for three ACHM types: coarse-graded, fine-graded with 0% RAP, and fine-graded with 15% RAP. A fully performance-based BMD Approach D was employed to identify the optimal performance zone. Four binder content levels (-0.5% P_{bi}, P_{bi}, +0.5% P_{bi}, and +1.0% P_{bi}) and four compaction levels (40, 55, 70, and 85 gyrations) were selected for each aggregate blend, resulting in a total of 48 mixtures. The performance of these mixtures was assessed using ARDOT's preferred tests, APA and IDEAL-CT, followed by supplementary evaluations with HWTT and TSR tests. The conclusions drawn from the study are as follows:

- Air voids were found to decrease as P_b and N levels increased. The highest V_a was observed at the lowest P_b and lowest N levels, while the lowest V_a occurred at the highest P_b and highest N levels. However, some exceptions were noted in both fine gradations with 0% RAP and with 15% RAP.

- The CT_{Index} increased with rising P_b levels across all three gradations. However, in the coarse gradation, an inverse relationship was observed between CT_{Index} and N. For both the fine gradations with 0% RAP and 15% RAP, no consistent trend was identified between CT_{Index} and N.

- The study did not reveal a clear relationship between P_b and APA rut depth for the coarse gradation. However, a consistent increase in rut depth was observed with an

increase in binder content in fine gradations with 0% RAP and 15% RAP. Additionally, APA rut depth consistently decreased with increasing N across all three gradations.

- Rutting did not pose any concern as all the mixtures exhibited APA rut depths below the recommended ARDOT maximum value of 8.0 mm. Based on this result, CT_{Index} was considered as the primary criterion affecting the overall ACHM performance in the current study.

- Five out of the sixteen ACHM in the coarse gradation failed in cracking, with a CT_{Index} below the ARDOT-recommended value of 50. In contrast, most zones in the other two gradations exhibited "Moderate" to "Excellent" performance, with CT_{Index} values ranging from 63 to 556 in fine gradation with 0% RAP and 71 to 357 in fine gradation with 15% RAP. It is possible, however, that the increased cost of adding the additional asphalt binder may outweigh the net crack resistance achieved. However, more research would need to be done to verify this cost-performance tradeoff.

- When mixtures from the initially identified optimal performance zones were evaluated for moisture susceptibility using HWTT and TSR tests, they exhibited significant moisture-related distress, evidenced by high rut depths and low TSR values. These findings underscore the importance of incorporating an ASA in the binder, as the binder used in this study did not contain any ASA.

- The outcomes also emphasize the need for supplementary testing to validate the results obtained from standard performance tests used by state agencies. As demonstrated in this study, mixtures that performed well in IDEAL-CT and APA tests still showed poor resistance to moisture damage.

- The final selection of optimal performance zones took economic factors into account. From a cost perspective, ACHM mixtures with both high P_b and high N are the least desirable due to increased material and production costs. Conversely, mixtures with lower P_b and N offer the most cost-effective option but may suffer from durability issues due to higher air voids. As a result, mixtures with higher P_b and lower N are considered the most suitable for ensuring long-term pavement durability and performance.

Chapter 3. BMD Field Projects

For this study, eight field projects were chosen, and performance tests were conducted on asphalt samples prepared using three different techniques: lab-mix lab-compacted (LMLC), plant-mix lab-compacted (PMLC), and reheated plant-mix lab-compacted (RPMLC).

For the LMLC samples, aggregates and binder were obtained from the plant, with both mixing and compaction carried out in the asphalt laboratory at the University of Arkansas (UARK). In contrast, the PMLC and RPMLC samples were produced using materials mixed at the plant, with loose mix samples collected directly from the truck. The PMLC samples were then compacted at the ARDOT laboratory at the plant. Meanwhile, the RPMLC samples were stored in metal buckets and allowed to cool to ambient temperature before being reheated and compacted at the UARK asphalt laboratory. A detailed illustration of the sample preparation process for each technique is provided in **Figure 44**.
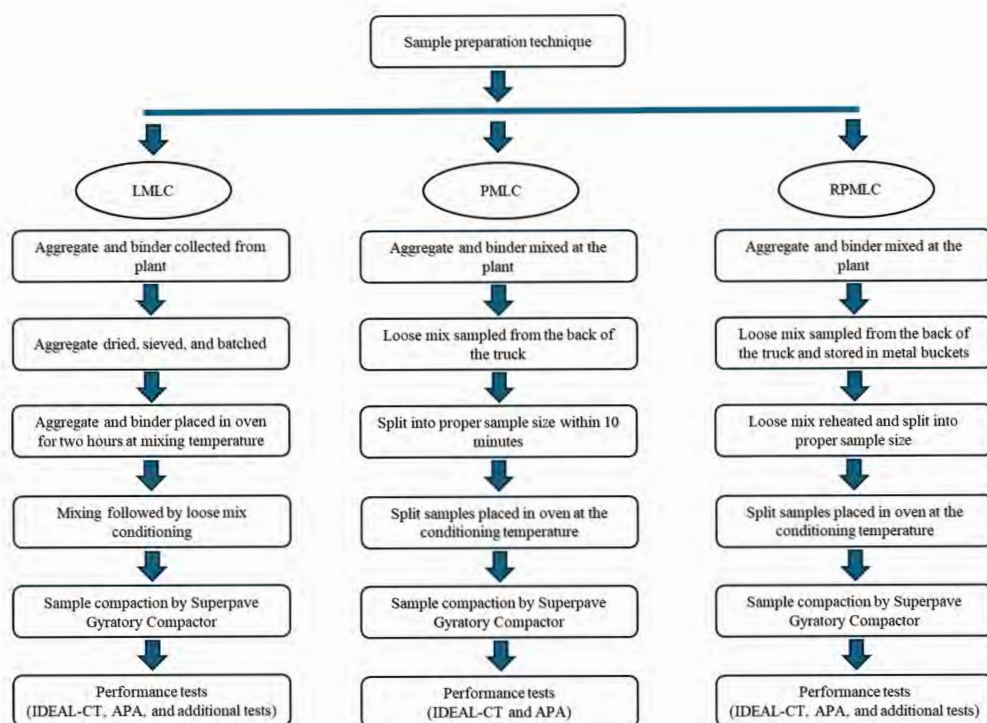
Figure 44. Flow chart for the different sample preparation techniques

3.1 Loose Mix Handling and Conditioning Protocol

This study assesses the effectiveness of BMD field projects approved by ARDOT in 2023 and 2024. The following loose mix conditioning protocol was applied in 2023:

For LMLC samples: In accordance with the previous version of AASHTO R 30 (43), both modified and unmodified binders were conditioned by spreading the loose mix evenly in a pan to a thickness of 1 to 2 inches. The mixture underwent short-term aging at a temperature of 275±5℉ for 4 hours ± 5 minutes. To ensure uniform conditioning, the mix was stirred at intervals of 60 ± 5 minutes. However, for the 2023 BMD projects, ARDOT followed the short-term aging protocol specified in the *Manual of Field Sampling and Testing Procedures* (40) during the mix design phase. Instead of aging the loose mix for 4 hours at 275°F, LMLC samples were conditioned for 2 hours at the compaction temperature.

For PMLC samples: Loose mix samples were collected from the back of the truck, after which volumetric tests were conducted to determine air voids. The mix was then divided into appropriately sized portions for IDEAL-CT and APA testing. Each portion was placed in a pan and heated in an oven set to the binder's compaction temperature. First, three IDEAL-CT sample splits were placed in the oven, followed by four APA sample splits. The three IDEAL-CT samples were compacted in the order they were placed in the oven, immediately after the APA samples were introduced. Once the IDEAL-CT samples were compacted, the APA samples were also compacted without delay.

For RPMLC samples: The conditioning procedure for RPMLC remained consistent across different asphalt binder types. Loose mix material was transferred from metal buckets to large trays and conditioned in an oven at the binder's compaction temperature for two hours. It was then portioned into required sample sizes using the quartering method, following AASHTO R 47 (39). The split samples were returned to the oven at the same compaction temperature for an additional two hours before compaction.

In 2024, ARDOT revised the short-term aging protocol to align with the latest AASHTO R 30 (41) specifications. Under this updated procedure, the following conditioning protocol was adopted for BMD field projects approved in 2024:

For LMLC samples: For unmodified binders, the loose mix is spread in a pan with a uniform thickness of 1 to 2 inches and subjected to short-term aging at 116 ± 3°C for warm-mix asphalt (WMA) or 135 ± 3°C for hot-mix asphalt (HMA) for 2 hours ± 5 minutes. The mixture is stirred after one hour. For polymer-modified binders, the same process is applied, except the oven temperature is set to the binder's compaction temperature for short-term aging.

The conditioning procedures for PMLC and RPMLC samples remain unchanged in 2024, following the same protocols as in 2023. Additionally, ARDOT increased the required number of IDEAL-CT replicates for BMD projects approved in 2024 from three to five.

Further details on the eight field projects are provided in **Table 24**, while their respective locations are illustrated in **Figure 45**.

Table 24. BMD field projects approved by ARDOT

Contractor Name	Project Number	Mix Design Number	Approved Year	Designated Number
Delta Asphalt	A00039	BHMA048-23	2023	AR01
Pine Bluff Sand & Gravel	A20022	BHMA262-23	2023	AR02
Rogers Group	A80021	BHMA272-23	2023	AR03
Atlas Asphalt	A90021	BHMA271-23	2023	AR04
Rogers Group	A60043	BHMA033-24	2024	AR05
Rogers Group	A80031	BHMA129-24	2024	AR06
APAC Central	09602	BHMA391-24	2024	AR07
Blackstone	A80031	BWMA476-24	2024	AR08

The selected projects cover diverse geographical regions across the state of Arkansas. **Table 25** and

Table *26* present mix design details, including nominal maximum aggregate size (NMAS), aggregate type, RAP percentage, total asphalt binder content (P_b), virgin asphalt binder content (P_{bv}), air voids (V_a), voids in mineral aggregates (VMA), and voids filled with asphalt (VFA), among other parameters. **Figure 46** and **Figure 47** illustrate the aggregate gradation for the various mixtures used in these field projects.
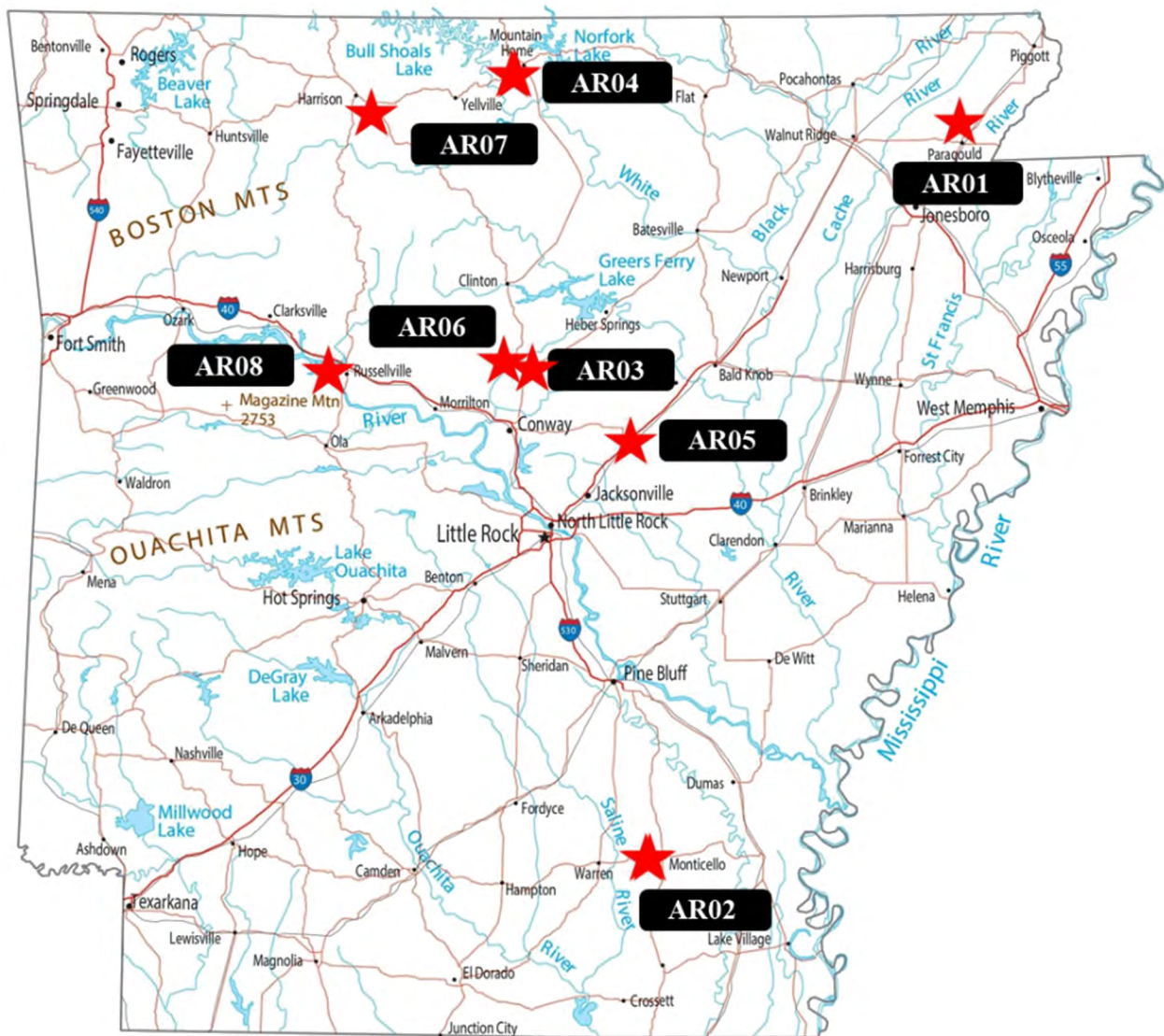
Figure 45. Location of BMD field projects

For all BMD projects, the NMAS is 12.5 mm, except for AR03, which has an NMAS of 9.5 mm. The maximum density line for the 12.5 mm NMAS is also depicted in **Figure 46** and **Figure 47**. The gradation of all projects intersects the maximum density line between 2.36 mm and 4.75 mm, except for AR02, which crosses it at the 0.3 mm size, and AR06, which intersects it between 4.75 mm and 9.5 mm.

Table 25. Mix design information for the BMD projects in 2023

Project/Properties	AR01	AR02	AR03	AR04
NMAS (mm)	12.5	12.5	9.5	12.5
Aggregate Type	Dolostone (50%) & Chert (25%)	Syenite (70%) & Sandstone (15%)	Sandstone (77%)	Sandstone (29%) & Dolostone (57%)
RAP (%)	25	15	20	14
P_b (%)	5.7	5.8	6.4	5.7
P_{bv} (%)	4.7	5.1	4.5	5
V_a (%)	4	3.5	3.3	3.5
VMA (%)	15.4	16	16.8	15.5
VFA (%)	77.4	77.9	80.4	78.2
Binder Grade	PG 64-22	PG 70-22	PG 67-22	PG 64-22
Mixing Temp (℉)	315	330	320	325
Compaction Temp (℉)	290	300	300	295

Table 26. Mix design information for the BMD projects in 2024

Project/Properties	AR05	AR06	AR07	AR08
NMAS (mm)	12.5	12.5	12.5	12.5
Aggregate Type	Sandstone (80%)	Sandstone (68%) & Limestone (12%)	Limestone (63%) & Sandstone (37%)	Limestone (55%) & Sandstone (31%)
RAP (%)	20	20	0	14
P_b (%)	6.4	6	5.7	6.1
P_{bv} (%)	5.3	4.9	5.7	5.4
V_a (%)	3.1	3	3	3

Project/Properties	AR05	AR06	AR07	AR08
VMA (%)	n/a	n/a	n/a	n/a
VFA (%)	n/a	n/a	n/a	n/a
Binder Grade	PG 70-22	PG 70-22	PG 64-22	PG 70-22
Mixing Temp (℉)	325	325	325	325
Compaction Temp (℉)	300	300	300	260
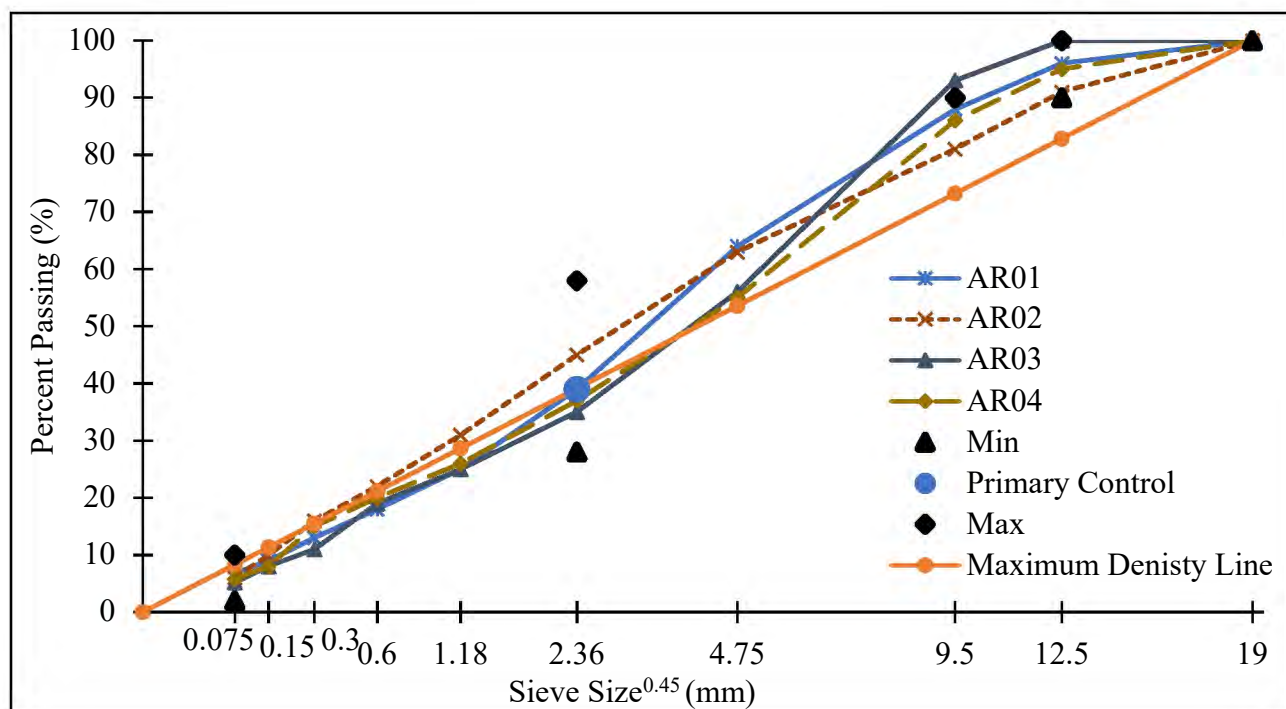
Figure 46. Gradation information for mixtures used in the BMD field projects in year 2023
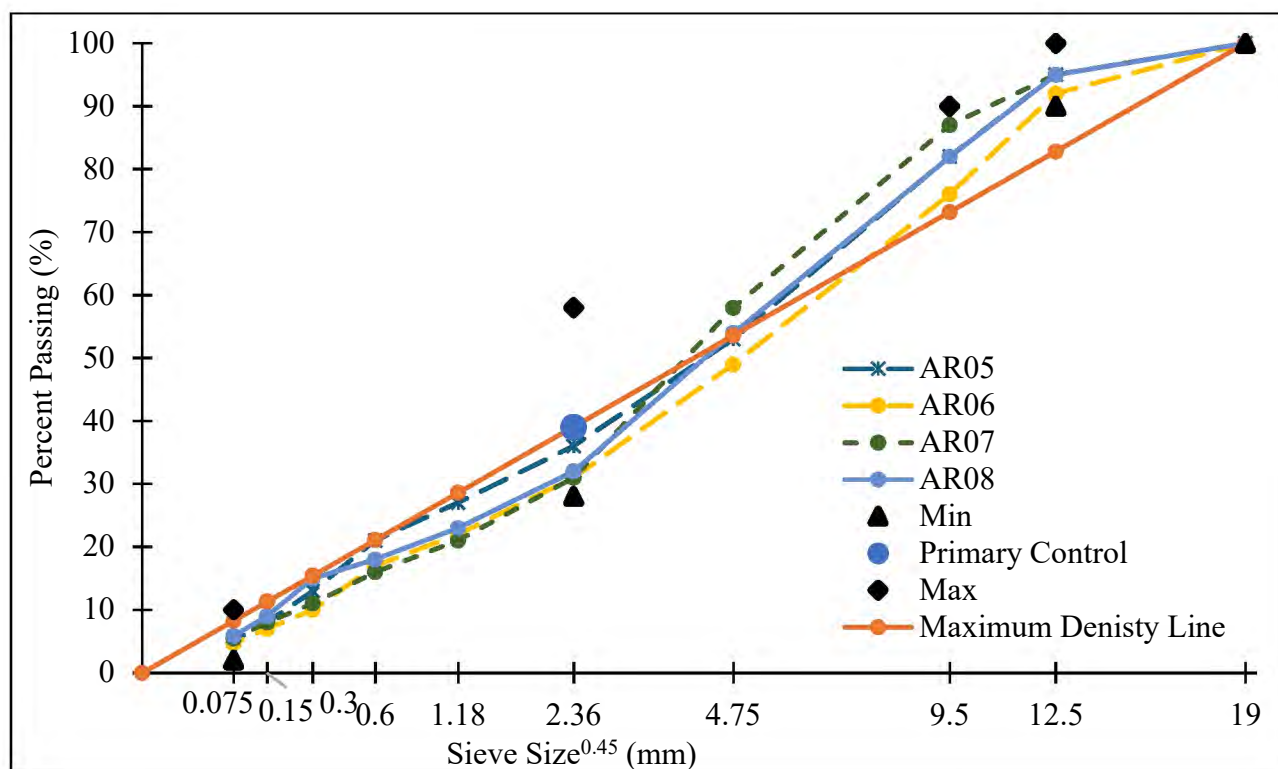
Figure 47. Gradation information for mixtures used in the BMD field projects in year 2024

Two performance tests—IDEAL-CT and APA—were performed on every BMD project using all three sample preparation methods. The remaining tests, including moisture-induced damage, I-FIT, HWTT, dynamic modulus, and flow number, were conducted using two preparation techniques: LMLC and RPMLC. The outcomes of these tests for each project are detailed in the sections that follow. The next section provides an overview of the performance test results for each project, followed by individual sections dedicated to each specific test.

3.2 AR01

Samples prepared using the three different sample preparation techniques underwent seven performance tests: IDEAL-CT, APA, moisture-induced damage, I-FIT, HWTT, dynamic modulus, and flow number. A summary of the six performance test results is provided in

Table 27, followed by additional details for each test.

Table 27. Summary of performance test results

Test	Result	LMLC	PMLC	RPMLC
IDEAL-CT	CT_{Index}	152	107	159
Asphalt Pavement Analyzer	Rut Depth (mm)	4.886	4.023	3.941
Moisture Induced Damage	TSR	0.90	N/A	0.92
Illinois Flexibility Index Test	FI	7.4	N/A	6.1
Hamburg Wheel Tracking Test	Rut depth (mm)	6.560	N/A	5.185
Flow Number	FN	184	N/A	-

3.2.1 IDEAL-CT

The details of the average $CT_{Index,}$ along with average air voids for all three sample preparation techniques, are given in **Table 28**. The Coefficient of Variation (CV) values are also provided. While there is no set standard for CV values, it is typical for asphalt mixture performance tests to have CV values in the 10-20% range.

Table 28. Results obtained from the IDEAL-CT test

Sample Type	Number of replicates	CT_{Index} Avg.	CT_{Index} CV (%)	Air Voids Avg. (%)	Air Voids CV (%)
LMLC	03	152	9	7.5	4
PMLC	03	107	20	7.3	2
RPMLC	03	159	9	7.3	4

3.2.2 APA

The details of the average APA rut depth, along with average air voids for all three-sample preparation techniques, are given in **Table 29**.

90

Table 29. Results obtained from the APA test

Sample Type	Number of replicates	Rut Depth Avg. (mm)	Rut Depth CV (%)	Air Voids Avg. (%)	Air Voids CV (%)
LMLC	04	4.886	4	7.9	2
PMLC	04	4.023	1	7.6	3
RPMLC	04	3.941	2	7.1	4

3.2.3 Moisture-Induced Damage

The details of average moisture conditioned strength, unconditioned strength, and tensile strength ratio, along with average air voids for two sample preparation techniques, are given in **Table 30**.

Table 30. Results obtained from the moisture-induced damage test

Sample Type	Number of replicates	Moisture conditioned strength		Air Voids		Unconditioned Strength (kPa)		Air Voids		Tensile Strength Ratio
		Avg (kPa)	CV (%)	Avg (%)	CV (%)	Avg (kPa)	CV (%)	Avg (%)	CV (%)	Avg
LMLC	03	874	7	7.8	2	968	2	7.8	2	0.90
RPMLC	03	1035	3	7.0	2	1126	2	7.0	4	0.92

3.2.4 Illinois Flexibility Index Test

The details of the average work of fracture, fracture energy, and flexibility index, along with average air voids for two sample preparation techniques, are given in **Table 31**.

91

Table 31. Results obtained from the I-FIT

Sample Type	Number of replicates	Air Voids		Work of fracture (Joules)		Fracture energy (Joules/m²)		Flexibility index	
		Avg.	CV (%)	Avg.	CV (%)	Avg.	CV (%)	Avg.	CV (%)
LMLC	03	6.2	5	8.8	1	2935	1	7.4	27
RPMLC	03	6.3	2	6.2	15	2051	15	6.5	3

3.2.5 Hamburg Wheel Tracking Test

The details of the average Hamburg wheel rut depth along with average air voids for two-sample preparation technique are given in **Table 32**.

Table 32. Results obtained from the Hamburg wheel tracking test

Sample Type	Number of replicates	Rut Depth Avg. (mm)	Rut Depth CV (%)	Air Voids Avg. (%)	Air Voids CV (%)
LMLC	04	6.560	25	7.0	5
RPMLC	04	5.185	14	7.1	2

3.2.6 Dynamic Modulus

Figure 48 illustrates the dynamic modulus master curve at a reference temperature of 20℃ for two sample preparation techniques. This data is the average of two replicates. The comparison of stiffness between the LMLC and RMPLC mixtures is represented using the line of equality curve, as shown in the **Figure 49**.
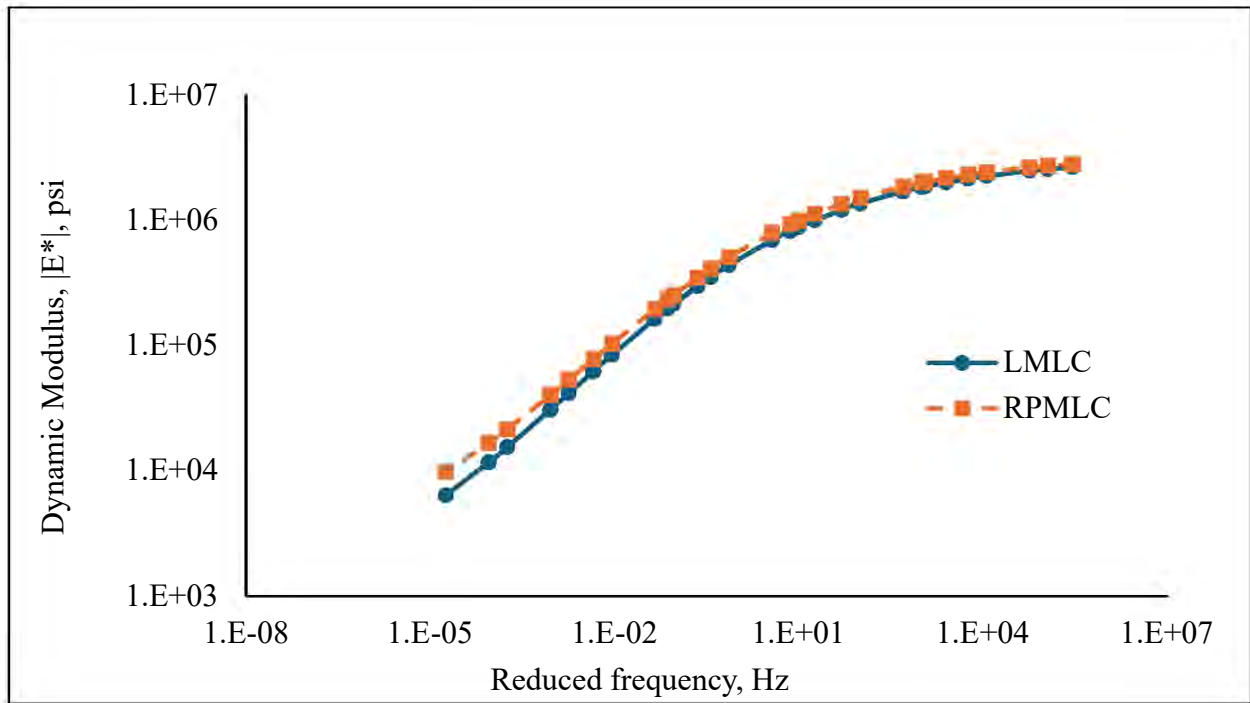
Figure 48. Dynamic Modulus at a reference temperature of 20℃ (AASHTO R 84)
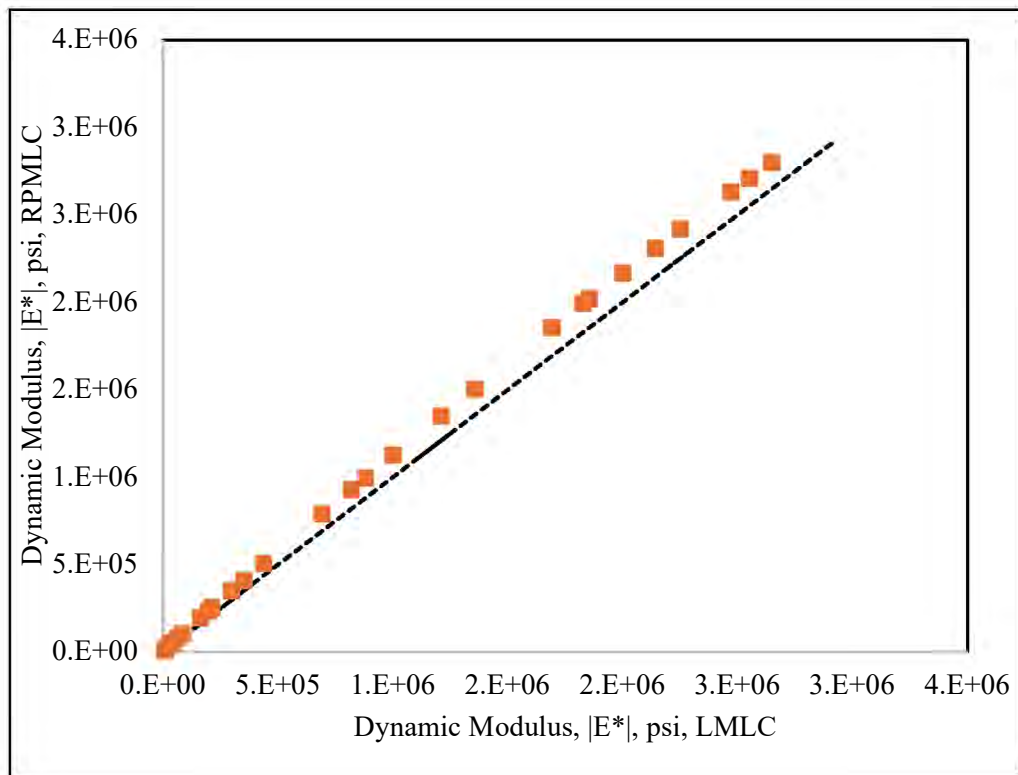
Figure 49. Line of equality, LMLC vs RPMLC

3.2.7 Flow Number

Table 33 presents the details of the average flow number, average micro strain at the flow point, and average air voids for the two sample preparation techniques.

Table 33. Results obtained from the flow number test

Sample Type	Number of replicates	Flow number		Micro strain at flow point		Air voids	
		Avg. (cycles)	CV (%)	Avg.	CV (%)	Avg. (%)	CV (%)
LMLC	02	184	54	21977	15	7.0	10
RPMLC	02	-	-	-	-	-	-

3.3 AR02

A summary of the performance test results for the AR02 project is provided in **Table 34**, along with additional details for each test.

Table 34. Summary of performance tests results

Test	Result	LMLC	PMLC	RPMLC
IDEAL-CT	CT_{Index}	83	56	51
Asphalt Pavement Analyzer	Rut Depth (mm)	2.847	3.733	2.886
Moisture Induced Damage	TSR	0.71	N/A	1.00
Illinois Flexibility Index Test	FI	3.5	N/A	4.2
Hamburg Wheel Tracking	Rut depth (mm)	2.910	N/A	2.430
Flow number	FN	106	N/A	155

3.3.1 IDEAL-CT

The details of the average CT_{Index} along with average air voids for all three-sample preparation techniques are given in **Table 35**.

Table 35. Results obtained from the IDEAL-CT test

Sample Type	Number of replicates	CT_{Index} Avg.	CT_{Index} CV (%)	Air Voids Avg. (%)	Air Voids CV (%)
LMLC	03	83	20	6.8	3
PMLC	03	56	17	7.2	6
RPMLC	03	51	11	7.0	4

3.3.2 APA

The details of average APA rut depth along with average air voids for all three-sample preparation techniques are given in **Table 36**.

Table 36. Results obtained from the APA test

Sample Type	Number of replicates	Rut Depth Avg. (mm)	Rut Depth CV (%)	Air Voids Avg. (%)	Air Voids CV (%)
LMLC	04	2.847	5	7.0	4
PMLC	04	3.733	24	N/A	N/A
RPMLC	04	2.886	9	6.6	7

3.3.3 Moisture Induced Damage

The details of average moisture conditioned strength, unconditioned strength, and tensile strength ratio along with average air voids for two sample preparation techniques are given in **Table 37**.

Table 37. Results obtained from the moisture induced damage test

Sample Type	Number of replicates	Moisture Conditioned Strength		Air Voids		Unconditioned Strength (kPa)		Air Voids		Tensile Strength Ratio
		Avg (kPa)	CV (%)	Avg (%)	CV (%)	Avg (kPa)	CV (%)	Avg (%)	CV (%)	Avg
LMLC	03	1136	14	7.2	2	1597	5	7.2	5	0.71
RPMLC	03	1680	1	6.7	3	1685	4	6.7	1	1.00

3.3.4 Illinois Flexibility Index Test

The details of average work of fracture, fracture energy, and flexibility index along with average air voids for two sample preparation techniques are given in **Table 38**.

Table 38. Results obtained from the I-FIT

Sample Type	Number of replicates	Air Voids		Work of fracture (Joules)		Fracture energy (Joules/m²)		Flexibility index	
		Avg.	CV (%)	Avg.	CV (%)	Avg.	CV (%)	Avg.	CV (%)
LMLC	03	6.6	2	7.9	16	2621	16	3.5	54
RPMLC	03	7.1	3	3.9	15	1309	15	4.2	50

3.3.5 Hamburg Wheel Tracking Test

The details of the average Hamburg wheel rut depth along with average air voids for two-sample preparation technique are given in **Table 39**.

Table 39. Results obtained from the Hamburg wheel tracking test

Sample Type	Number of replicates	Rut Depth Avg. (mm)	Rut Depth CV (%)	Air Voids Avg. (%)	Air Voids CV (%)
LMLC	04	2.910	13	7.0	2
RPMLC	04	2.430	1	7.1	4

3.3.6 Dynamic Modulus

Figure 50 illustrates the dynamic modulus master curve at a reference temperature of 20℃ for two sample preparation techniques. The comparison of stiffness between the LMLC and RMPLC mixtures is represented using the line of equality curve, as shown in the **Figure 51**.
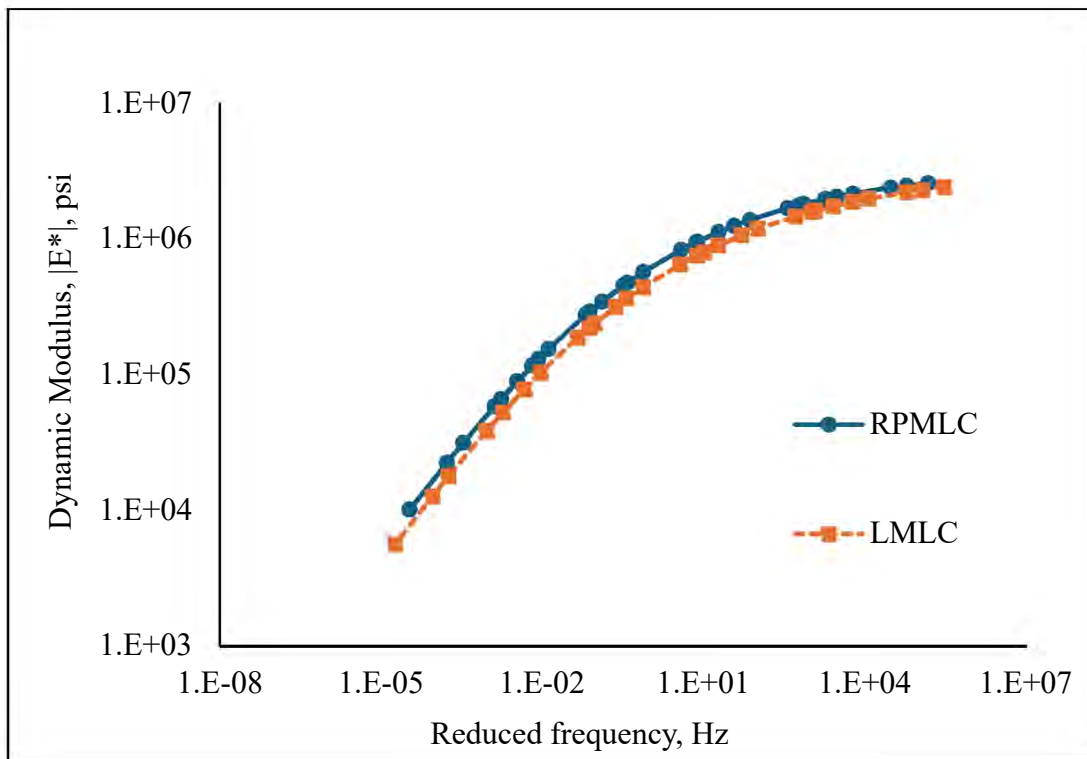
Figure 50. Dynamic Modulus at a reference temperature of 20℃

97
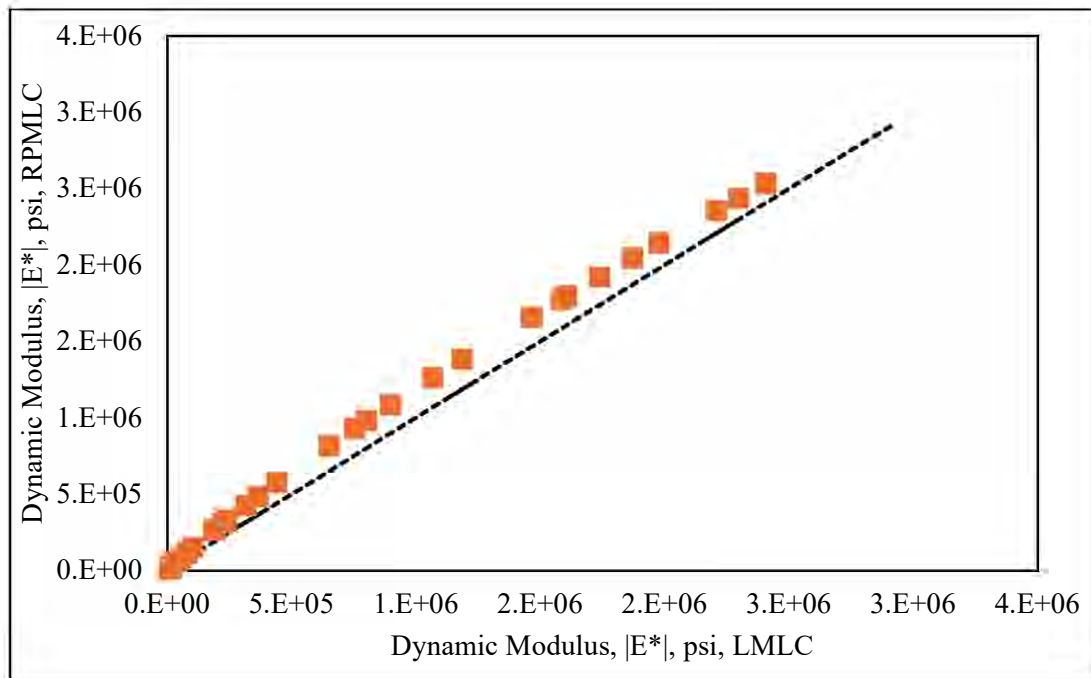
Figure 51. Line of equality, LMLC vs RPMLC

3.3.7 Flow Number

Table 40 presents the details of the average flow number, average micro strain at the flow point, and average air voids for the two sample preparation techniques.

Table 40. Results obtained from the flow number test

Sample Type	Number of replicates	Flow number		Micro strain at flow point		Air voids	
		Avg. (cycles)	CV (%)	Avg.	CV (%)	Avg. (%)	CV (%)
LMLC	02	106	9	21420	1	7.4	2
RPMLC	02	155	9	23445	11	6.7	1

3.4 AR03

A summary of the performance test results for the AR03 project is provided in **Table 41**, along with additional details for each test.

Table 41. Summary of performance tests results

Test	Result	LMLC	PMLC	RPMLC
IDEAL-CT	CT_{Index}	42	54	33
Asphalt Pavement Analyzer	Rut Depth (mm)	2.601	1.429	1.441
Moisture Induced Damage	TSR	0.87	N/A	0.94
Illinois Flexibility Index Test	FI	2.7	N/A	0.6
Hamburg Wheel Tracking	Rut depth (mm)	2.490	N/A	2.410
Flow number	FN	189	N/A	1060

3.4.1 IDEAL-CT

The details of the average CT_{Index} along with average air voids for all three sample preparation techniques are given in **Table 42**.

Table 42. Results obtained from the IDEAL-CT test

Sample Type	Number of replicates	CT_{Index} Avg.	CT_{Index} CV (%)	Air Voids Avg. (%)	Air Voids CV (%)
LMLC	03	42	20	7.2	4
PMLC	03	54	50	6.7	1
RPMLC	03	33	31	6.8	5

3.4.2 APA

The details of average APA rut depth along with average air voids for all three-sample preparation techniques are given in **Table 43**.

Table 43. Results obtained from the APA test

Sample Type	Number of replicates	Rut Depth Avg. (mm)	Rut Depth CV (%)	Air Voids Avg. (%)	Air Voids CV (%)
LMLC	04	2.601	8	6.6	8
PMLC	04	1.429	4	6.7	2
RPMLC	04	1.441	5	6.3	4

3.4.3 Moisture Induced Damage

The details of average moisture conditioned strength, unconditioned strength, and tensile strength ratio along with average air voids for two sample preparation techniques are given in **Table 44**.

Table 44. Results obtained from the moisture induced damage test

Sample Type	Number of replicates	Moisture Conditioned Strength		Air Voids		Unconditioned Strength (kPa)		Air Voids		Tensile Strength Ratio
		Avg (kPa)	CV (%)	Avg (%)	CV (%)	Avg (kPa)	CV (%)	Avg (%)	CV (%)	Avg
LMLC	03	1272	18	7.1	3	1455	2	7.0	7	0.87
RPMLC	03	1843	3	6.8	4	1961	4	7.0	4	0.94

3.4.4 Illinois Flexibility Index Test

The details of average work of fracture, fracture energy, and flexibility index along with average air voids for two sample preparation techniques are given in **Table 45**.

Table 45. Results obtained from the I-FIT

Sample Type	Number of replicates	Air Voids		Work of fracture (Joules)		Fracture energy (Joules/m^2)		Flexibility index	
		Avg. (%)	CV (%)	Avg.	CV (%)	Avg.	CV (%)	Avg.	CV (%)
LMLC	03	6.8	2	5.2	13	1733	11	2.7	11
RPMLC	03	6.8	0	1.1	30	1197	27	0.6	31

100

3.4.5 Hamburg Wheel Tracking Test

The details of the average Hamburg wheel rut depth along with average air voids for two-sample preparation technique are given in **Table 46**.

Table 46. Results obtained from the Hamburg wheel tracking test

Sample Type	Number of replicates	Rut Depth Avg. (mm)	Rut Depth CV (%)	Air Voids Avg. (%)	Air Voids CV (%)
LMLC	04	2.490	27	7.1	6
RPMLC	04	2.410	15	7.1	6

3.4.6 Dynamic Modulus

Figure 52 illustrates the dynamic modulus master curve at a reference temperature of 20℃ for two sample preparation techniques. The comparison of stiffness between the LMLC and RMPLC mixtures is represented using the line of equality curve, as shown in the **Figure 53**.

Figure 52. Dynamic Modulus at a reference temperature of 20℃

Figure 53. Line of equality, LMLC vs RPMLC

3.4.7 Flow Number

Table 47 presents the details of the average flow number, average micro strain at the flow point, and average air voids for the two sample preparation techniques.

Table 47. Results obtained from the flow number test

Sample Type	Number of replicates	Flow number Avg. (cycles)	Flow number CV (%)	Micro strain at flow point Avg.	Micro strain at flow point CV (%)	Air voids Avg. (%)	Air voids CV (%)
LMLC	02	189	57	16931	43	7.1	4
RPMLC	02	1060	36	29682	5	7.0	6

102

3.5 AR04

A summary of the performance test results for the AR04 project is provided in **Table 48**, along with additional details for each test.

Table 48. Summary of performance tests results

Test	Result	LMLC	PMLC	RPMLC
IDEAL-CT	CT_{Index}	77	56	38
Asphalt Pavement Analyzer	Rut Depth (mm)	2.270	3.293	3.881
Moisture Induced Damage	TSR	0.87	N/A	0.94
Illinois Flexibility Index Test	FI	3.5	N/A	4.2
Hamburg Wheel Tracking	Rut depth (mm)	2.490	N/A	2.410
Flow number	FN	78	N/A	290

3.5.1 IDEAL-CT

The details of the average CT_{Index}, along with average air voids for all three-sample preparation techniques are given in **Table 49**.

Table 49. Results obtained from the IDEAL-CT test

Sample Type	Number of replicates	CT_{Index} Avg.	CT_{Index} CV (%)	Air Voids Avg. (%)	Air Voids CV (%)
LMLC	03	77	28	6.8	4
PMLC	03	56	22	6.8	1
RPMLC	03	38	33	7.4	1

3.5.2 APA

The details of average APA rut depth, along with average air voids for all three-sample preparation techniques are given in

Table 50.

Table 50. Results obtained from the APA test

Sample Type	Number of replicates	Rut Depth Avg. (mm)	Rut Depth CV (%)	Air Voids Avg. (%)	Air Voids CV (%)
LMLC	04	2.270	10	6.2	1
PMLC	04	3.293	10	N/A	N/A
RPMLC	04	3.881	29	6.6	2

3.5.3 Moisture Induced Damage

The details of average moisture conditioned strength, unconditioned strength, and tensile strength ratio along with average air voids for two sample preparation techniques are given in **Table 51**.

Table 51. Results obtained from the moisture induced damage test

Sample Type	Number of replicates	Moisture Conditioned Strength		Air Voids		Unconditioned Strength (kPa)		Air Voids		Tensile Strength Ratio
		Avg (kPa)	CV (%)	Avg (%)	CV (%)	Avg (kPa)	CV (%)	Avg (%)	CV (%)	Avg
LMLC	03	934	5	6.8	7	951	8	7.2	5	0.98
RPMLC	03	1487	5	6.7	1	1595	3	6.8	4	0.93

3.5.4 Illinois Flexibility Index Test

The details of average work of fracture, fracture energy, and flexibility index along with average air voids for two sample preparation techniques are given in **Table 52**.

104

Table 52. Results obtained from the I-FIT

Sample Type	Number of replicates	Air Voids		Work of fracture (Joules)		Fracture energy (Joules/m²)		Flexibility index	
		Avg.	CV (%)	Avg.	CV (%)	Avg.	CV (%)	Avg.	CV (%)
LMLC	03	7.0	18	7.8	1	2606	1	5.0	26
RPMLC	03	6.8	12	5.2	19	1702	17	1.5	44

3.5.5 Hamburg Wheel Tracking Test

The details of the average Hamburg wheel rut depth along with average air voids for two-sample preparation techniques are given in **Table 53**.

Table 53. Hamburg Wheel Tracking

Sample Type	Number of replicates	Rut Depth Avg. (mm)	Rut Depth CV (%)	Air Voids Avg. (%)	Air Voids CV (%)
LMLC	02	20.020	0	6.8	6
RPMLC	02	3.085	6	7.2	2

3.5.6 Dynamic Modulus

Figure 54 illustrates the dynamic modulus master curve at a reference temperature of 20℃ for two sample preparation techniques. The comparison of stiffness between the LMLC and RMPLC mixtures is represented using the line of equality curve, as shown in the **Figure 55**.
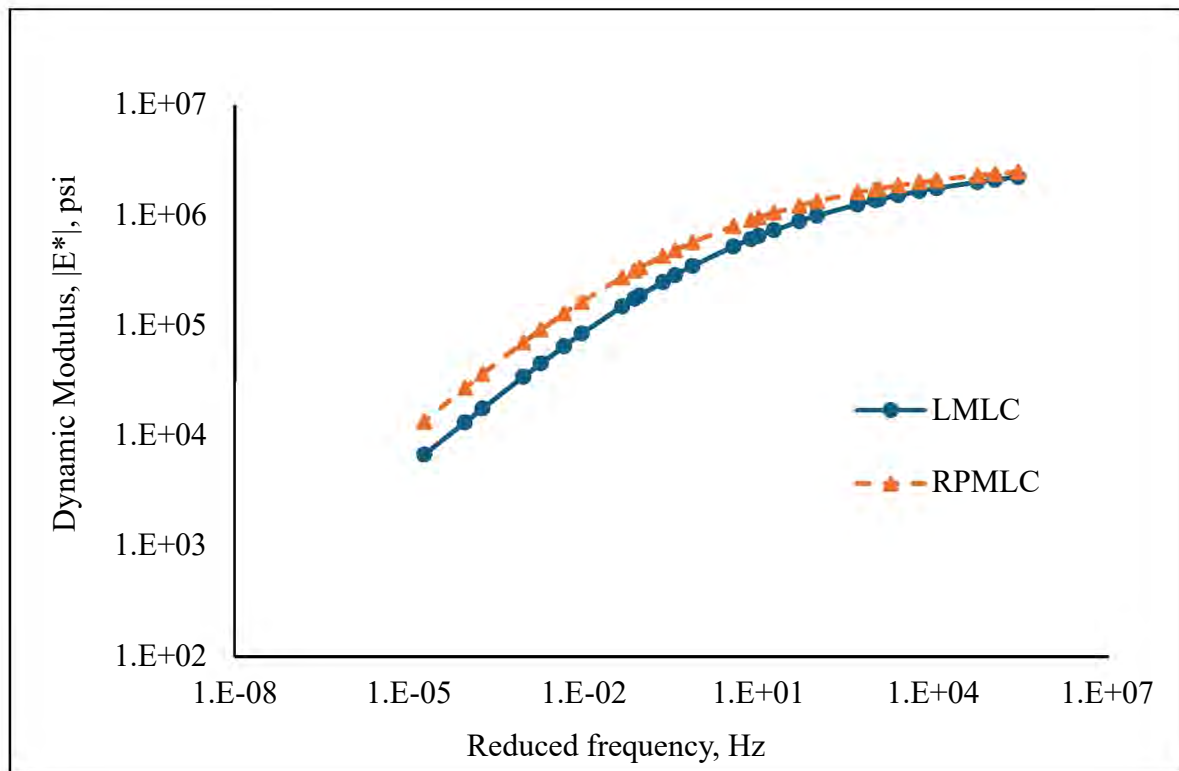
Figure 54. Dynamic Modulus
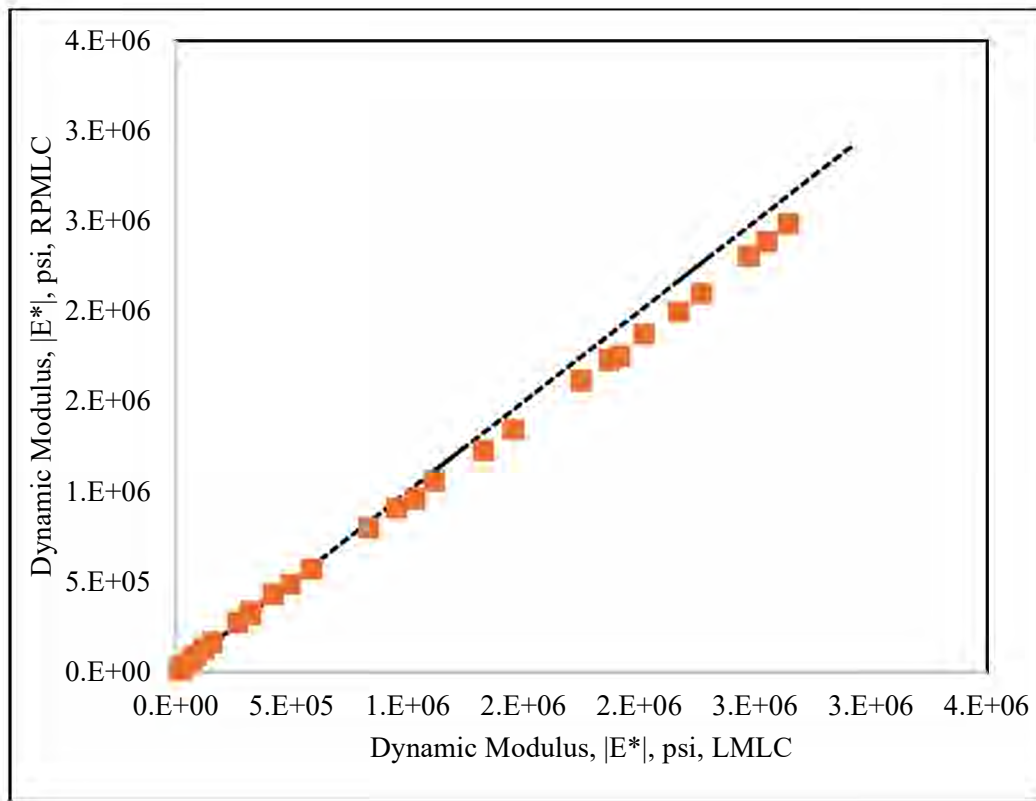

Figure 55. Line of equality, LMLC vs RPMLC

106

3.5.7 Flow Number

Table 54 presents the details of the average flow number, average micro strain at the flow point, and average air voids for the two sample preparation techniques.

Table 54. Results obtained from the flow number test

Sample Type	Number of replicates	Flow number		Micro strain at flow point		Air voids	
		Avg. (cycles)	CV (%)	Avg.	CV (%)	Avg. (%)	CV (%)
LMLC	02	78	11	24932	4	7.1	8
RPMLC	02	290	20	18973	16	7.3	2

3.6 AR05

A summary of the performance test results for the AR04 project is provided in **Table 55**, along with additional details for each test.

Table 55. Summary of performance tests results

Test	Result	LMLC	PMLC	RPMLC
IDEAL-CT	CT_{Index}	196	215	200
Asphalt Pavement Analyzer	Rut Depth (mm)	2.452	3.494	5.520
Moisture Induced Damage	TSR	0.96	N/A	0.95
Illinois Flexibility Index Test	FI	5.2	N/A	4.3
Hamburg Wheel Tracking	Rut depth (mm)	2.145	N/A	2.695
Flow number	FN	904	N/A	304

3.6.1 IDEAL-CT

The details of the average CT_{Index} along with average air voids for all three sample preparation techniques are given in

Table 56.

Table 56. Results obtained from the IDEAL-CT test

Sample Type	Number of replicates	CT_{Index} Avg.	CT_{Index} CV (%)	Air Voids Avg. (%)	Air Voids CV (%)
LMLC	05	196	23	7.0	4
PMLC	05	215	18	6.6	3
RPMLC	05	200	26	7.3	3

3.6.2 APA

The details of the average APA rut depth along with average air voids for all three-sample preparation techniques are given in **Table 57**.

Table 57. Results obtained from the APA test

Sample Type	Number of replicates	Rut Depth Avg. (mm)	Rut Depth CV (%)	Air Voids Avg. (%)	Air Voids CV (%)
LMLC	04	2.452	14	6.9	10
PMLC	04	3.494	51	6.8	10
RPMLC	04	5.520	3	6.8	6

3.6.3 Moisture Induced Damage

The details of average moisture conditioned strength, unconditioned strength, and tensile strength ratio along with average air voids for two sample preparation techniques are given in **Table 58**.

Table 58. Results obtained from the moisture induced damage test

Sample Type	Number of replicates	Moisture Conditioned Strength		Air Voids		Unconditioned Strength (kPa)		Air Voids		Tensile Strength Ratio
		Avg (kPa)	CV (%)	Avg (%)	CV (%)	Avg (kPa)	CV (%)	Avg (%)	CV (%)	Avg
LMLC	03	1344	3	6.9	6	1396	2	6.8	5	0.96
RPMLC	03	1371	2	6.8	3	1439	4	6.9	4	0.95

3.6.4 Illinois Flexibility Index Test

The details of average work of fracture, fracture energy, and flexibility index along with average air voids for two sample preparation techniques are given in **Table 59**.

Table 59. Results obtained from the I-FIT

Sample Type	Number of replicates	Air Voids		Work of fracture (Joules)		Fracture energy (Joules/m²)		Flexibility index	
		Avg.	CV (%)	Avg.	CV (%)	Avg.	CV (%)	Avg.	CV (%)
LMLC	03	6.2	0	8.9	31	2974	31	5.2	15
RPMLC	03	7.1	1	7.8	11	2583	11	4.3	24

3.6.5 Hamburg Wheel Tracking Test

The details of the average Hamburg wheel rut depth along with average air voids for two-sample preparation technique are given in

Table 60.

109

Table 60. Results obtained from the Hamburg wheel tracking test

Sample Type	Number of replicates	Rut Depth Avg. (mm)	Rut Depth CV (%)	Air Voids Avg. (%)	Air Voids CV (%)
LMLC	04	2.145	6	7.3	4
RPMLC	04	2.695	34	6.8	2

3.6.6 Dynamic Modulus

Figure 56 illustrates the dynamic modulus master curve at a reference temperature of 20℃ for two sample preparation techniques. The comparison of stiffness between the LMLC and RMPLC mixtures is represented using the line of equality curve, as shown in the **Figure 57**.
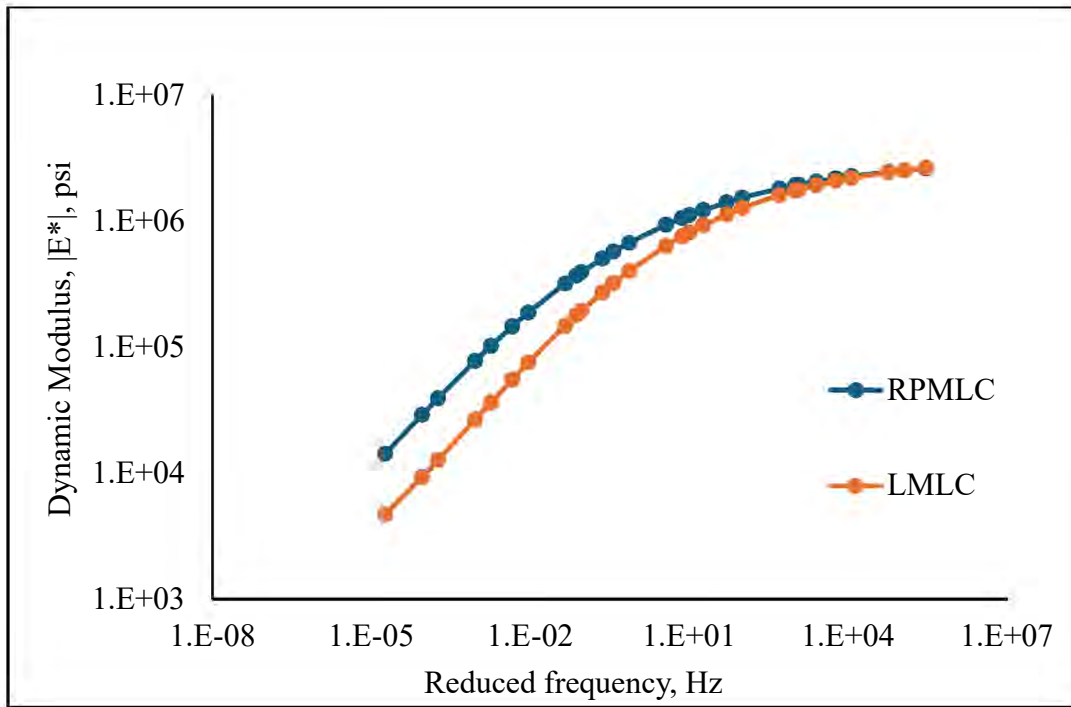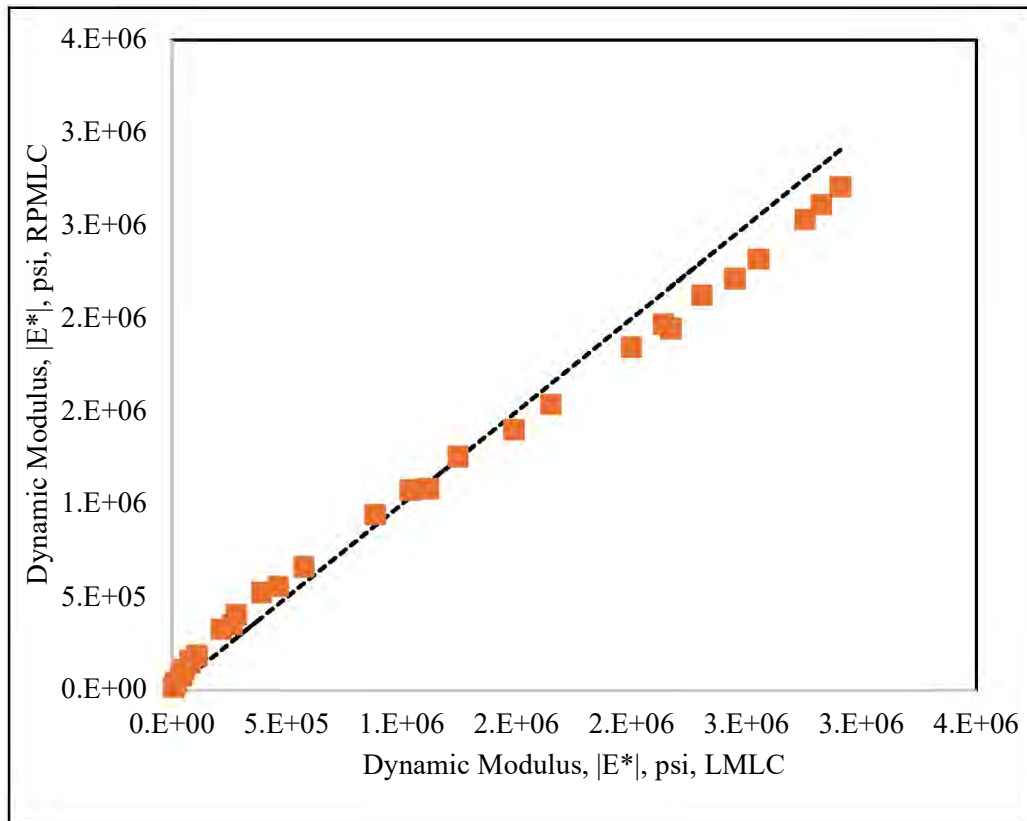

Figure 56. Dynamic Modulus at a reference temperature of 20℃

Figure 57. Line of equality, LMLC vs RPMLC

3.6.7 Flow Number

Table 61 presents the details of the average flow number, average micro strain at the flow point, and average air voids for the two sample preparation techniques.

Table 61. Results obtained from the flow number test

Sample Type	Number of replicates	Flow number		Micro strain at flow point		Air voids	
		Avg. (cycles)	CV (%)	Avg.	CV (%)	Avg. (%)	CV (%)
LMLC	02	904	22	41380	11	6.9	8
RPMLC	02	304	16	34224	3	6.9	1

3.7 AR06

A summary of the performance test results for the AR04 project is provided in **Table 62**, along with additional details for each test.

Table 62. Summary of performance test results

Test	Result	LMLC	PMLC	RPMLC
IDEAL-CT	CT_{Index}	123	90	53
Asphalt Pavement Analyzer	Rut Depth (mm)	3.135	2.804	2.487
Moisture Induced Damage	TSR	0.95	N/A	0.75
Illinois Flexibility Index Test	FI	3.4	N/A	2.5
Hamburg Wheel Tracking	Rut depth (mm)	3.425	N/A	1.640
Flow number	FN	587	N/A	1346

3.7.1 IDEAL-CT

The details of the average CT_{Index} along with average air voids for all three-sample preparation techniques are given in **Table 63**.

Table 63. Results obtained from the IDEAL-CT test

Sample Type	Number of replicates	CT_{Index} Avg.	CT_{Index} CV (%)	Air Voids Avg. (%)	Air Voids CV (%)
LMLC	05	123	19	7.1	5
PMLC	05	90	19	6.9	4
RPMLC	05	53	31	7.0	5

3.7.2 APA

The details of the average APA rut depth along with average air voids for all three-sample preparation techniques are given in **Table 64**.

Table 64. Results obtained from the APA test

Sample Type	Number of replicates	Rut Depth Avg. (mm)	Rut Depth CV (%)	Air Voids Avg. (%)	Air Voids CV (%)
LMLC	04	3.135	25	7.2	1
PMLC	04	2.804	0	6.8	4
RPMLC	04	2.487	28	6.9	1

3.7.3 Moisture Induced Damage

The details of average moisture conditioned strength, unconditioned strength and tensile strength ratio along with average air voids for two sample preparation techniques are given in

Table *65*.

Table 65. Results obtained from the moisture induced damage test

Sample Type	Number of replicates	Moisture Conditioned Strength		Air Voids		Unconditioned Strength (kPa)		Air Voids		Tensile Strength Ratio
		Avg (kPa)	CV (%)	Avg (%)	CV (%)	Avg (kPa)	CV (%)	Avg (%)	CV (%)	Avg
LMLC	03	1345	3	7.1	5	1411	2	6.8	5	0.95
RPMLC	03	1356	5	6.8	2	1810	4	6.8	3	0.75

3.7.4 Illinois Flexibility Index Test

The details of average work of fracture, fracture energy, and flexibility index along with average air voids for two sample preparation techniques are given in **Table 66**.

Table 66. Results obtained from the I-FIT

Sample Type	Number of replicates	Air Voids		Work of fracture (Joules)		Fracture energy (Joules/m²)		Flexibility index	
		Avg.	CV (%)	Avg.	CV (%)	Avg.	CV (%)	Avg.	CV (%)
LMLC	03	7.3	8	6.7	13	2215	13	3.4	24
RPMLC	03	6.1	1	6.3	30	1985	28	2.5	118

3.7.5 Hamburg Wheel Tracking Test

The details of the average Hamburg wheel rut depth along with average air voids for two-sample preparation technique are given in

Table 67.

Table 67. Results obtained from the Hamburg wheel tracking test

Sample Type	Number of replicates	Rut Depth Avg. (mm)	Rut Depth CV (%)	Air Voids Avg. (%)	Air Voids CV (%)
LMLC	04	3.425	12	7.4	2
RPMLC	04	1.640	1	6.8	4

3.7.6 Dynamic Modulus

Figure 58 illustrates the dynamic modulus master curve at a reference temperature of 20℃ for two sample preparation techniques. The comparison of stiffness between the LMLC and RMPLC mixtures is represented using the line of equality curve, as shown in the **Figure 59**.
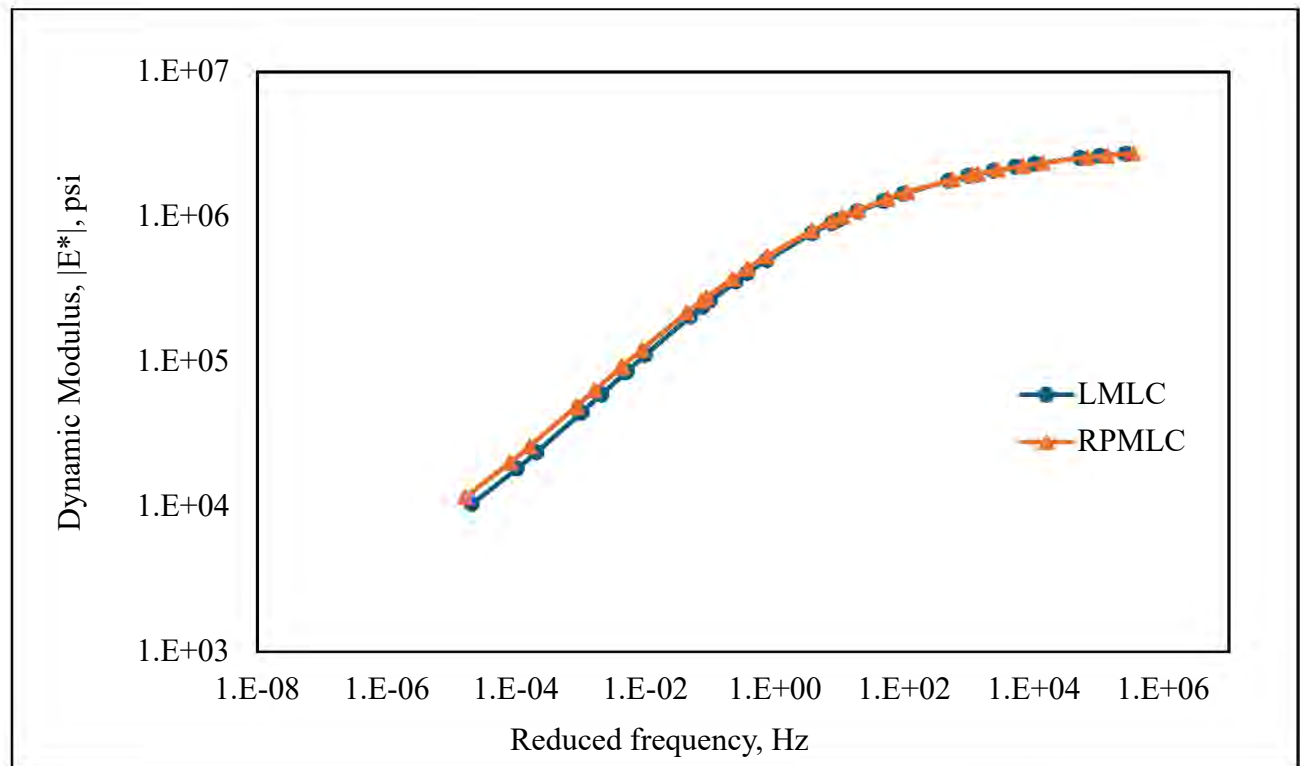
114

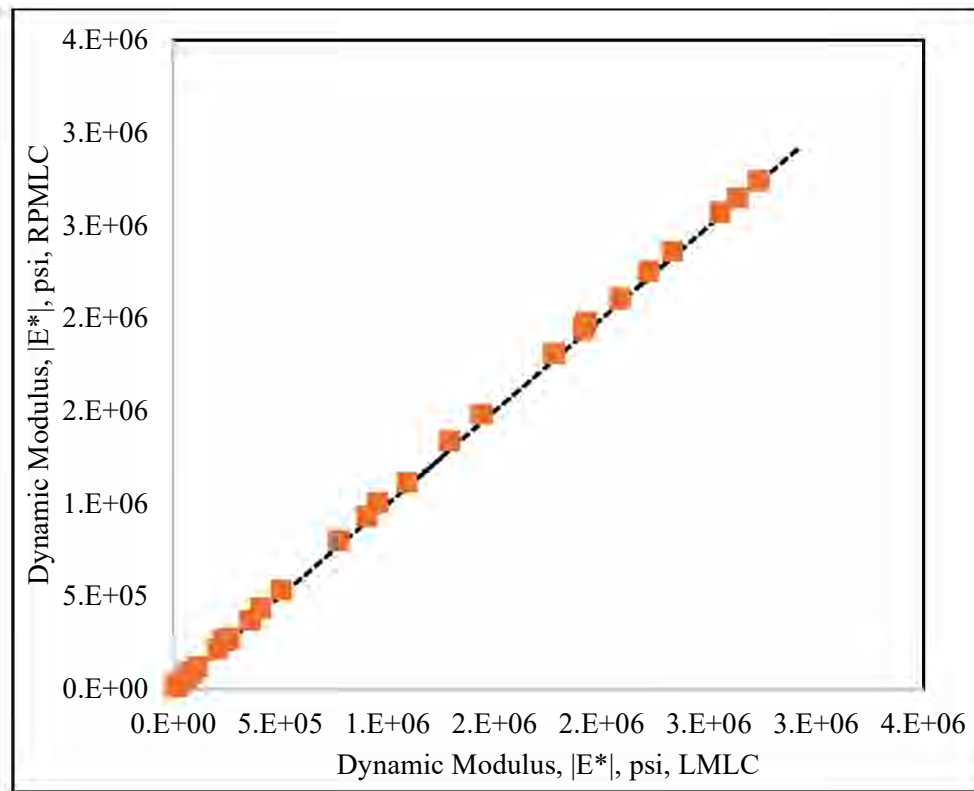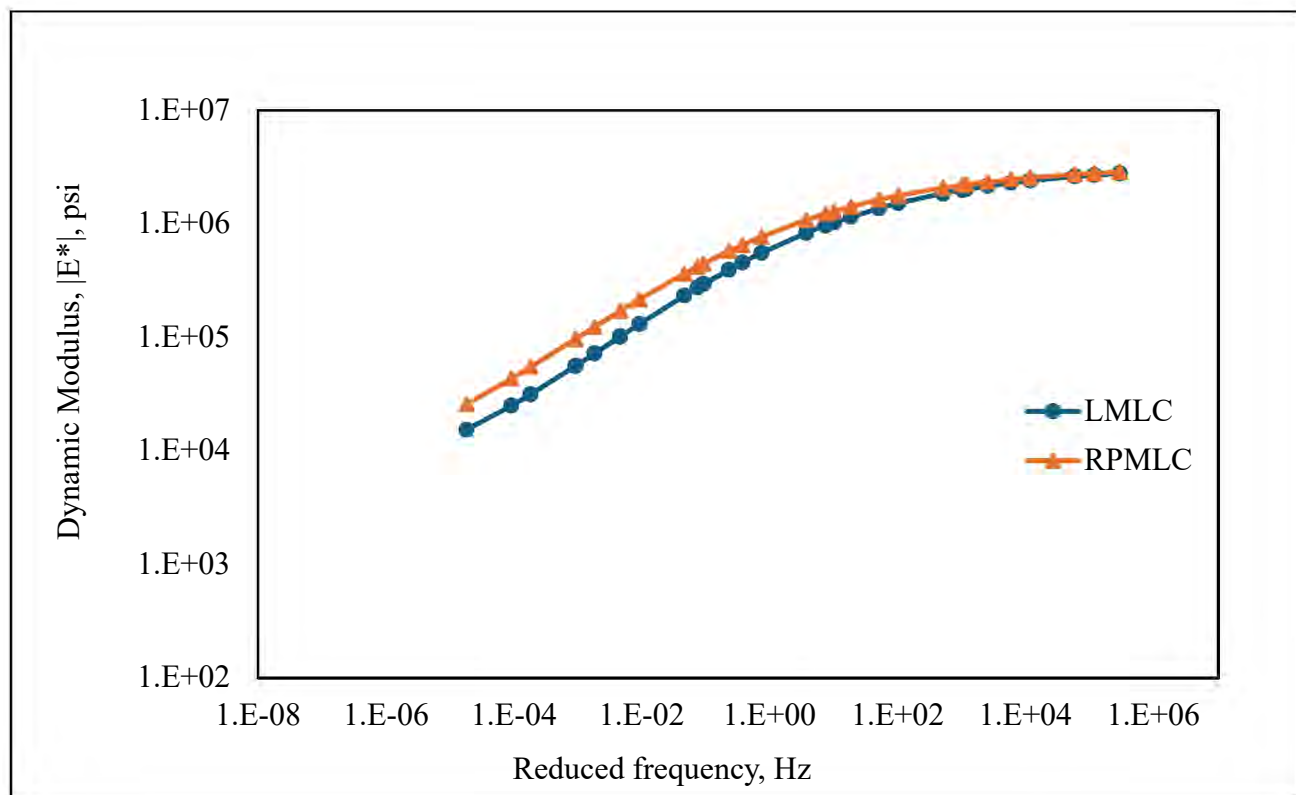**Figure 58. Dynamic Modulus at a reference temperature of 20℃**
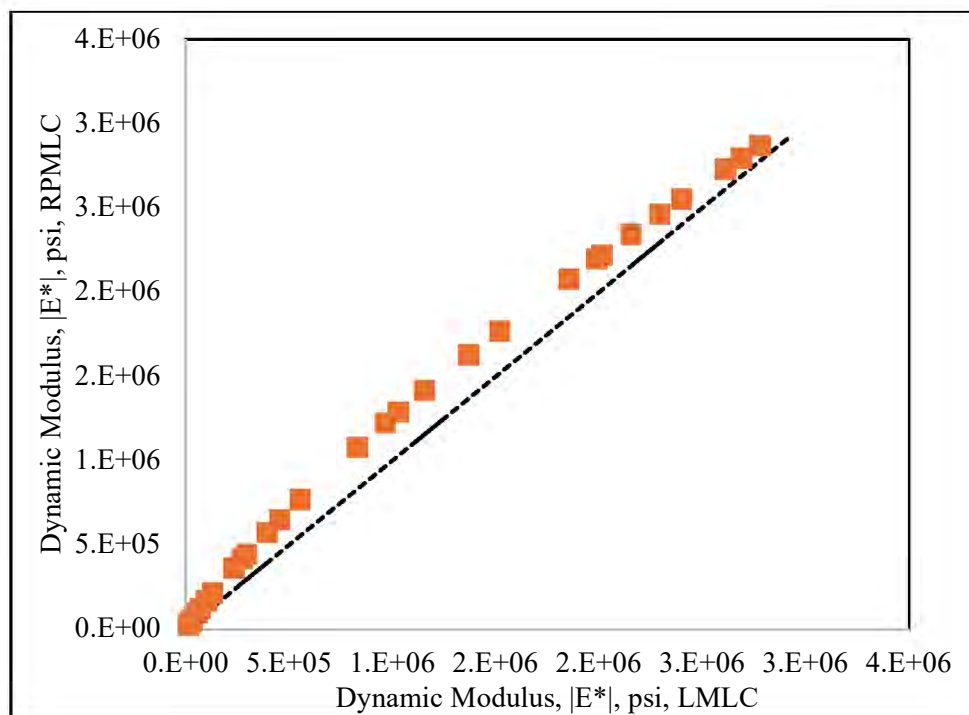
Figure 59. Line of equality, LMLC vs RPMLC

3.7.7 Flow Number

Table 68 presents the details of the average flow number, average micro strain at the flow point, and average air voids for the two sample preparation techniques.

Table 68. Results obtained from the flow number test

Sample Type	Number of replicates	Flow number		Micro strain at flow point		Air voids	
		Avg. (cycles)	CV (%)	Avg.	CV (%)	Avg. (%)	CV (%)
LMLC	02	587	37	28910	32	7.0	7
RPMLC	02	1346	15	27166	11	6.8	1

3.8 AR07

A summary of the performance test results for the AR04 project is provided in **Table 69**, along with additional details for each test.

Table 69. Summary of performance test results

Test	Result	LMLC	PMLC	RPMLC
IDEAL-CT	CT_{Index}	205	173	244
Asphalt Pavement Analyzer	Rut Depth (mm)	3.567	5.549	5.099
Moisture Induced Damage	TSR	0.88	N/A	0.64
Illinois Flexibility Index Test	FI	7.5	N/A	6.8
Hamburg Wheel Tracking	Rut depth (mm)	19.300	N/A	20.030
Flow number	FN	65	N/A	156

3.8.1 IDEAL-CT

The details of the average CT_{Index} along with average air voids for all three sample preparation techniques are given in **Table 70**.

Table 70. Results obtained from the IDEAL-CT test

Sample Type	Number of replicates	CT_{Index} Avg.	CT_{Index} CV (%)	Air Voids Avg. (%)	Air Voids CV (%)
LMLC	05	205	14	7.2	3
PMLC	05	173	9	6.8	2
RPMLC	05	244	26	7.1	5

3.8.2 APA

The details of the average APA rut depth along with average air voids for all three-sample preparation techniques are given in **Table 71**.

Table 71. Results obtained from the APA test

Sample Type	Number of replicates	Rut Depth Avg. (mm)	Rut Depth CV (%)	Air Voids Avg. (%)	Air Voids CV (%)
LMLC	04	3.567	27	7.0	1
PMLC	04	5.549	75	6.3	1
RPMLC	04	5.099	1	7.1	0

3.8.3 Moisture Induced Damage

The details of average moisture conditioned strength, unconditioned strength and tensile strength ratio along with average air voids for two sample preparation techniques are given in **Table 72**.

Table 72. Results obtained from the moisture induced damage test

Sample Type	Number of replicates	Moisture Conditioned Strength		Air Voids		Unconditioned Strength (kPa)		Air Voids		Tensile Strength Ratio
		Avg (kPa)	CV (%)	Avg (%)	CV (%)	Avg (kPa)	CV (%)	Avg (%)	CV (%)	Avg
LMLC	03	812	6	7.0	1	927	4	7.0	7	0.88
RPMLC	03	684	2	6.9	3	1061	2	7.0	6	0.64

3.8.4 Illinois Flexibility Index Test

The details of average work of fracture, fracture energy, and flexibility index along with average air voids for two sample preparation techniques are given in **Table 73**.

Table 73. Results obtained from the I-FIT

Sample Type	Number of replicates	Air Voids		Work of fracture (Joules)		Fracture energy (Joules/m^2)		Flexibility index	
		Avg.	CV (%)	Avg.	CV (%)	Avg.	CV (%)	Avg.	CV (%)
LMLC	03	6.4	4	7.2	10	2391	10	7.5	32
RPMLC	03	7.2	2	8.4	16	2778	16	6.8	29

3.8.5 Hamburg Wheel Tracking Test

The details of the average Hamburg wheel rut depth along with average air voids for two-sample preparation technique are given in **Table 74**.

Table 74. Results obtained from the Hamburg wheel tracking test

Sample Type	Number of replicates	Rut Depth Avg. (mm)	Rut Depth CV (%)	Air Voids Avg. (%)	Air Voids CV (%)
LMLC	02	19.300	5	6.9	2
RPMLC	02	20.030	2	7.0	6

3.8.6 Dynamic Modulus

Figure 60 illustrates the dynamic modulus master curve at a reference temperature of 20℃ for two sample preparation techniques. The comparison of stiffness between the LMLC and RMPLC mixtures is represented using the line of equality curve, as shown in the **Figure 61**.
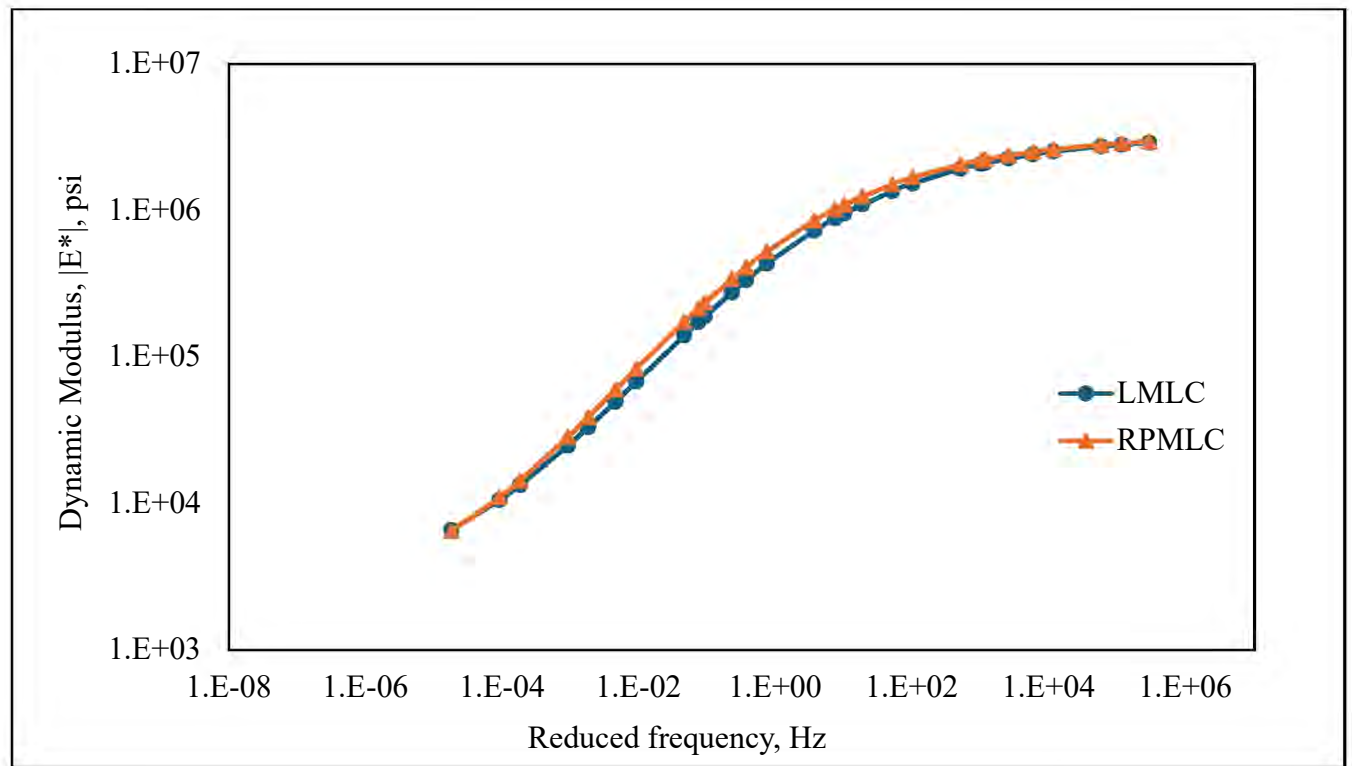
Figure 60. Dynamic Modulus at a reference temperature of 20℃
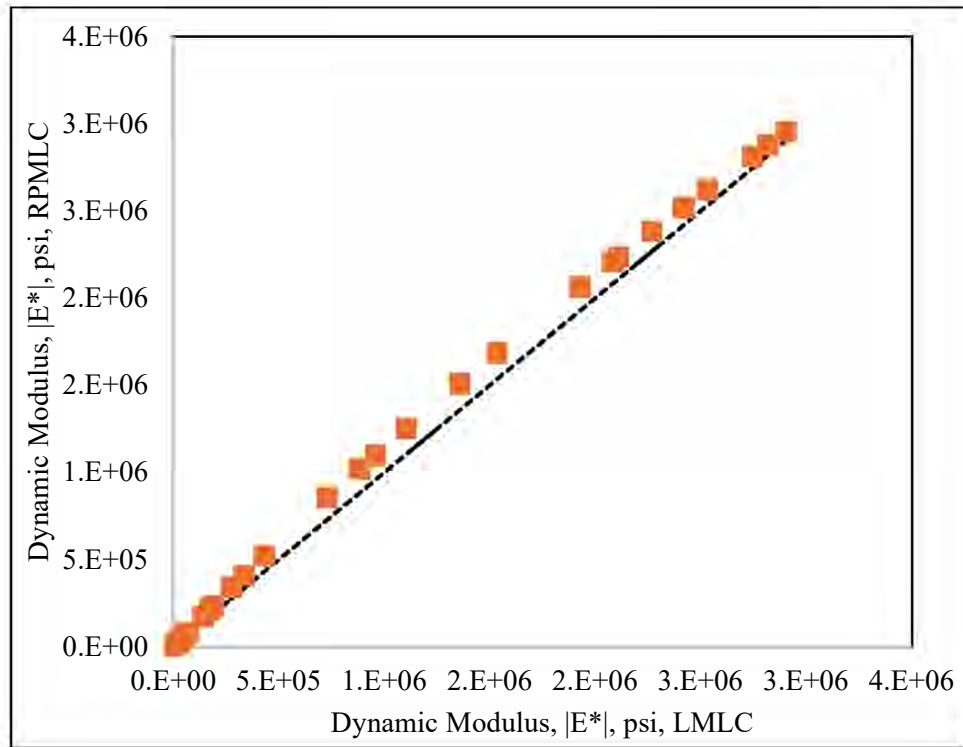
Figure 61. Line of equality, LMLC vs RPMLC

3.8.7 Flow Number

Table 75 presents the details of the average flow number, average micro strain at the flow point, and average air voids for the two sample preparation techniques.

Table 75. Results obtained from the flow number test

Sample Type	Number of replicates	Flow number		Micro strain at flow point		Air voids	
		Avg. (cycles)	CV (%)	Avg.	CV (%)	Avg. (%)	CV (%)
LMLC	02	65	15	21503	8	6.7	0
RPMLC	02	156	22	34304	8	7.4	2

3.9 AR08

A summary of the performance test results for the AR04 project is provided in **Table 76**, along with additional details for each test.

Table 76. Summary of performance test results

Test	Result	LMLC	PMLC	RPMLC
IDEAL-CT	CT_{Index}	170	251	189
Asphalt Pavement Analyzer	Rut Depth (mm)	2.408	3.871	2.740
Moisture Induced Damage	TSR	0.72	N/A	0.73
Illinois Flexibility Index Test	FI	3.3	N/A	3.6
Hamburg Wheel Tracking	Rut depth (mm)	3.270	N/A	4.265
Flow number	FN	611	N/A	415

3.9.1 IDEAL-CT

The details of the average CT_{Index} along with average air voids for all three sample preparation techniques are given in **Table 77**.

Table 77. Results obtained from the IDEAL-CT test

Sample Type	Number of replicates	CT_{Index} Avg.	CT_{Index} CV (%)	Air Voids Avg. (%)	Air Voids CV (%)
LMLC	05	170	17	7.2	2
PMLC	05	251	18	7.0	4
RPMLC	05	189	21	7.3	2

3.9.2 APA

The details of the average APA rut depth along with average air voids for all three-sample preparation techniques are given in **Table 78**.

121

Table 78. Results obtained from the APA test

Sample Type	Number of replicates	Rut Depth Avg. (mm)	Rut Depth CV (%)	Air Voids Avg. (%)	Air Voids CV (%)
LMLC	04	2.408	35	7.2	0
PMLC	04	3.871	46	6.7	0
RPMLC	04	2.740	20	7.7	1

3.9.3 Moisture Induced Damage

The details of average moisture conditioned strength, unconditioned strength and tensile strength ratio along with average air voids for two sample preparation techniques are given in **Table 79**.

Table 79. Results obtained from the moisture induced damage test

Sample Type	Number of replicates	Moisture Conditioned Strength		Air Voids		Unconditioned Strength (kPa)		Air Voids		Tensile Strength Ratio
		Avg (kPa)	CV (%)	Avg (%)	CV (%)	Avg (kPa)	CV (%)	Avg (%)	CV (%)	Avg
LMLC	03	944	7	7.1	6	1315	6	6.8	5	0.72
RPMLC	03	891	4	6.6	3	1220	1	6.8	8	0.73

3.9.4 Illinois Flexibility Index Test

The details of average work of fracture, fracture energy, and flexibility index along with average air voids for two sample preparation techniques are given in **Table 80**.

122

Table 80. Results obtained from the I-FIT

Sample Type	Number of replicates	Air Voids		Work of fracture (Joules)		Fracture energy (Joules/m²)		Flexibility index	
		Avg.	CV (%)	Avg.	CV (%)	Avg.	CV (%)	Avg.	CV (%)
LMLC	02			4.1	7	1357	8	3.3	17
RPMLC	03	6.8	1	6.8	18	2257	18	3.6	11

3.9.5 Hamburg Wheel Tracking Test

The details of the average Hamburg wheel rut depth along with average air voids for two-sample preparation technique are given in

Table 81.

Table 81. Results obtained from the Hamburg wheel tracking test

Sample Type	Number of replicates	Rut Depth Avg. (mm)	Rut Depth CV (%)	Air Voids Avg. (%)	Air Voids CV (%)
LMLC	02	3.270	10	6.8	3
RPMLC	02	4.270	5	7.5	1

3.9.6 Dynamic Modulus

Figure 62 illustrates the dynamic modulus master curve at a reference temperature of 20℃ for two sample preparation techniques. The comparison of stiffness between the LMLC and RMPLC mixtures is represented using the line of equality curve, as shown in the **Figure 63**.
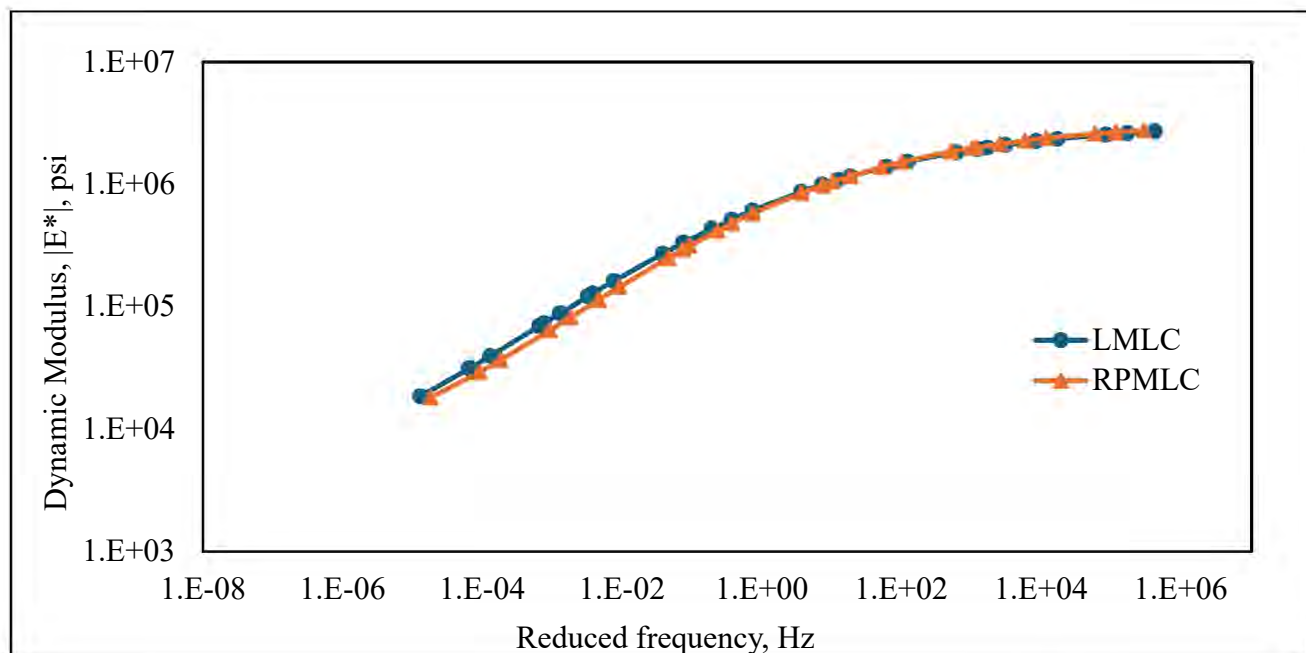
Figure 62. Dynamic Modulus at a reference temperature of 20℃
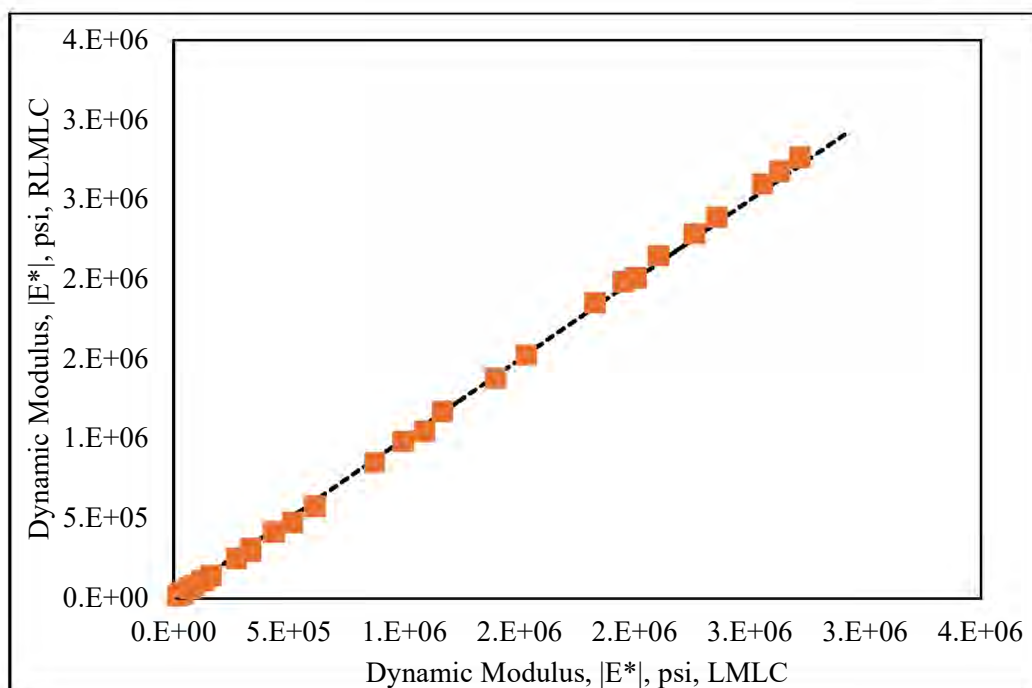

Figure 63. Line of equality, LMLC vs RPMLC

3.9.7 Flow Number

Table 82 presents the details of the average flow number, average micro strain at the flow point, and average air voids for the two sample preparation techniques.

Table 82. Results obtained from the flow number test

Sample Type	Number of replicates	Flow number		Micro strain at flow point		Air voids	
		Avg. (cycles)	CV (%)	Avg.	CV (%)	Avg. (%)	CV (%)
LMLC	02	611	52	25591	13	7.0	8
RPMLC	02	415	13	33088	1	6.9	4

3.10 Comparison of Performance Test Results for All the Field BMD Projects

3.10.1 IDEAL-CT

The CT_{Index} values for the eight BMD projects across the three sample preparation techniques are illustrated in **Figure 64**. The line of equality plots comparing CT_{Index} values of LMLC with PMLC, as well as LMLC with RPMLC, are shown in **Figure 65 and Figure 66**, respectively. These plots indicate that at lower CT_{Index} values, LMLC exhibits slightly greater crack resistance than both PMLC and RPMLC. This trend may be attributed to increased aging and higher stiffness in ACHM produced at the plant compared to those prepared in the laboratory. However, at higher CT_{Index} values, PMLC and RPMLC appear to be slightly more crack resistant than LMLC, while considering the variation in the data, all three LMLC, PMLC, and RPMLC demonstrate comparable cracking resistance. Previous studies (43, 44) have reported higher stiffness in RPMLC mixtures compared to PMLC mixtures, likely due to reheating effects. Interestingly, these findings contrast with those of Johnson et al. (42), who observed greater stiffness in lab-produced mixtures than in plant-produced ones. Conversely, another study (45) found no significant stiffness differences between plant-produced and lab-produced mixtures. It can be concluded here that with considering high variability in the cracking index data, the three sample preparation techniques yield similar performance outcomes. It should be noted that the time that PMLC mixtures were "reheated" in the oven was not recorded, as from the time the mixtures were sampled in the field to the time they were taken to the lab for testing, there was some cooling. The longer the PMLC mixtures were in the oven in an attempt to bring

the mixture back up to compaction temperature, the more aging could occur, which could result in different IDEAL-CT and APA test results. Similar issues could also occur with the RPMLC samples. This was addressed with the "Proposed Specification for Handling Plant-Produced Asphalt Concrete Hot Mix in Laboratory" document provided to ARDOT by the University of Arkansas in March 2023.
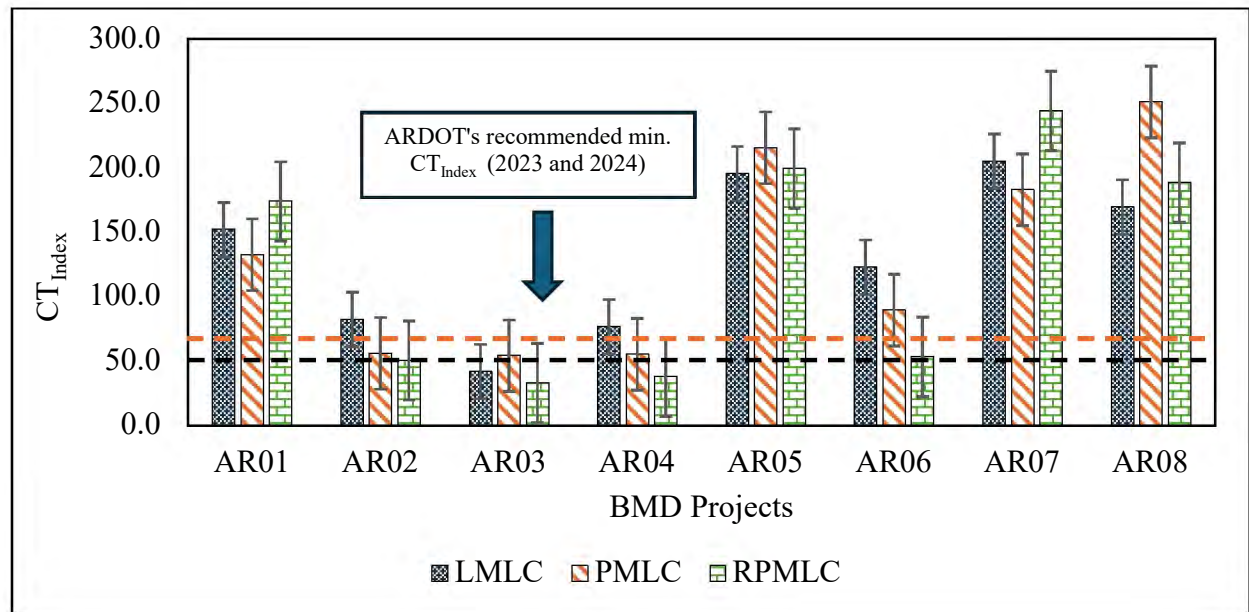
Figure 64. CT$_{Index}$ obtained for the BMD field projects
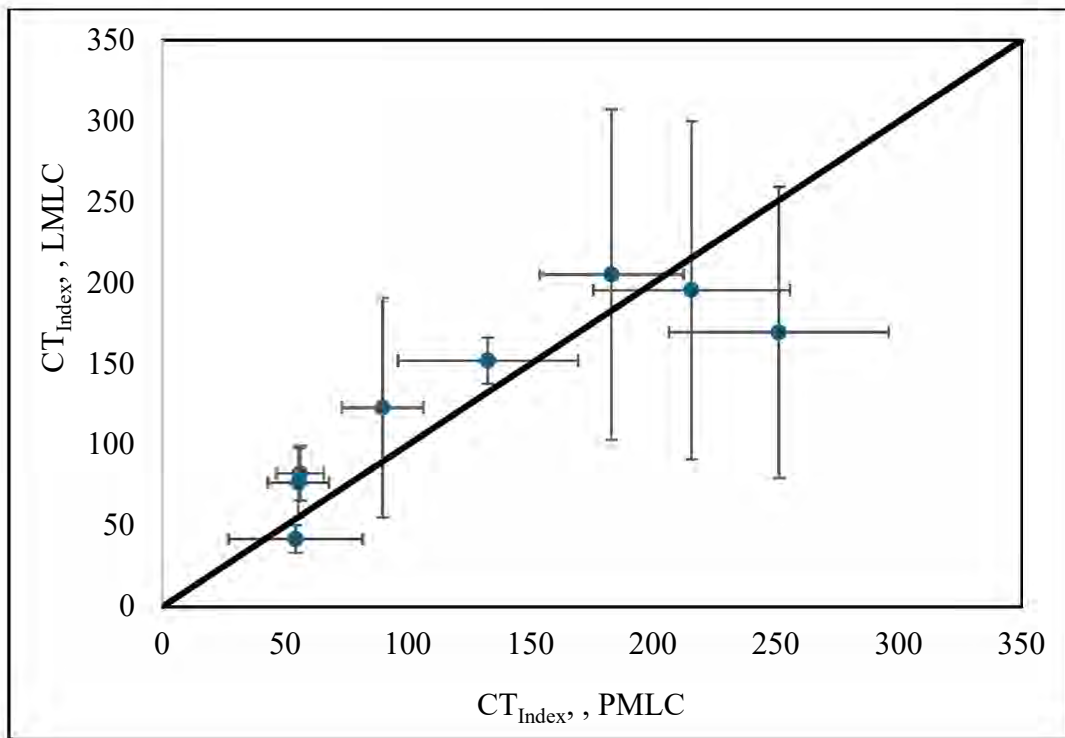
Figure 65. Line of equality plot comparing CT$_{Index}$ values of LMLC and PMLC
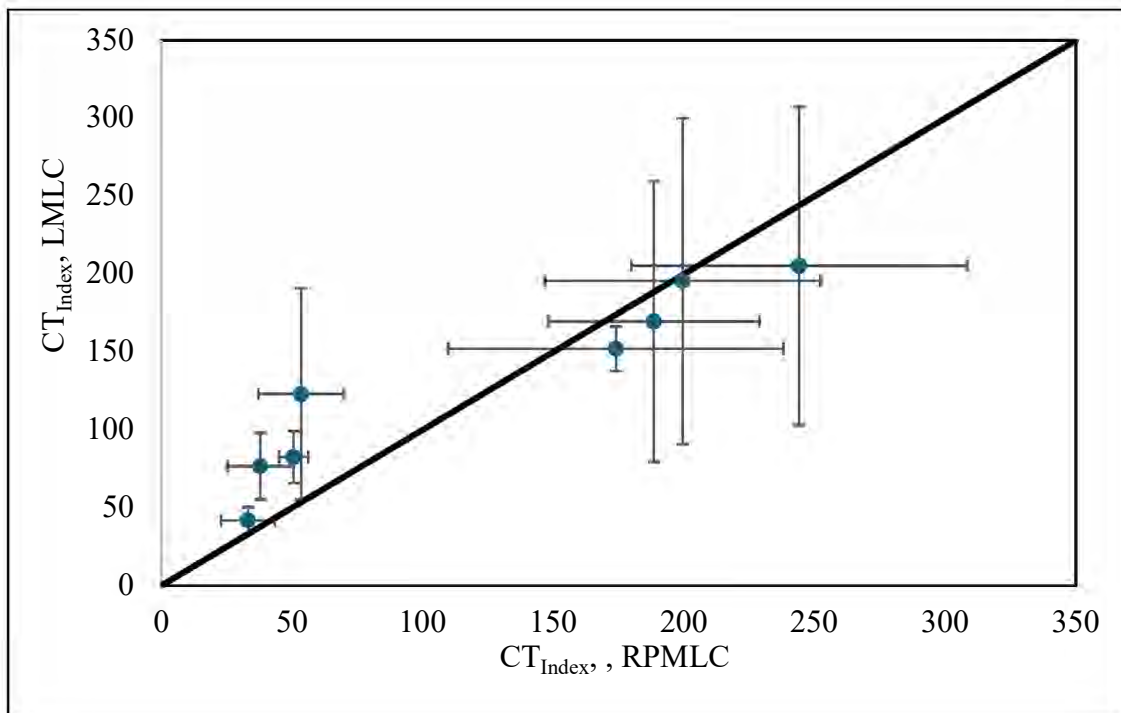
Figure 66. Line of equality plot comparing CT$_{Index}$ values of LMLC and RPMLC

3.10.2 APA

Figure 67 presents the APA rut depth values for the eight BMD projects corresponding to the three sample preparation techniques. The line of equality plots comparing APA rut depth values between LMLC and PMLC, as well as between LMLC and RPMLC, are shown in **Figure 68** and **Figure 69,** respectively. The data reveals no clear pattern in APA rut depth concerning the different sample fabrication methods. Furthermore, the variations in rut depths among the three sample types for each project remain within one standard deviation. Notably, across all eight projects, the rut depth stayed below the maximum values recommended by ARDOT. Based on the available dataset, it can be concluded that rutting is not a concern for ACHM designed within the state. This is likely because contractors have refined their mix designs to enhance rut resistance, particularly since the APA test is an older method compared to the IDEAL-CT test.
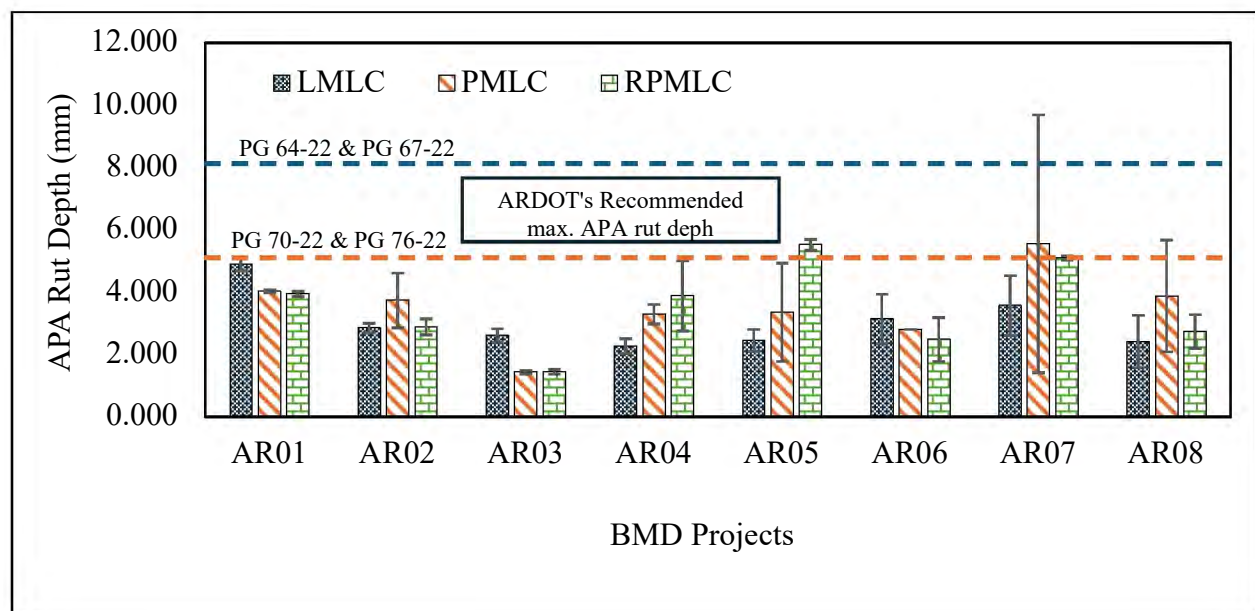
Figure 67. APA rut depth obtained for the BMD field projects
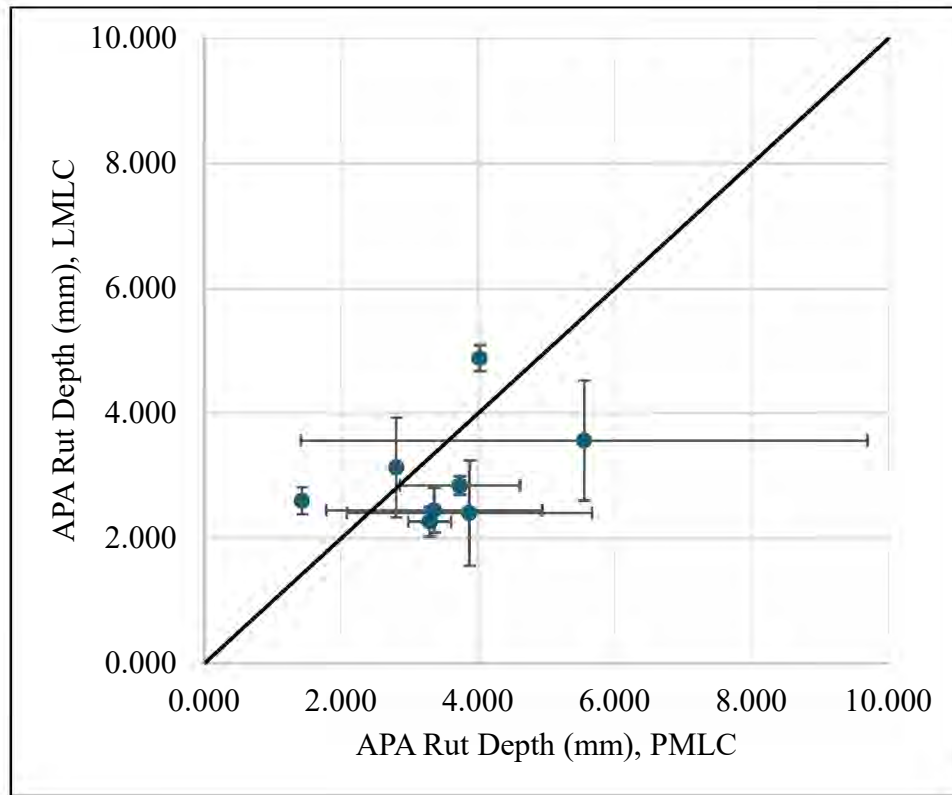
Figure 68. Line of equality plot comparing APA rut depth values of LMLC and PMLC
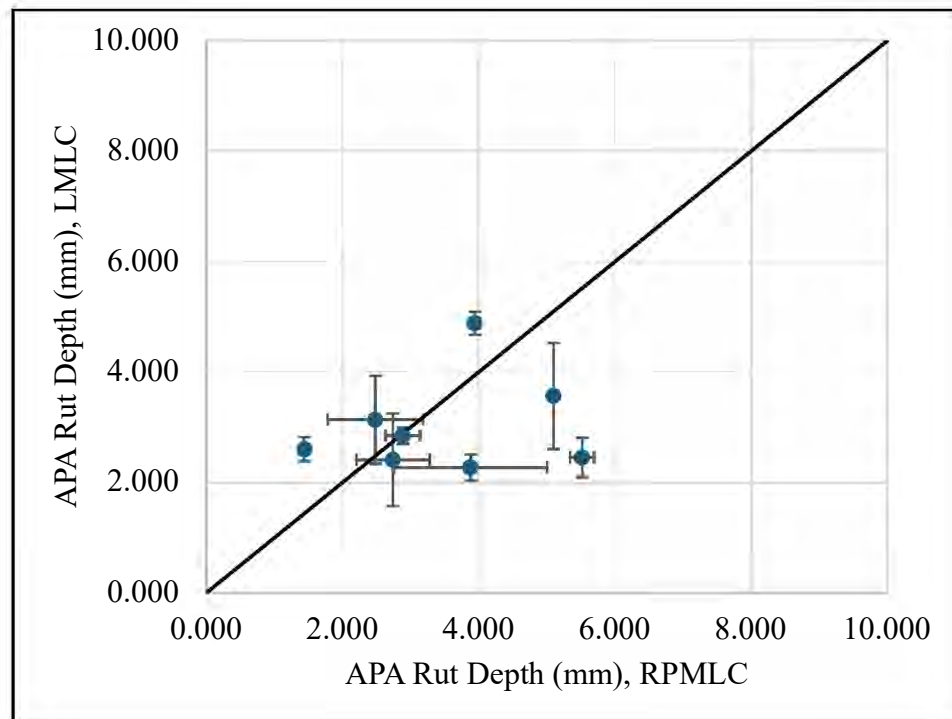
Figure 69. Line of equality plot comparing APA rut depth values of LMLC and RPMLC

3.10.3 Moisture-Induced Damage

Figure 70 presents the results of the moisture conditioned tensile strength and TSR values from the eight BMD projects. The line of equality plots comparing the conditioned and unconditioned strength values between LMLC and PMLC, as well as between LMLC and RPMLC, are shown in **Figure 71** and **Figure 72**, respectively. It was noted that RPMLC samples exhibited higher conditioned and unconditioned strengths than LMLC at higher tensile strengths. However, at lower strength, both methods show similar performance. However, unclear trends for TSR were obtained between the three sample preparation techniques. This reinforces the results obtained from the IDEAL-CT and APA tests that the three sample preparation techniques produce samples exhibiting almost similar performance. Additionally, except for a few mixtures (AR02_LMLC, AR08_LMLC, AR06_RPMLC, AR07_RPMLC, and AR08_RPMLC), all other mixtures have TSR values exceeding the recommended threshold of 0.80.
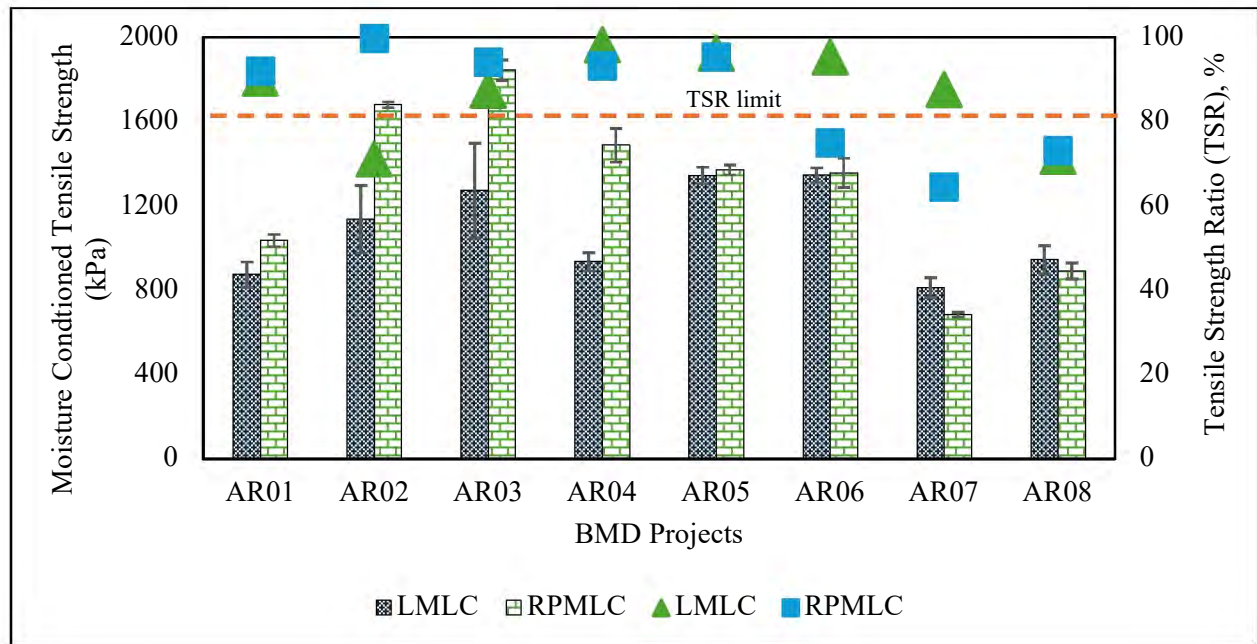
Figure 70. Moisture conditioned tensile strength and TSR values for the BMD field projects. The bars indicated moisture conditioned tensile strength, while the triangle and square icons indicated LMLC and RPMLC TSR values, respectively.

130
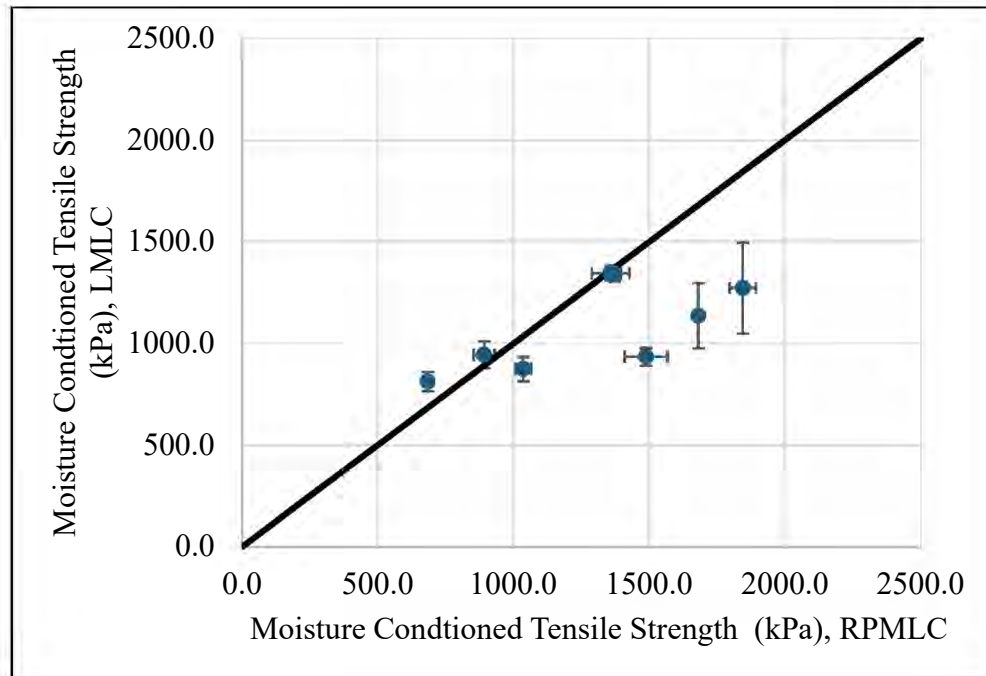
Figure 71. Line of equality plot comparing conditioned strength of LMLC and RPMLC
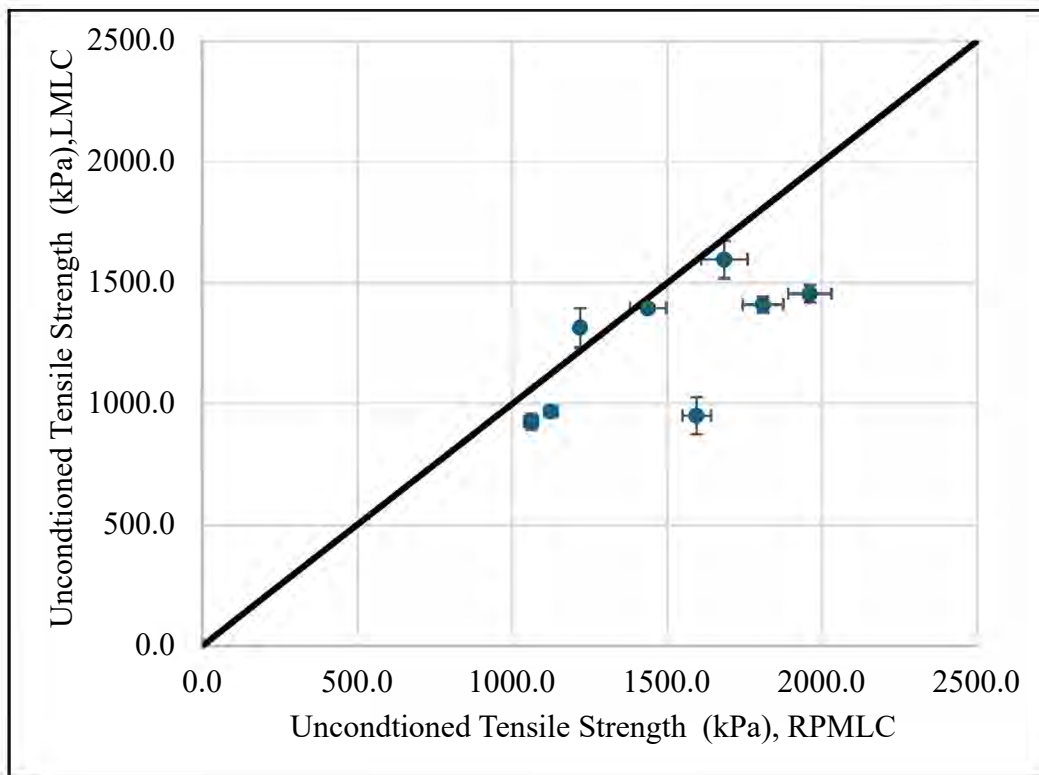
Figure 72. Line of equality plot comparing unconditioned strength of LMLC and RPMLC

3.10.4 HWTT

Figure 73 presents the rut depths measured using the HWTT. In Arkansas, there are no specific standards for HWTT rut depths, as the APA test is the preferred method for evaluating the rutting resistance of ACHM. Therefore, the results obtained from the study have been compared with the HWTT recommendations from Texas, Louisiana, and Oklahoma. Both Texas (46) and Oklahoma (47) set a maximum allowable rut depth of 12.5 mm, while Louisiana (48) recommends a limit of 10.0 mm for Level 1 mixes. The findings from this study indicate that, except for AR04_LMLC and AR07_LMLC, and AR07_RPMLC, all projects had HWTT rut depths below 10.0 mm. This aligns with the results from the APA test, reinforcing that ACHM designed roads in Arkansas do not exhibit significant rutting issues. The line of equality plots comparing rut depth values between LMLC and RPMLC is shown in **Figure 74**, revealing that the rut depths for these two sample types are comparable.
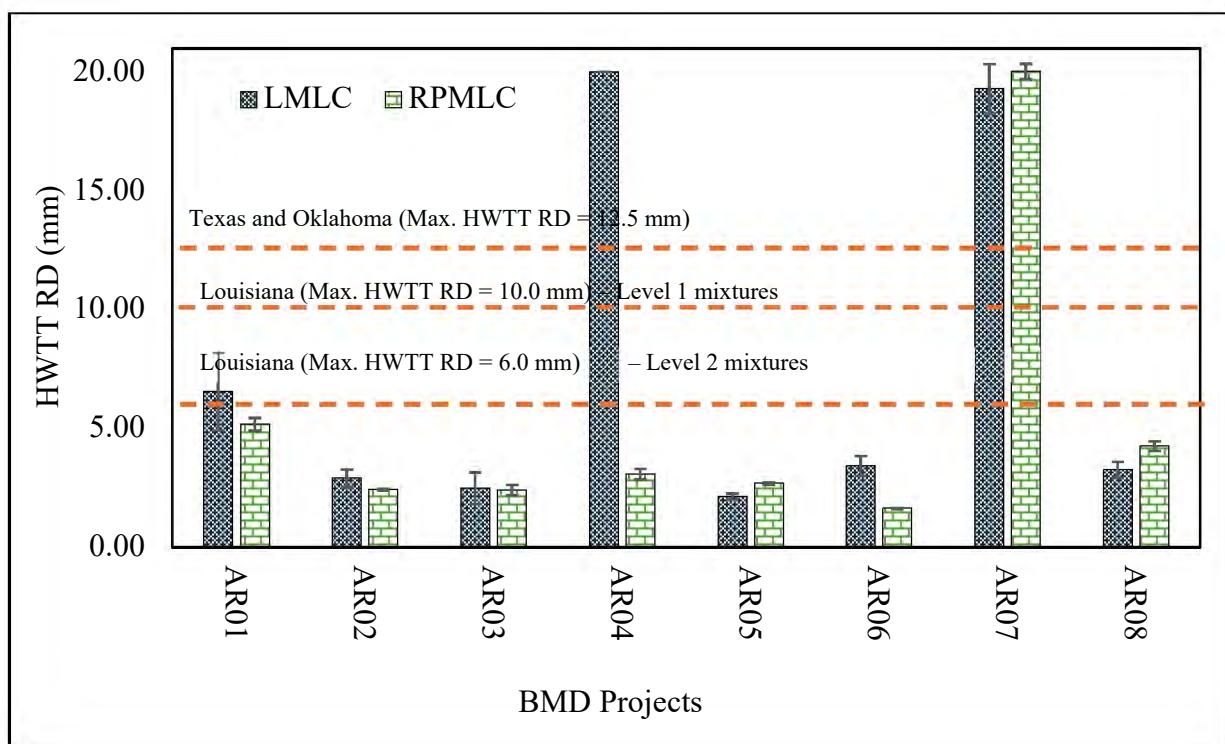
Figure 73. HWTT rut depth for the BMD field projects
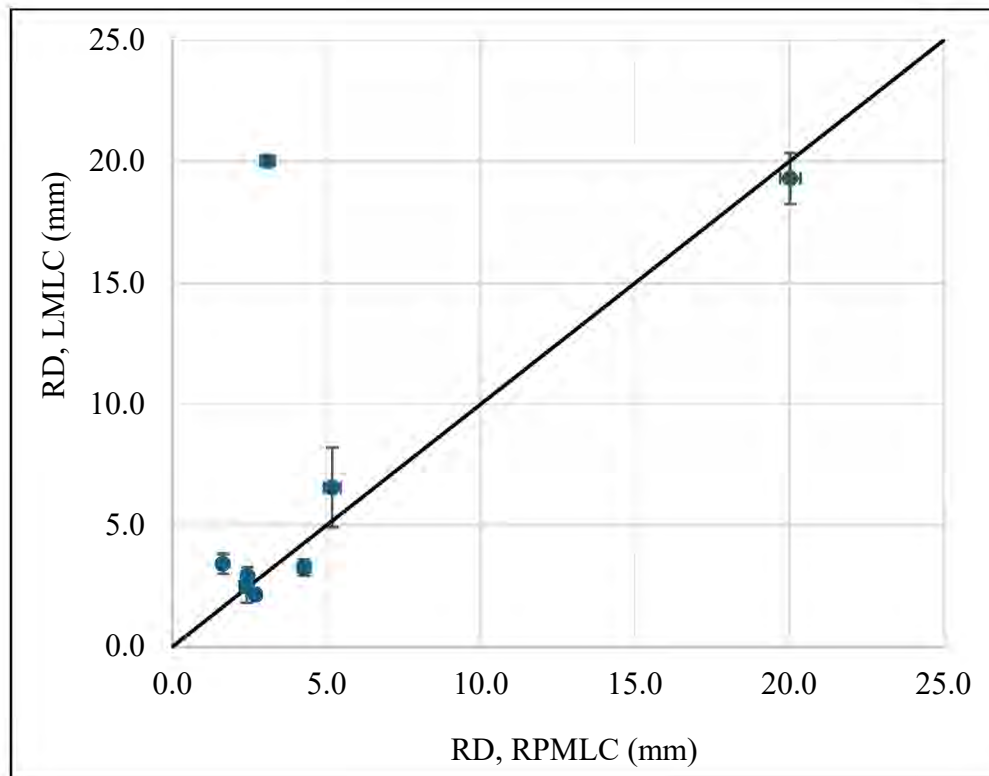
Figure 74. Line of equality plot comparing rut depth of LMLC and RPMLC sample

3.10.5 I-FIT

Figure 75 displays the FI values obtained for the eight BMD field projects. In Arkansas, there are no established standards for I-FIT, as the IDEAL-CT test is the preferred method for assessing the cracking resistance of ACHM. Consequently, the results obtained from the study have been compared with FI recommendations from Illinois and New York, both of which set a minimum FI threshold of 8.0. The study's findings reveal that the average FI values for all eight field projects fall below this recommended minimum. The line of equality plots comparing FI values between LMLC and RPMLC is shown in **Figure 76**, demonstrating that LMLC samples exhibit slightly higher FI values than RPMLC samples; however, considering the variability in the results, both show almost similar performance. This trend aligns with the IDEAL-CT findings at lower CT_{Index} values. Additionally, a notably higher variability in FI values compared to CT_{Index} values was observed. To further validate these results, a larger dataset is needed.
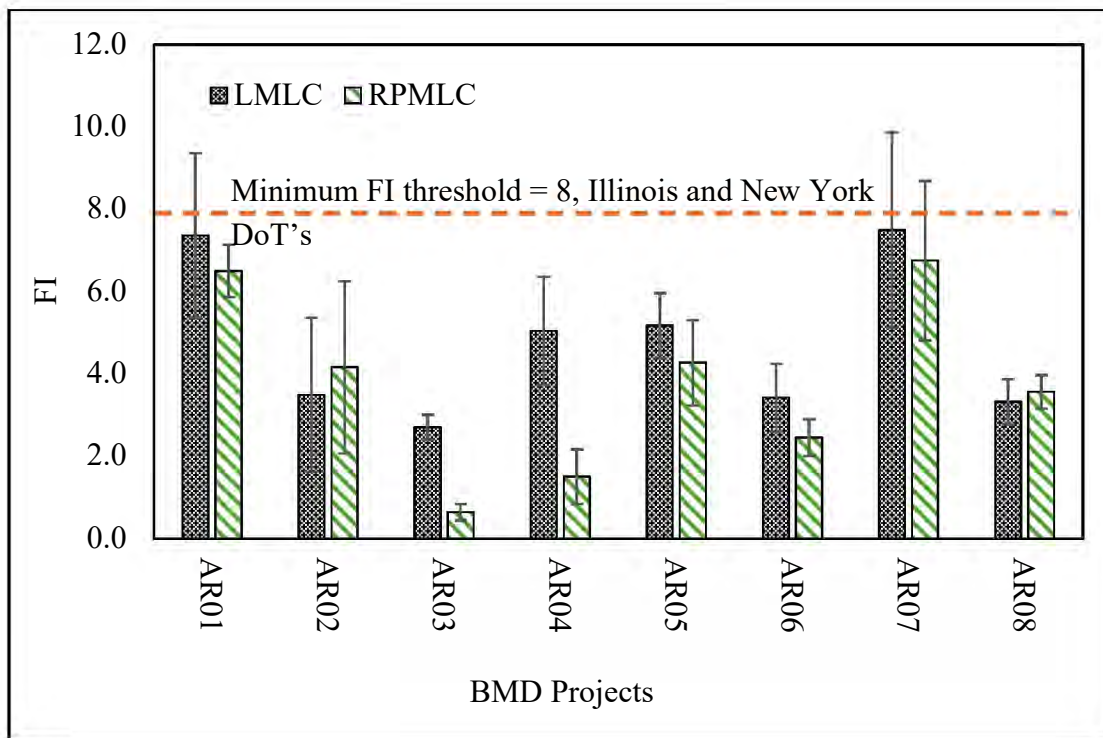
Figure 75. FI obtained for the BMD field projects
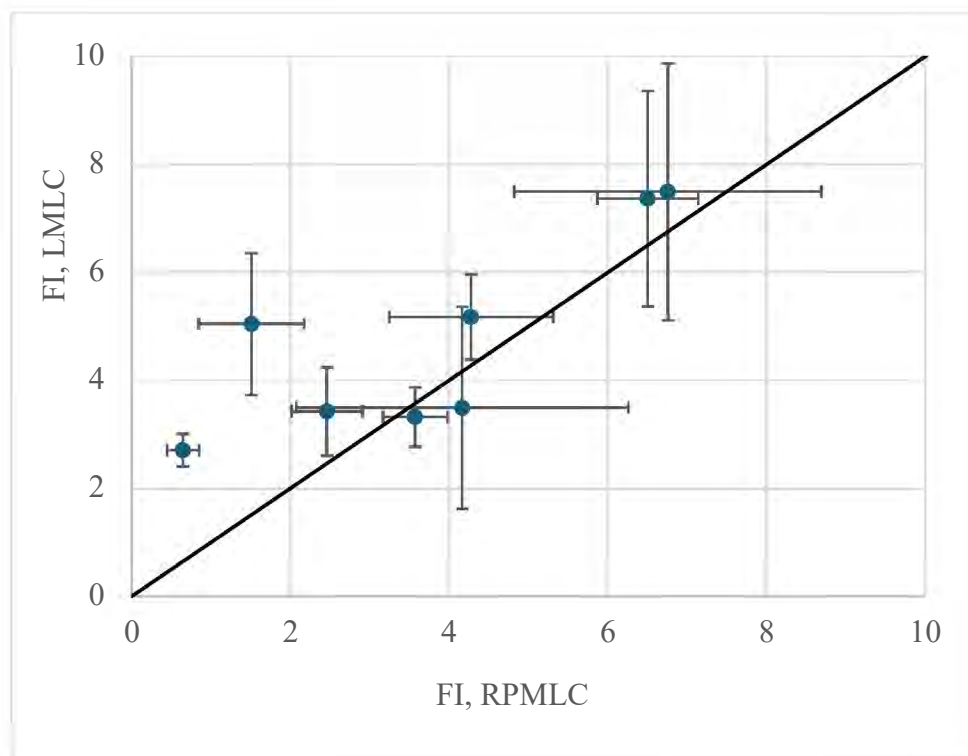
Figure 76. Line of equality plot comparing FI of LMLC and RPMLC samples

3.10.6 Dynamic Modulus

Figure 77 and **Figure 78** present the dynamic modulus master curve for LMLC samples from the BMD field projects approved in 2023 and 2024, respectively. A comparison of stiffness between LMLC and RPMLC samples is illustrated using the line of equality in **Figure 79** and **Figure 80**. The results indicate that RPMLC samples generally exhibit higher stiffness than LMLC samples across most projects. Notably, these findings contradict those of Johnson et al. (42), who reported greater stiffness in lab-produced mixtures compared to plant-produced ones. Previous studies (43, 44) have also found that RMPLC mixtures tend to have higher stiffness than plant-produced mixtures, likely due to reheating effects.
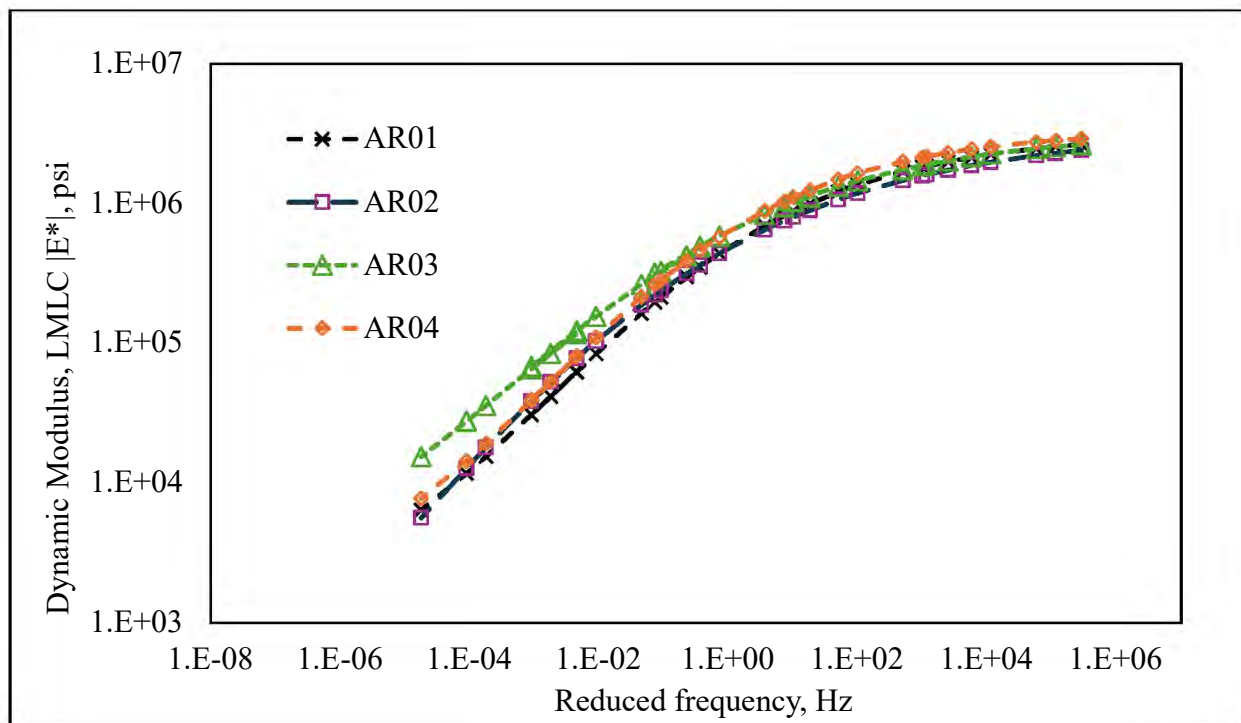
Figure 77. Dynamic modulus master curve plotted at a reference temperature of 20 ℃ for AR01 through AR04
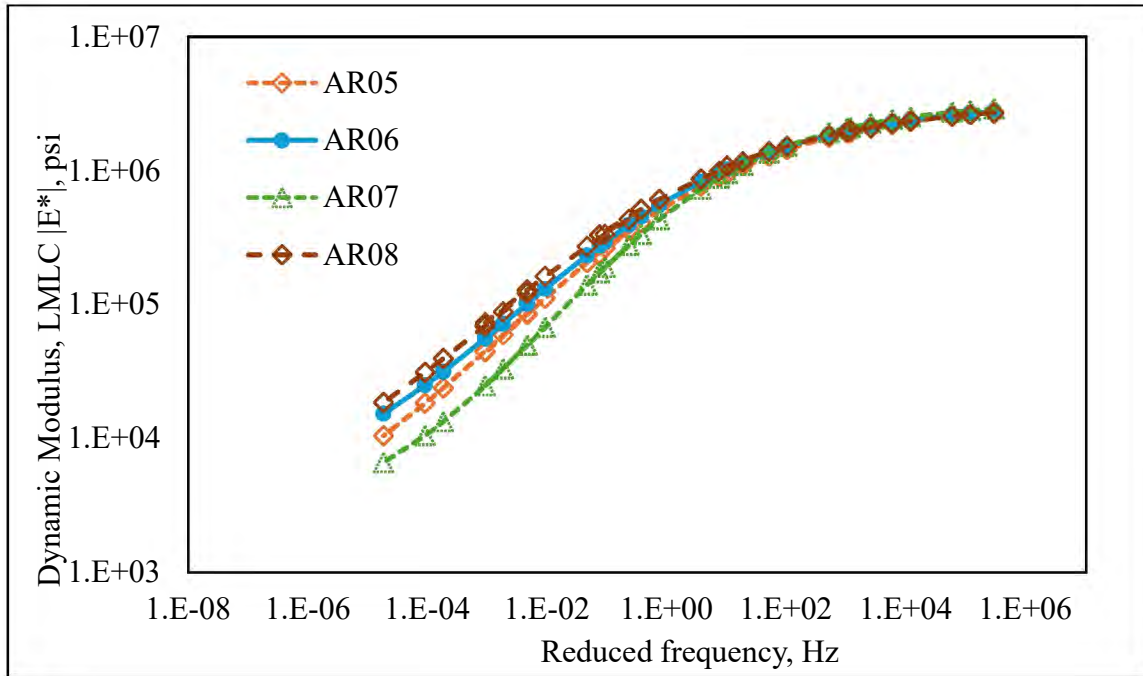
Figure 78. Dynamic modulus master curve plotted at a reference temperature of 20 ℃ for AR05 through AR06
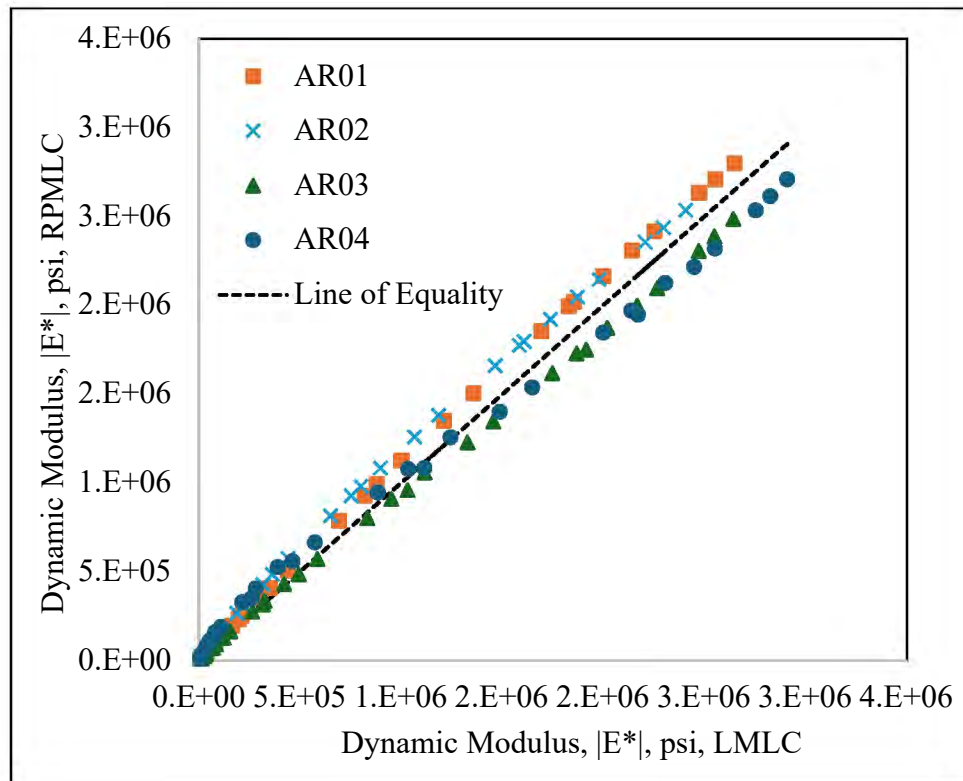
Figure 79. Line of equality comparing the stiffness of LMLC and RPMLC mixture for AR01 through AR04
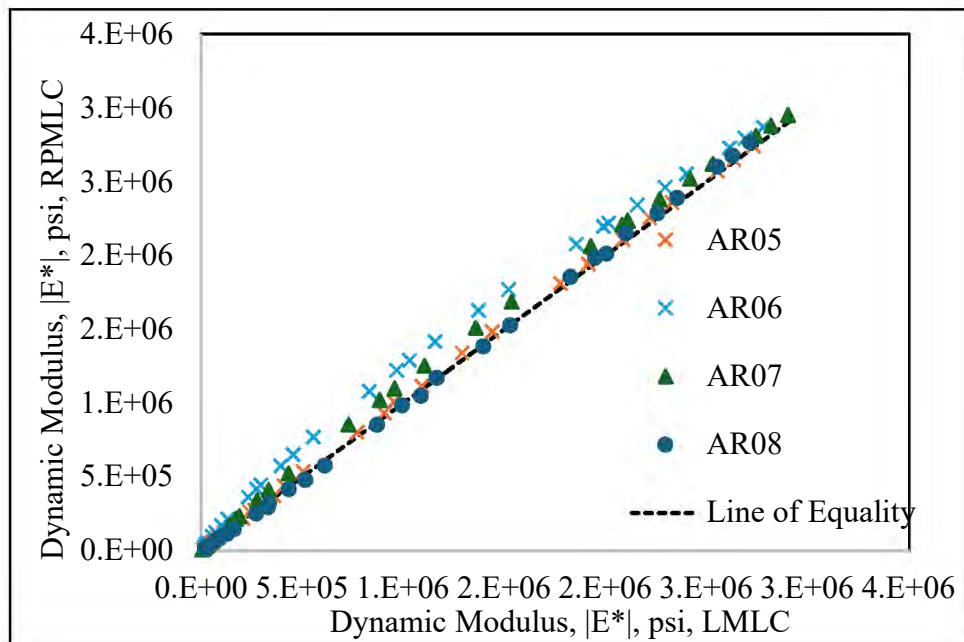
Figure 80. Line of equality comparing the stiffness of LMLC and RPMLC mixture for AR05 through AR06

3.10.7 Flow Number

Figure 81 displays the FN values obtained for the eight BMD field projects. In Arkansas, there are no established standards for FN, as the IDEAL-CT test is the preferred method for assessing the cracking resistance of ACHM. The line of equality plots comparing FI values between LMLC and RPMLC are shown in **Figure 82**, demonstrating that RPMLC samples generally exhibit higher FN values than RPMLC samples, suggesting greater rutting resistance in RPMLC. However, considering the variability in the tests' results, both sample preparation methods show comparable performance.
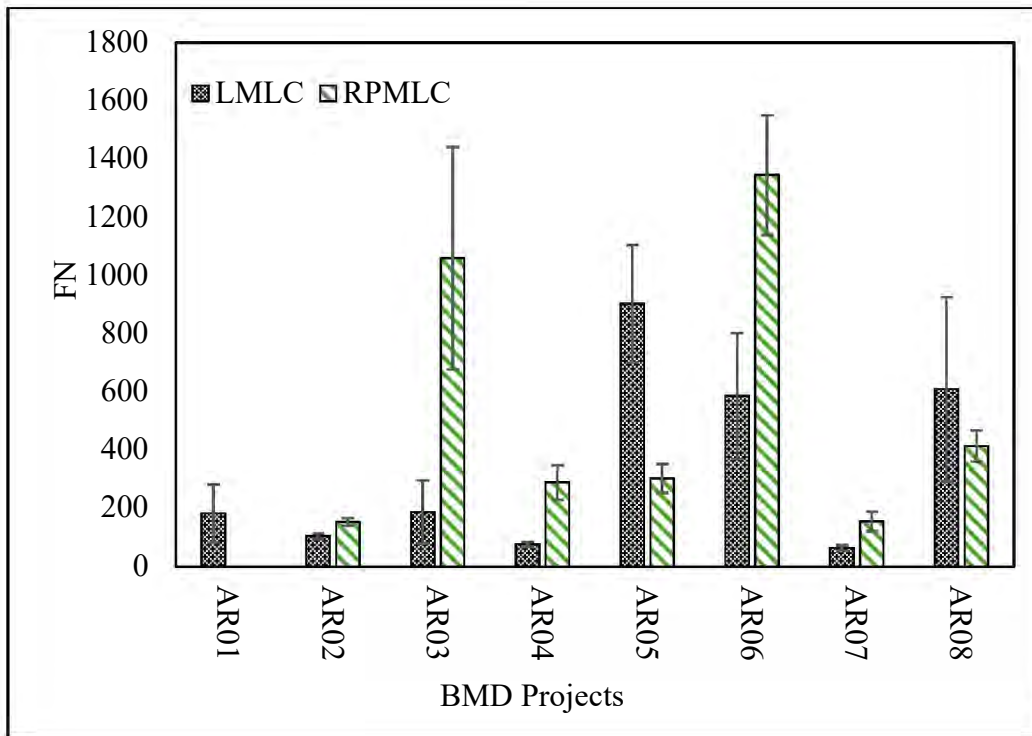
Figure 81. FN obtained for the BMD field projects
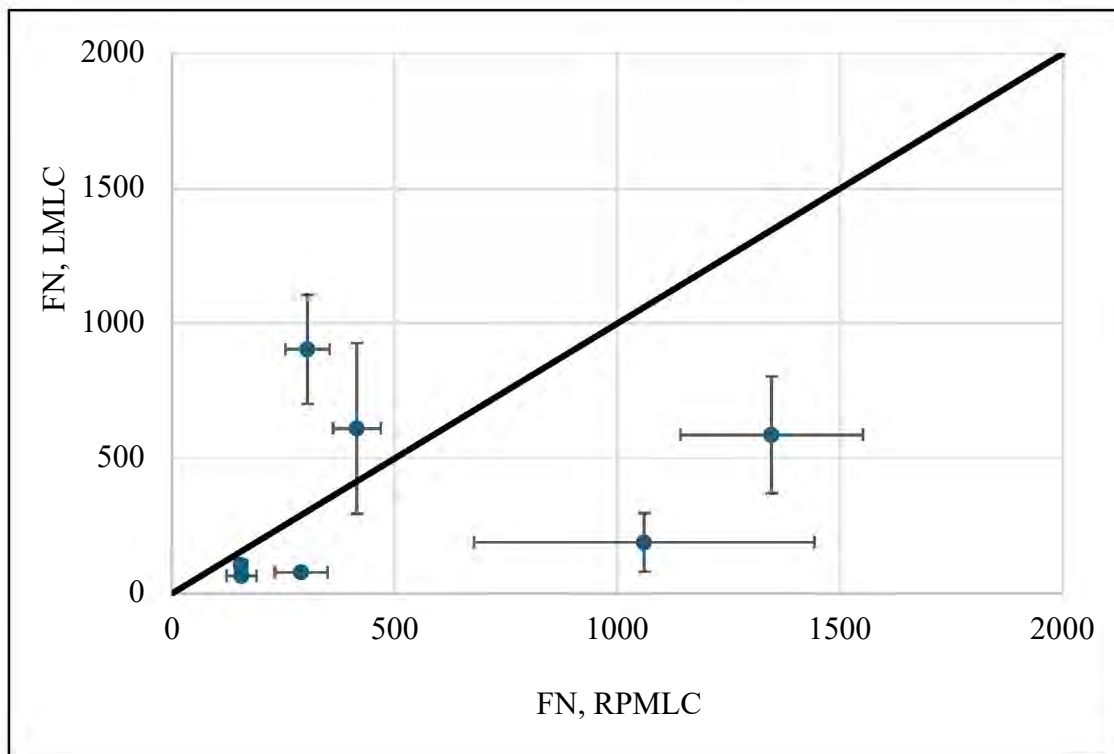
Figure 82. Line of equality plot comparing Flow number of LMLC and RPMLC samples

138

3.11 Conclusions

Rutting and cracking are the primary pavement distresses targeted in BMD, with various methods developed to evaluate ACHM performance in both laboratory and field settings. A comprehensive understanding of the performance characteristics and distinctions between laboratory-produced and plant-produced ACHM is essential for the successful implementation of BMD.

The second part of this study focused on eight field projects approved by ARDOT in 2023 and 2024. The research aimed to compare asphalt samples fabricated using three different methods: LMLC, PMLC, and RPMLC. Initial assessments of rutting and cracking performance were conducted using the APA and IDEAL-CT tests, ARDOT's preferred evaluation methods. Additionally, five supplementary performance tests—moisture-induced damage, HWTT, I-FIT, dynamic modulus, and flow number—were performed to further validate the findings. The study yielded the following key conclusions:

- The CT_{Index} results for the eight BMD projects show that LMLC has slightly better crack resistance at lower values, while PMLC and RPMLC perform slightly better at higher values. Despite some variability, all three sample preparation techniques demonstrate comparable cracking performance overall.

- No consistent trend was observed in APA rut depth across the three fabrication methods. The variability in rut depth among the sample types was minimal, with all rut depths remaining within ARDOT's recommended limits for the eight BMD projects.

- RPMLC samples generally exhibited higher strength than LMLC at higher values, while both performed similarly at lower strengths. TSR values showed no clear trend among the techniques, supporting earlier findings from IDEAL-CT and APA tests that all three methods yield comparable performance. Most mixtures met the recommended TSR threshold of 0.80, with only a few exceptions.

- HWTT rut depths for the eight BMD projects show that with most results falling below the 10.0 mm limit recommended by Louisiana. Only AR04_LMLC, AR07_LMLC, and AR07_RPMLC exceeded this threshold. These findings, supported by APA test results,

confirm that ACHM mixtures in Arkansas generally show good rutting resistance, with comparable performance between LMLC and RPMLC.

- FI values for all eight BMD field projects fall below the minimum threshold of 8.0 recommended by Illinois and New York. LMLC samples generally exhibit slightly higher FI values than RPMLC, though both show similar performance when accounting for variability. The findings align with IDEAL-CT results at lower CT_{Index} values, but the higher variability in FI suggests that additional data is needed for validation.

- Dynamic modulus test results indicated that RPMLC samples generally exhibited higher stiffness than LMLC samples across most projects. These findings both align with and contradict previous studies, highlighting the need for further validation with a larger dataset.

- RPMLC samples generally have higher FN values than LMLC, indicating potentially better rutting resistance. However, due to variability in results, both preparation methods demonstrate comparable overall performance.

Chapter 4. AASHTOWare Pavement Me

The influence of sample fabrication technique on the long-term performance of pavement was evaluated using the AASHTOWare Pavement ME software, referred to as Pavement ME in this study. The software offers three levels of analysis: Level 1, Level 2, and Level 3 (**54**) as shown in **Figure 83**. Level 1 analysis requires binder's viscoelastic properties (complex shear modulus, G*, and phase angle, δ) and ACHM's stiffness properties (|E*|) as inputs, which were used in this study to compare the long-term performance of LMLC mixture to RPMLC mixture.
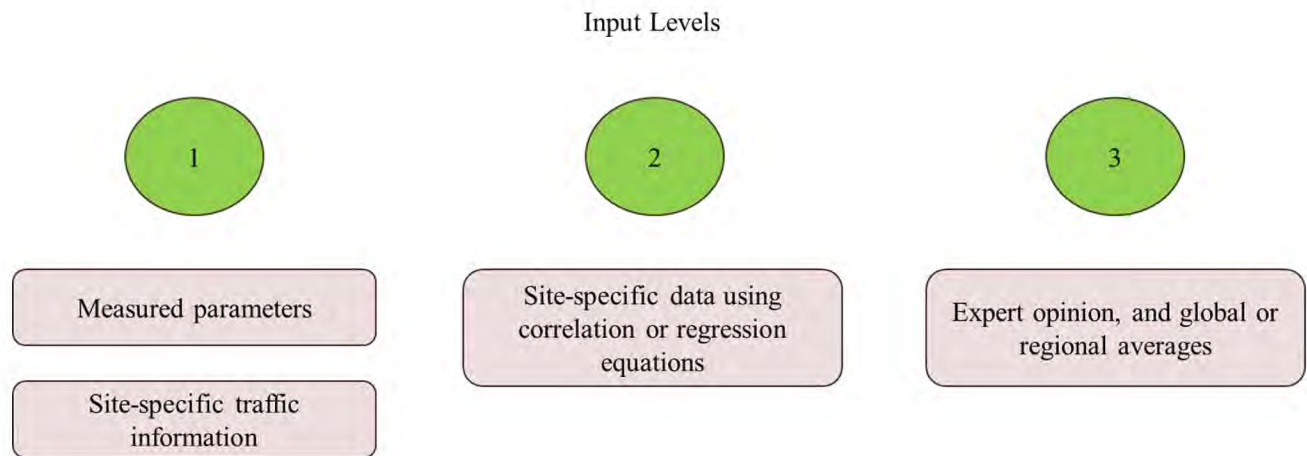
Figure 83. Input levels in Pavement ME software

4.1 Input details

This study analyzed four pavement sections that differed in terms of asphalt layer thicknesses and traffic levels. The four-pavement structures used for the analysis are shown in **Figure 84** and the location of each section is shown in **Figure 85**. The traffic and truck percentage for all four sections is given in **Table 83** and the inputs required for traffic calculation in MEPDG are mentioned in **Table 84.** The total number of trucks over the 20-year design life is also presented in **Table 84**. Among the roads, I-40 experiences the highest truck traffic over this period, while County Road sees the lowest.

Table 83: Traffic and truck percentage for each project

Cross-Section Location	Design Lanes	Design Year AADT	Percent Trucks (%)	Design Speed (mph)
I-40	2	41,000	56	70
I-555	2	45,000	15	55
I-49 North	2 (North Only)	15,000	20	70
County Rd.	1	500	10	40

Table 84: MEPDG inputs for traffic calculation

Pavement cross sections	R (%)	DDF	LDF	Two-way AADTT	Heavy Trucks (cumulative)
I-40	90	0.50	0.80	22,960	102.37
I-555	90	0.50	0.80	6,750	30.09
I-49 North	90	1.00	0.80	3,000	26.75
County Rd.	90	0.50	1.00	50	0.45

All four-pavement sections used the same climate data obtained from the weather station located in Paragould, Arkansas. The base and subgrade layer properties were kept constant between the pavement sections and for the BMD projects. The properties of the ACHM layers within each section were uniform but varied according to the BMD project. For each BMD project, the asphalt layer properties ($|E^*|$, V_a, P_b, G^*, δ, aggregate gradation) were varied as per the data obtained from mix designs and laboratory tests. The viscoelastic properties of the binder, including the complex shear modulus (G) and phase angle (δ), are provided in **Table 85. Table 86 (55)** presents the performance criteria for each type of pavement distress, which will be used to evaluate the long-term performance of the ARDOT balanced mix design mixture. The default MEPDG values were used in this study to evaluate mixture performance. Since the comparison focuses on LMLC vs. RPMLC and BMD vs. Superpave mixtures, the terminal distress values do not influence the comparative results.
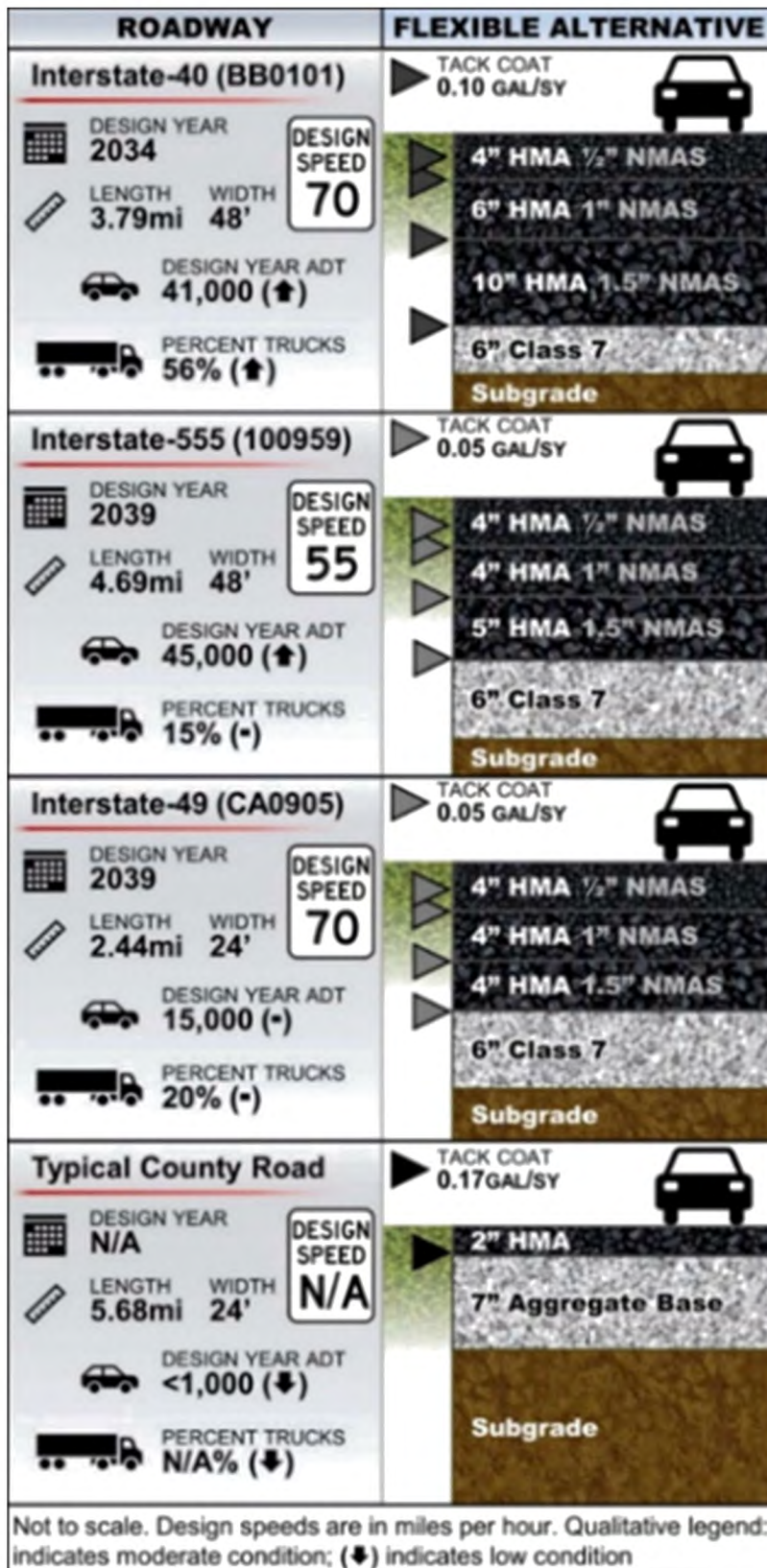
Figure 84: Pavement structure for Pavement ME (56)

Figure 85: Pavement cross section location in Arkansas state

Table 85. Binder's viscoelastic properties for all BMD projects

BMD Project/Temperature (° F)	Binder G* (Pa)			Phase angle (deg)		
	147.2	158	168.8	147.2	158	168.8
AR01	1190	574	297	87.50	88.50	89.20
AR02	2940	1555	840	73.65	74.60	75.40
AR03	2135	985	493	83.10	83.10	81.35
AR04	1290	630	331	84.10	82.35	78.50
AR05	5580	3230	1943	61.57	61.37	61.20
AR06	4795	2670	1535	66.20	66.85	67.75
AR07	1447	696	358	84.97	83.90	80.63
AR08	7917	4360	2447	62.23	64.63	66.97

Table 86. Performance criteria for pavement distress

Distress	Pavement ME default value	Indiana DOT	Colorado DOT
International Roughness Index, IRI (in/mi)	172	160	160
AC top-down fatigue cracking (%lane area)	25	-	-
AC bottom-up fatigue cracking (%lane area)	25	10	10
AC thermal cracking (ft/mile)	1000	500	1500
Total permanent deformation (in)	0.75	-	0.4
Asphalt layer deformation (in)	0.25	0.4	0.25

4.2 LMLC vs RPMLC

Pavement ME predicts distress progression over a 20-year pavement life. **Figure 86** illustrates the progression of the International Roughness Index (IRI) in BMD project AR01 with LMLC samples for all cross sections, showing a steady rate of increase over time. **Figure 87** illustrate the progression of total permanent deformation.

(a)

(b)

(c)

(d)
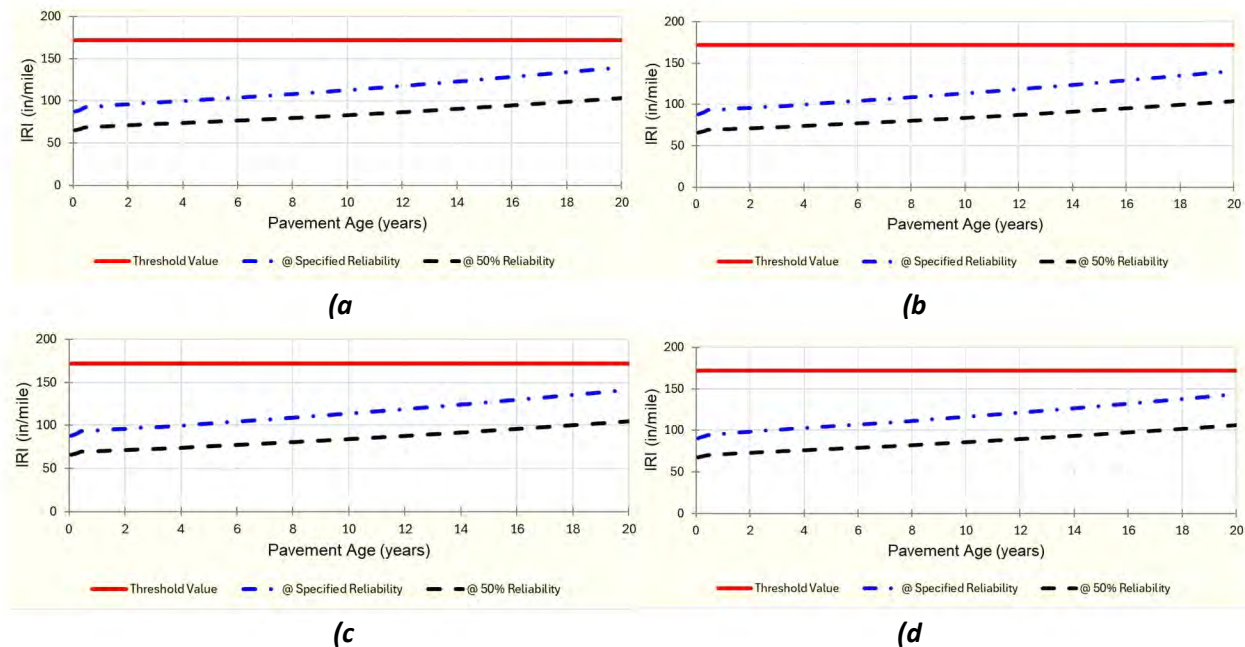
Figure 86: IRI progression in 20 years of life for BMD project AR01 with LMLC samples; a) I-40, b) I-555, c) I-49, d) County Road

145
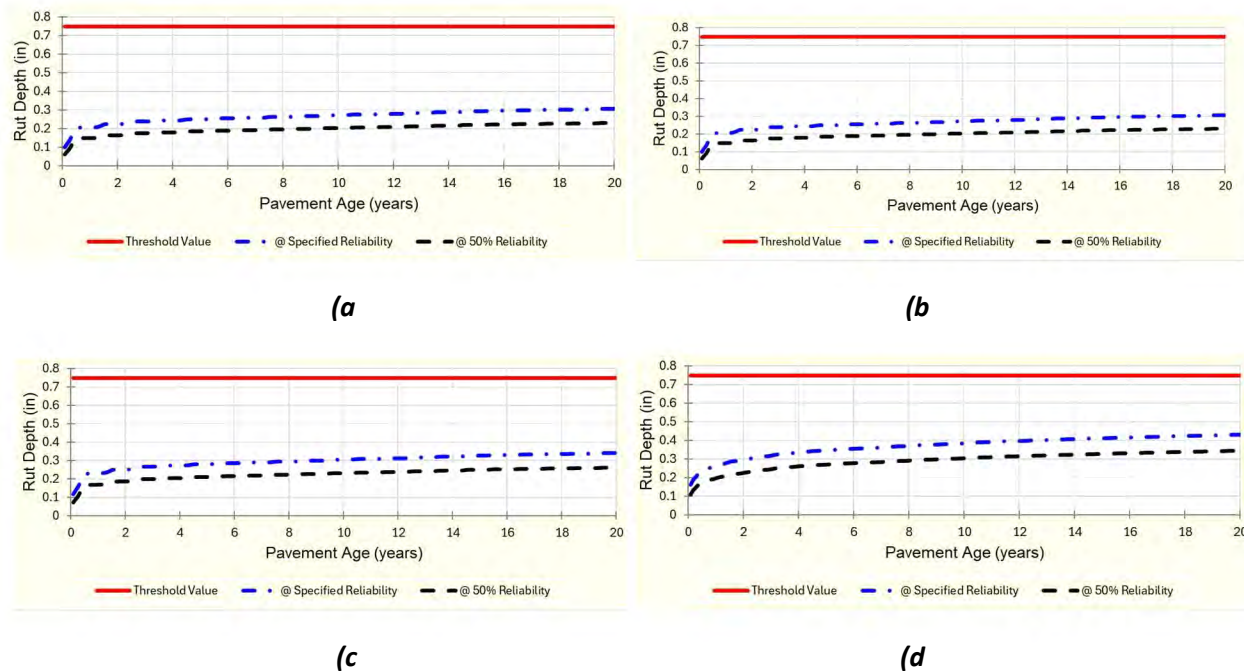
Figure 87: Total permanent deformation progression in 20 years of life BMD project AR01 with LMLC samples; a) I-40, b) I-555, c) I-49, d) County Road

Pavement distress for all BMD projects, using both LMLC and RPMLC, was calculated and is presented in **Table 87** to **Table 90** for the pavement cross-sections I-40, I-555, I-49, and the County Road, respectively. The values shown represent the predicted distress at the end of a 20-year service life.

Table 87. Average pavement distress at the end of 20 years of life in pavement cross section I-40

Project		AR01	AR02	AR03	AR04	AR05	AR06	AR07	AR08
LMLC	Terminal IRI (in/mile)	140.00	140.00	139.20	138.30	138.90	138.70	140.00	138.90
	Permanent deformation - total pavement (in)	0.31	0.30	0.28	0.27	0.28	0.27	0.31	0.28
	AC bottom-up fatigue cracking (% lane area)	1.45	1.45	1.45	1.45	1.45	1.45	1.45	1.45
	AC thermal cracking (ft/mile)	442.97	440.58	495.83	440.57	440.57	440.57	440.61	440.75
	AC top-down fatigue cracking (% lane area)	14.16	14.22	14.26	14.17	14.20	14.23	14.01	14.26
	Permanent deformation - AC only (in)	0.14	0.14	0.11	0.10	0.12	0.11	0.15	0.11
RPMLC	Terminal IRI (in/mile)	139.20	138.50	139.10	137.40	138.80	137.30	139.00	139.10
	Permanent deformation - total pavement (in)	0.29	0.27	0.27	0.24	0.28	0.24	0.28	0.28
	AC bottom-up fatigue cracking (% lane area)	1.45	1.45	1.45	1.45	1.45	1.45	1.45	1.45
	AC thermal cracking (ft/mile)	442.97	440.58	495.83	440.57	440.57	440.57	440.61	440.75
	AC top-down fatigue cracking (% lane area)	14.20	14.25	14.26	14.25	14.23	14.26	14.01	14.25
	Permanent deformation - AC only (in)	0.12	0.10	0.11	0.08	0.11	0.08	0.12	0.12

Table 88. Average pavement distress at the end of 20 years of life in pavement cross section I-555

Project		AR01	AR02	AR03	AR04	AR05	AR06	AR07	AR08
LMLC	Terminal IRI (in/mile)	140.90	140.80	140.60	139.30	139.80	139.70	140.70	139.90
	Permanent deformation - total pavement (in)	0.33	0.32	0.30	0.29	0.30	0.30	0.33	0.30
	AC bottom-up fatigue cracking (% lane area)	1.55	1.56	1.52	1.50	1.50	1.51	1.53	1.53
	AC thermal cracking (ft/mile)	448.26	440.59	550.30	440.58	440.57	440.57	440.68	441.57
	AC top-down fatigue cracking (% lane area)	13.66	14.00	14.20	13.76	13.92	14.10	12.75	14.20
	Permanent deformation - AC only (in)	0.13	0.13	0.10	0.09	0.11	0.10	0.14	0.10
RPMLC	Terminal IRI (in/mile)	140.20	139.50	140.50	138.50	139.70	138.40	139.70	140.10
	Permanent deformation - total pavement (in)	0.31	0.29	0.30	0.27	0.30	0.27	0.31	0.31
	AC bottom-up fatigue cracking (% lane area)	1.52	1.51	1.53	1.49	1.45	1.48	1.51	1.53
	AC thermal cracking (ft/mile)	448.26	440.60	550.30	440.58	440.57	440.57	440.68	441.57
	AC top-down fatigue cracking (% lane area)	13.89	14.14	14.20	14.16	14.06	14.22	12.79	14.16
	Permanent deformation - AC only (in)	0.11	0.09	0.10	0.07	0.10	0.07	0.11	0.11

Table 89. Average pavement distress at the end of 20 years of life in pavement cross section I-49

Project		AR01	AR02	AR03	AR04	AR05	AR06	AR07	AR08
	Terminal IRI (in/mile)	141.40	141.50	141.20	139.70	140.30	140.20	141.10	140.40
	Permanent deformation - total pavement (in)	0.34	0.34	0.31	0.30	0.31	0.31	0.34	0.31
LMLC	AC bottom-up fatigue cracking (% lane area)	1.75	1.80	1.68	1.59	1.61	1.62	1.70	1.69
	AC thermal cracking (ft/mile)	449.13	440.61	560.08	440.58	440.57	440.57	440.70	441.87
	AC top-down fatigue cracking (% lane area)	13.56	13.95	14.19	13.67	13.88	14.07	12.44	14.19
	Permanent deformation - AC only (in)	0.14	0.14	0.11	0.10	0.11	0.11	0.14	0.11
	Terminal IRI (in/mile)	140.60	140.00	141.10	138.90	140.20	138.80	140.00	140.60
	Permanent deformation - total pavement (in)	0.32	0.30	0.31	0.28	0.31	0.28	0.32	0.32
RPMLC	AC bottom-up fatigue cracking (% lane area)	1.67	1.65	1.69	1.56	1.60	1.54	1.62	1.70
	AC thermal cracking (ft/mile)	449.13	440.61	560.08	440.58	440.57	440.57	440.70	441.87
	AC top-down fatigue cracking (% lane area)	13.84	14.13	14.20	14.14	14.01	14.20	12.50	14.13
	Permanent deformation - AC only (in)	0.12	0.10	0.10	0.08	0.11	0.07	0.12	0.11

Table 90. Average pavement distress at the end of 20 years of life in pavement cross section County Road

Project		AR01	AR02	AR03	AR04	AR05	AR06	AR07	AR08
	Terminal IRI (in/mile)	143.40	142.60	147.40	141.50	141.70	141.60	142.50	142.20
	Permanent deformation - total pavement (in)	0.43	0.43	0.42	0.41	0.41	0.41	0.43	0.42
LMLC	AC bottom-up fatigue cracking (% lane area)	1.45	1.45	1.45	1.45	1.45	1.45	1.45	1.45
	AC thermal cracking (ft/mile)	551.82	444.35	1130.41	440.76	440.57	440.58	452.59	474.19
	AC top-down fatigue cracking (% lane area)	4.69	4.69	4.69	4.69	4.69	4.69	4.69	4.69
	Permanent deformation - AC only (in)	0.10	0.10	0.08	0.08	0.09	0.08	0.10	0.09
	Terminal IRI (in/mile)	142.90	141.80	147.40	141.10	141.60	140.80	142.00	142.30
	Permanent deformation - total pavement (in)	0.42	0.41	0.42	0.40	0.41	0.39	0.42	0.42
RPMLC	AC bottom-up fatigue cracking (% lane area)	1.45	1.45	1.45	1.45	1.45	1.45	1.45	1.45
	AC thermal cracking (ft/mile)	551.82	444.35	1130.41	440.76	440.57	440.58	452.59	474.19
	AC top-down fatigue cracking (% lane area)	4.69	4.69	4.69	4.69	4.69	4.69	4.69	4.69
	Permanent deformation - AC only (in)	0.09	0.08	0.08	0.07	0.09	0.07	0.09	0.09

The comparison of pavement distress for BMD Project AR01 at pavement cross-section I-555 is illustrated in **Figure 88** through **Figure 93**. The IRI is slightly higher for LMLC samples than for RPMLC. Rutting is also greater in LMLC, which can be attributed to its lower dynamic modulus compared to RPMLC. AC bottom-up cracking is more pronounced in LMLC, while RPMLC, having a higher modulus, shows less of this distress. AC thermal cracking is similar for both sample preparation methods. However, AC top-down cracking is more significant in RPMLC than in LMLC. Permanent deformation is also higher in LMLC. These results suggest that higher dynamic modulus tends to reduce rutting-related distress but may increase cracking-related distress, such as top-down cracking. On the other hand, the lower modulus in LMLC is associated with greater bottom-up cracking.
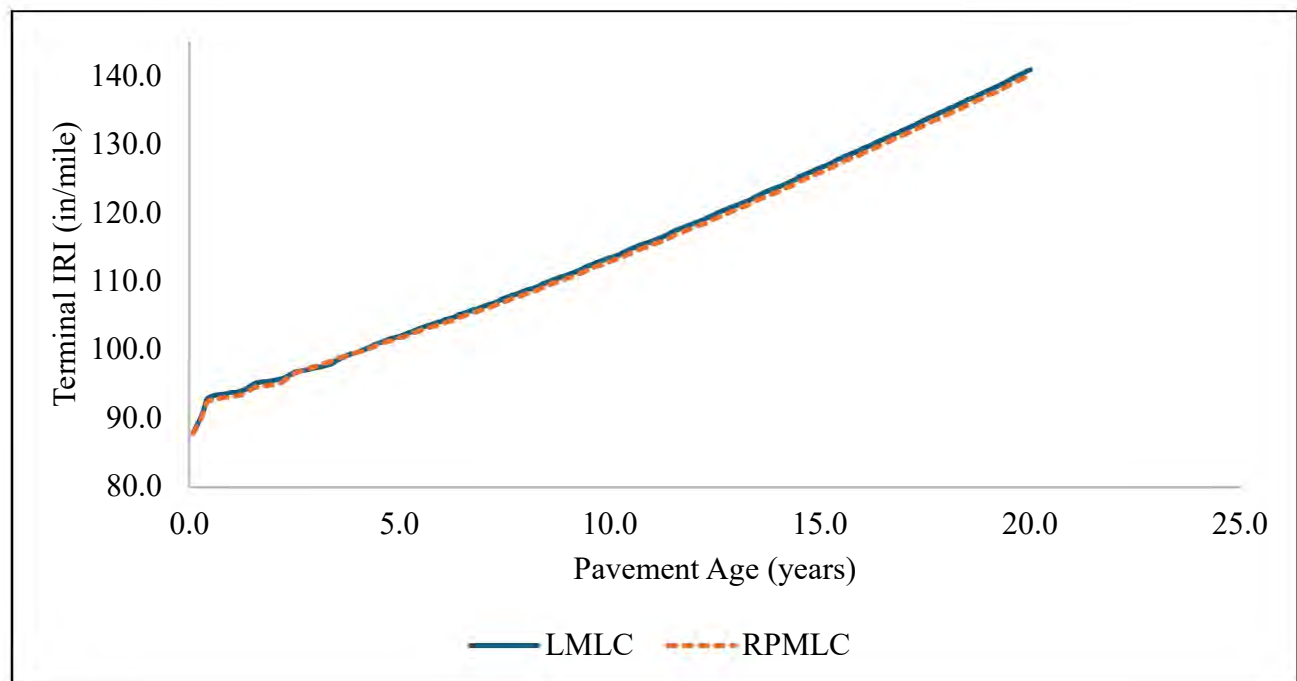
Figure 88: Comparison of International Roughness Index for LMLC and RPMLC mixtures at I-555 section in BMD project AR01.

Figure 89: Comparison of Permanent deformation - total pavement for LMLC and RPMLC mixtures at I-555 section in BMD project AR01.
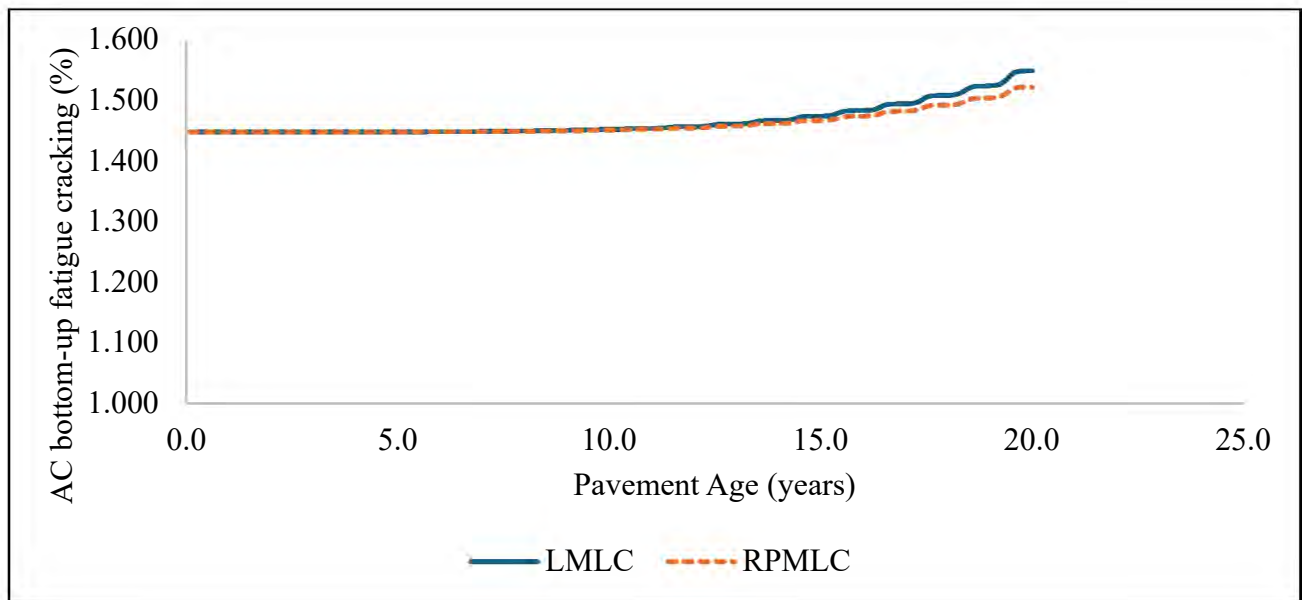
Figure 90: Comparison of AC bottom-up fatigue cracking for LMLC and RPMLC mixtures at I-555 section in BMD project AR01.
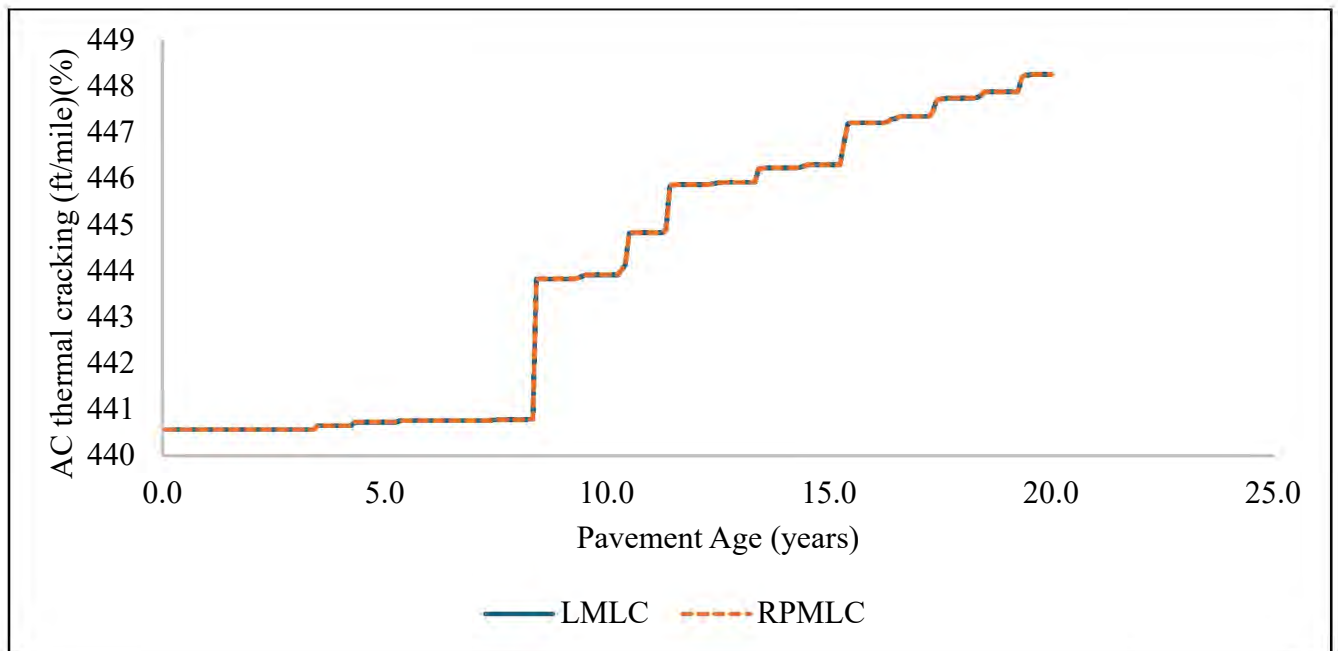
Figure 91: Comparison of AC thermal cracking (ft/mile) for LMLC and RPMLC mixtures at I-555 section in BMD project AR01.

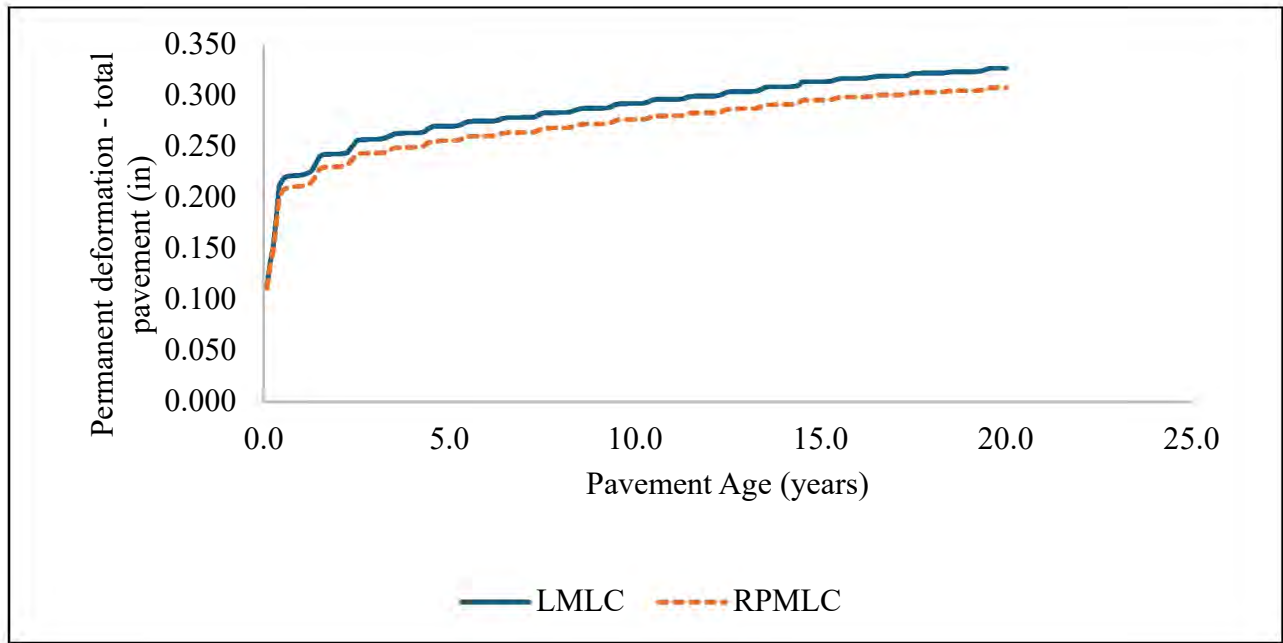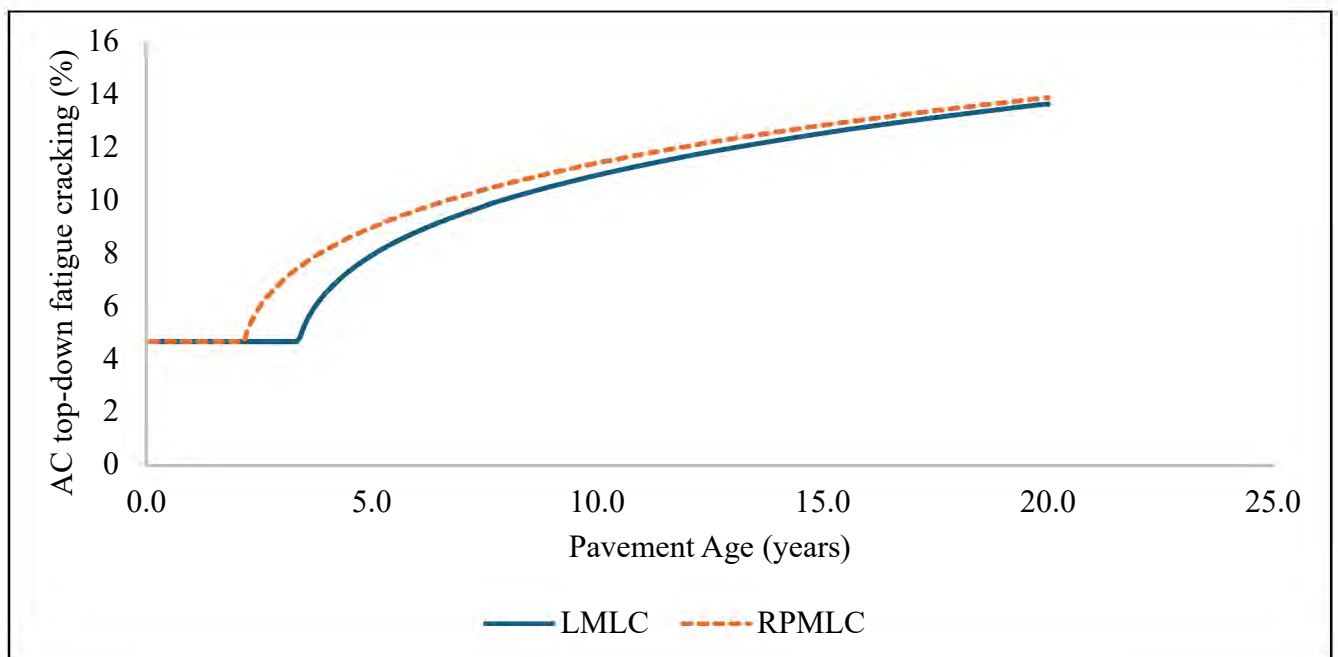**Figure 92: Comparison of AC top-down fatigue cracking for LMLC and RPMLC mixtures at I-555 section in BMD project AR01.**

151
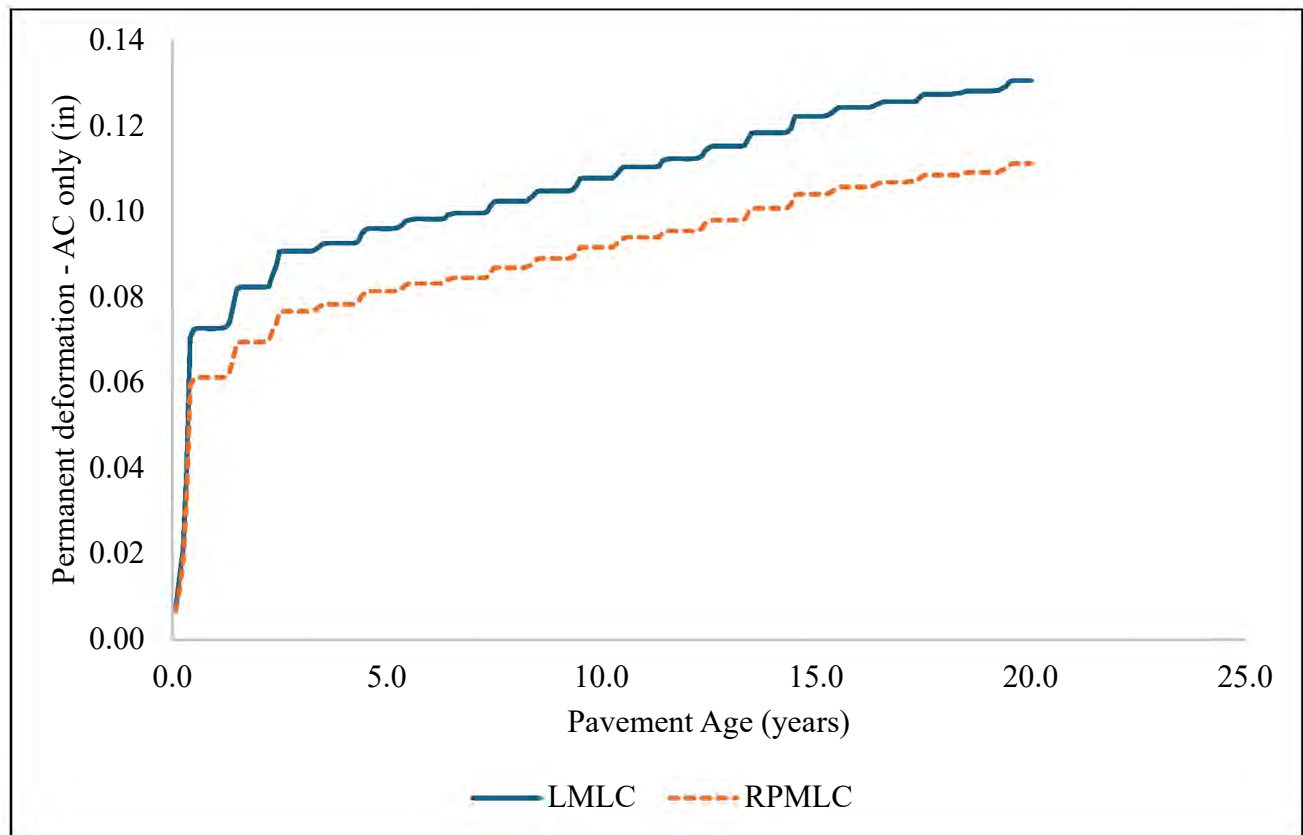
Figure 93: Comparison of Permanent deformation - AC only for LMLC and RPMLC mixtures at I-555 section in BMD project AR01.

4.3 BMD vs Superpave (Nam Tran)

To compare the BMD mixture with the Superpave mixture, data from Nam Tran (**54**) were utilized in this study. Four mixtures with comparable binder contents and aggregate sources were selected. **Figure 94** Illustrates the comparison of dynamic modulus between the BMD and Superpave mixtures. The Superpave mixtures exhibited higher dynamic modulus values, particularly at higher frequencies (i.e., lower temperatures). In the lower portion of the master curve, the dynamic modulus of the Superpave mixtures was generally equal to or lower than that of the BMD mixtures, except in the case of AR02 compared to GMQ.
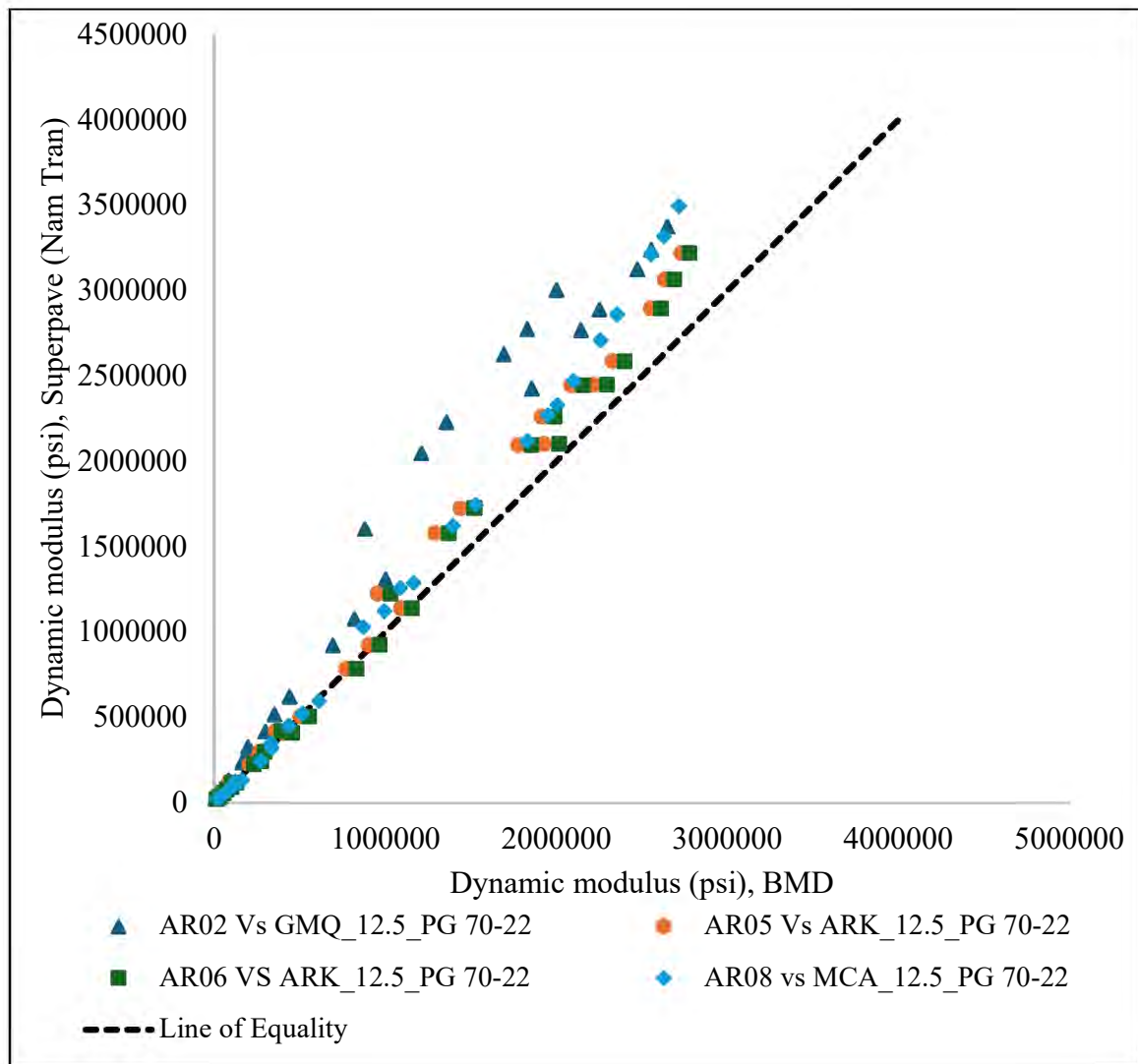
Figure 94: Comparison of dynamic modulus with Nam Tran Thesis (Superpave mixture)

Pavement distress for both BMD and Super mixture was calculated and is presented in **Table 91** to **Table 94** for the pavement cross-sections I-40, I-555, I-49, and the County Road, respectively. The values shown represent the predicted distress at the end of a 20-year service life.

Table 91. Average pavement distress at the end of 20 years of life in pavement cross section I-40

| Project		AR02 vs GMQ	AR05 VS ARK	AR06 VS ARK	AR08 VS MCA
BMD	Terminal IRI (in/mile)	140.00	138.90	138.70	138.90
	Permanent deformation - total pavement (in)	0.30	0.28	0.27	0.28
	AC bottom-up fatigue cracking (% lane area)	1.45	1.45	1.45	1.45
	AC thermal cracking (ft/mile)	440.58	440.57	440.57	440.75
	AC top-down fatigue cracking (% lane area)	14.22	14.20	14.23	14.26
	Permanent deformation - AC only (in)	0.14	0.12	0.11	0.11
Nam Tran	Terminal IRI (in/mile)	148.30	148.50	148.50	148.10
	Permanent deformation - total pavement (in)	0.29	0.29	0.29	0.28
	AC bottom-up fatigue cracking (% lane area)	1.45	1.45	1.45	1.45
	AC thermal cracking (ft/mile)	1581.31	1586.82	1586.82	1584.06
	AC top-down fatigue cracking (% lane area)	14.25	14.23	14.23	14.25
	Permanent deformation - AC only (in)	0.12	0.13	0.13	0.12

Table 92. Average pavement distress at the end of 20 years of life in pavement cross section I-555

Project		AR02 vs GMQ	AR05 VS ARK	AR06 VS ARK	AR08 VS MCA
BMD	Terminal IRI (in/mile)	140.80	139.80	139.70	139.90
	Permanent deformation - total pavement (in)	0.32	0.30	0.30	0.30
	AC bottom-up fatigue cracking (% lane area)	1.56	1.50	1.51	1.53
	AC thermal cracking (ft/mile)	440.59	440.57	440.57	441.57
	AC top-down fatigue cracking (% lane area)	14.00	13.92	14.10	14.20
	Permanent deformation - AC only (in)	0.13	0.11	0.10	0.10
Nam Tran	Terminal IRI (in/mile)	154.20	153.10	153.10	154.50
	Permanent deformation - total pavement (in)	0.31	0.31	0.31	0.30
	AC bottom-up fatigue cracking (% lane area)	1.52	1.53	1.53	1.52
	AC thermal cracking (ft/mile)	2204.57	2052.89	2052.89	2273.51
	AC top-down fatigue cracking (% lane area)	14.16	14.04	14.04	14.14
	Permanent deformation - AC only (in)	0.11	0.12	0.12	0.11

Table 93. Average pavement distress at the end of 20 years of life in I-49

Project		AR02 vs GMQ	AR05 VS ARK	AR06 VS ARK	AR08 VS MCA
BMD	Terminal IRI (in/mile)	141.50	140.30	140.20	140.40
	Permanent deformation - total pavement (in)	0.34	0.31	0.31	0.31
	AC bottom-up fatigue cracking (% lane area)	1.80	1.61	1.62	1.69
	AC thermal cracking (ft/mile)	440.61	440.57	440.57	441.87
	AC top-down fatigue cracking (% lane area)	13.95	13.88	14.07	14.19
	Permanent deformation - AC only (in)	0.14	0.11	0.11	0.11
Nam Tran	Terminal IRI (in/mile)	155.20	155.60	155.60	155.60
	Permanent deformation - total pavement (in)	0.32	0.32	0.32	0.31
	AC bottom-up fatigue cracking (% lane area)	1.65	1.69	1.69	1.65
	AC thermal cracking (ft/mile)	2273.51	2301.09	2301.09	2356.25
	AC top-down fatigue cracking (% lane area)	14.14	14.01	14.01	14.13
	Permanent deformation - AC only (in)	0.12	0.12	0.12	0.11

Table 94. Average pavement distress at the end of 20 years of life in County Road

Project		AR02 vs GMQ	AR05 VS ARK	AR06 VS ARK	AR08 VS MCA
BMD	Terminal IRI (in/mile)	142.60	141.70	141.60	142.20
	Permanent deformation - total pavement (in)	0.43	0.41	0.41	0.42
	AC bottom-up fatigue cracking (% lane area)	1.45	1.45	1.45	1.45
	AC thermal cracking (ft/mile)	444.35	440.57	440.58	474.19
	AC top-down fatigue cracking (% lane area)	4.69	4.69	4.69	4.69
	Permanent deformation - AC only (in)	0.10	0.09	0.08	0.09
Nam Tran	Terminal IRI (in/mile)	163.40	163.70	163.70	163.40
	Permanent deformation - total pavement (in)	0.41	0.42	0.42	0.41
	AC bottom-up fatigue cracking (% lane area)	1.45	1.45	1.45	1.45
	AC thermal cracking (ft/mile)	3197.38	3197.38	3197.38	3197.38
	AC top-down fatigue cracking (% lane area)	4.69	4.69	4.69	4.69
	Permanent deformation - AC only (in)	0.09	0.09	0.09	0.09

The comparison of pavement distress for BMD Project AR08 and Nam Tran _MCA at pavement cross-section I-555 is illustrated in **Figure 95** through **Figure 100**. The Superpave mixture exhibits a higher IRI compared to the BMD mixture, which may be attributed to its higher dynamic modulus, particularly in the upper portion of the master curve. Thermal cracking is also more severe in the Superpave mixture, likely due to the elevated modulus in

155

this region, which increases the pavement's susceptibility to such distress. Additionally, the Superpave mixture shows greater permanent deformation when compared to the BMD mixture. This could be related to its lower modulus in the lower portion of the master curve, as seen in the comparison between AR08 and MCA. Overall, while the higher modulus of the Superpave mixture may reduce some types of distress, it appears to contribute to increased thermal cracking and IRI.
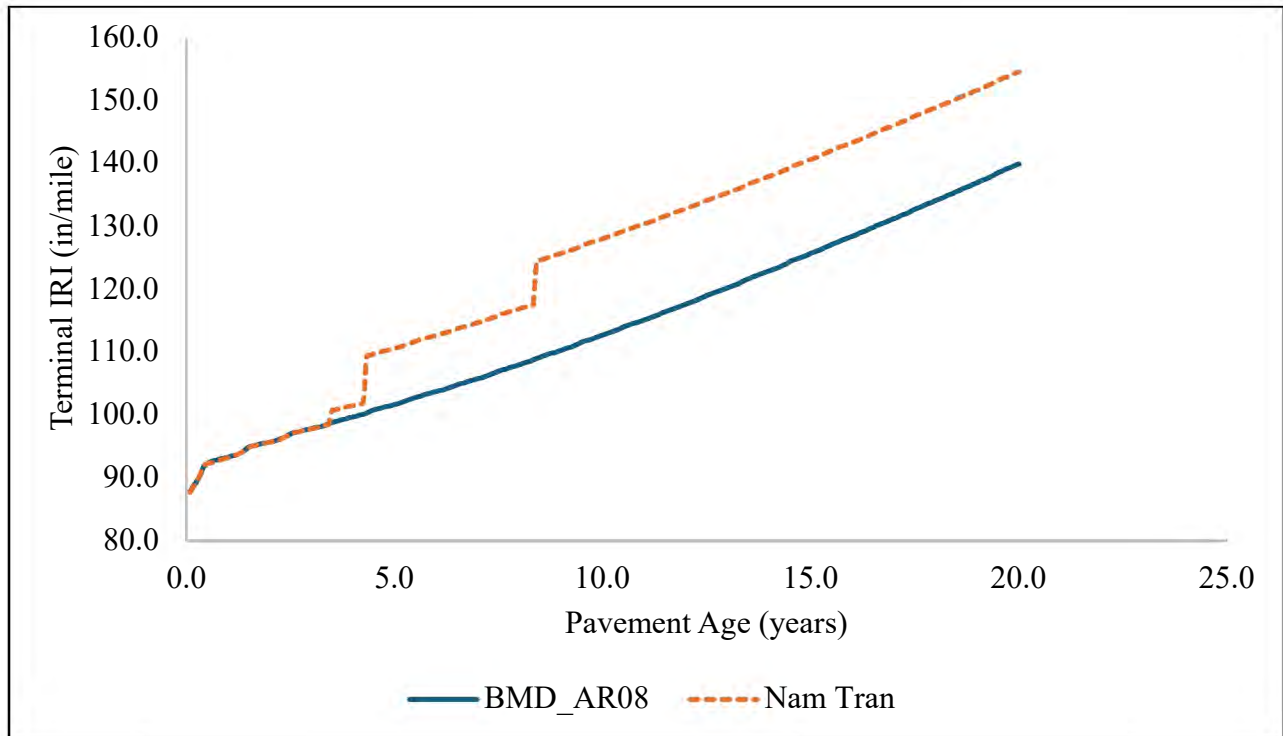
Figure 95: Comparison of International Roughness Index for BMD and Superpave mixture (Nam Tran) mixtures at I-555 section in BMD project AR08.

Figure 96: Comparison of Permanent deformation - total pavement for BMD and Superpave mixture (Nam Tran) mixtures at I-555 section in BMD project AR08.

Figure 97: Comparison of AC bottom-up fatigue cracking for BMD and Superpave mixture (Nam Tran) mixtures at I-555 section in BMD project AR08.

Figure 98: Comparison of AC thermal cracking for BMD and Superpave mixture (Nam Tran) mixtures at I-555 section in BMD project AR08.

Figure 99: Comparison of AC top-down fatigue cracking for BMD and Superpave mixture (Nam Tran) mixtures at I-555 section in BMD project AR08.

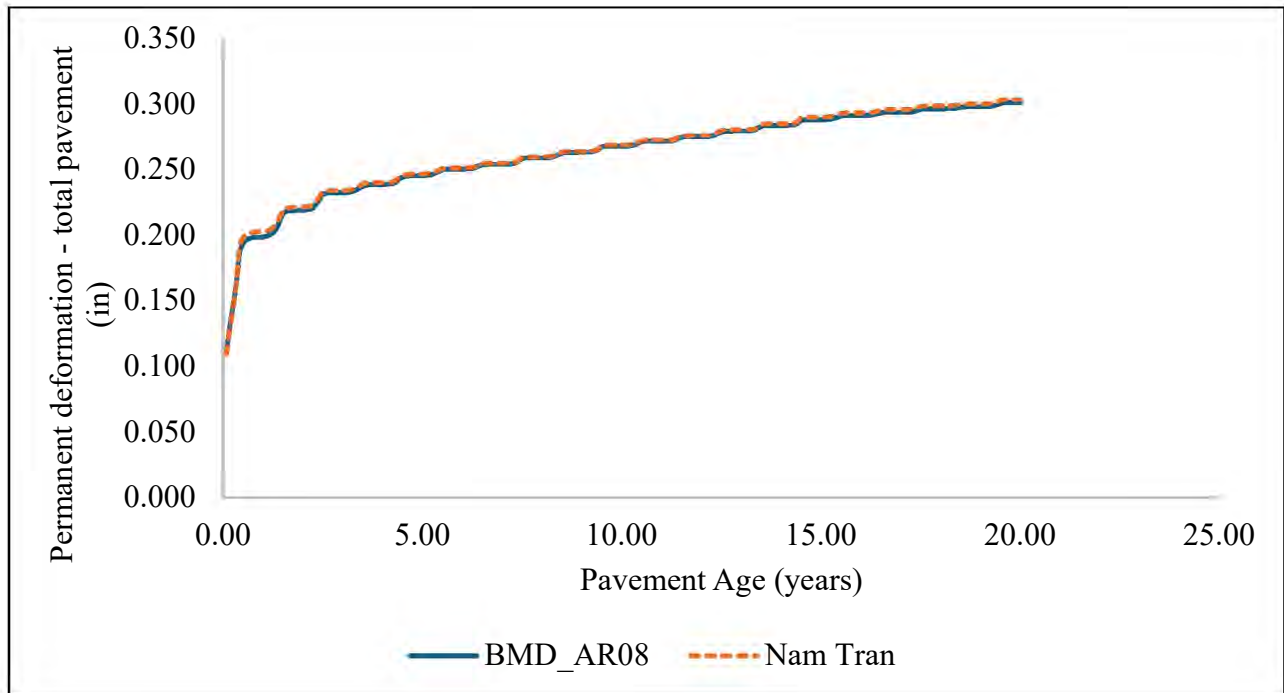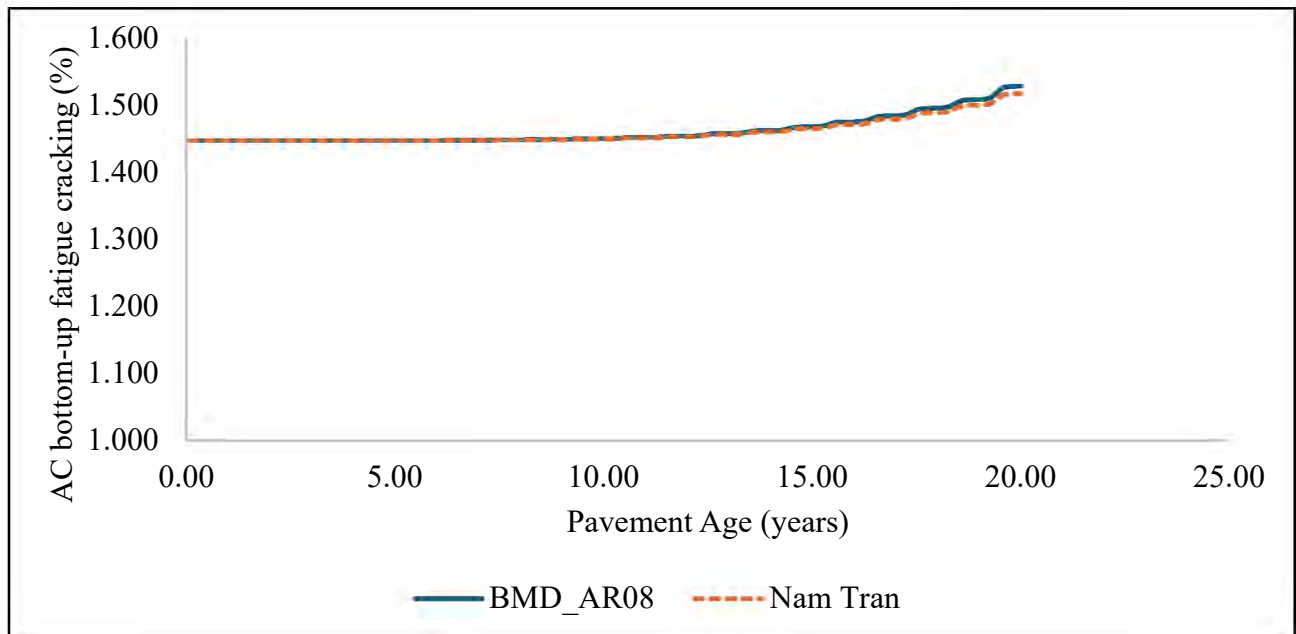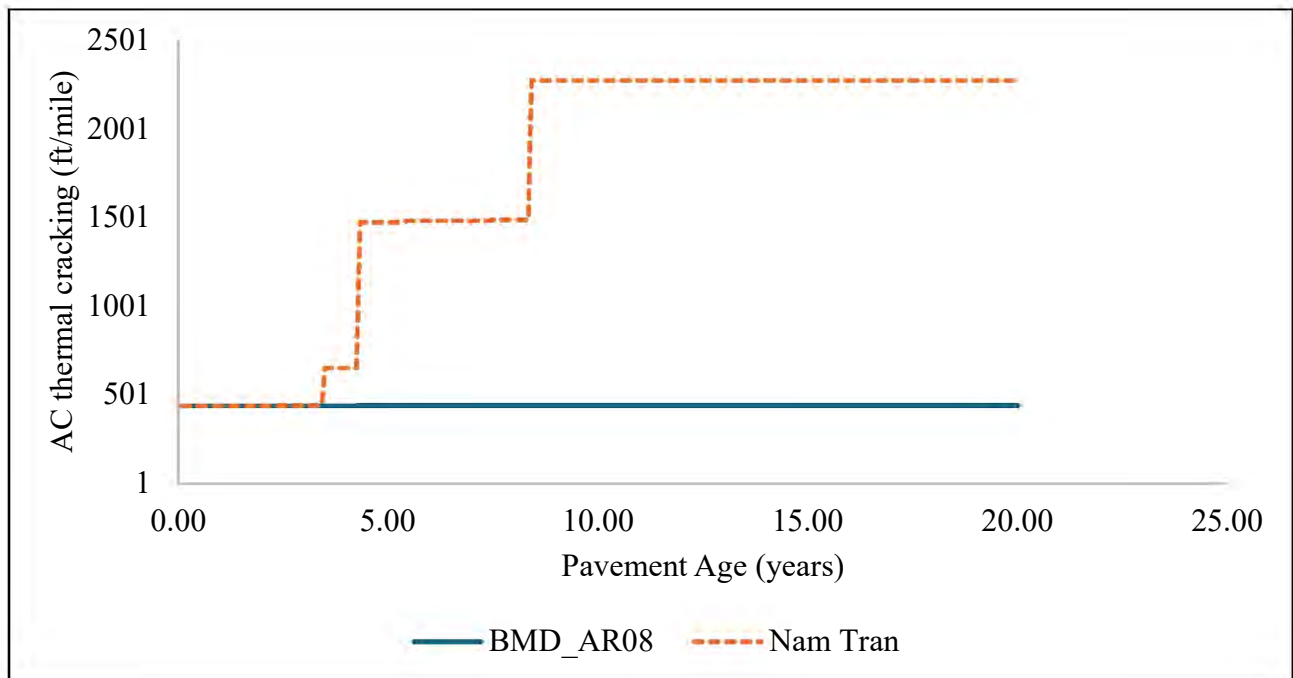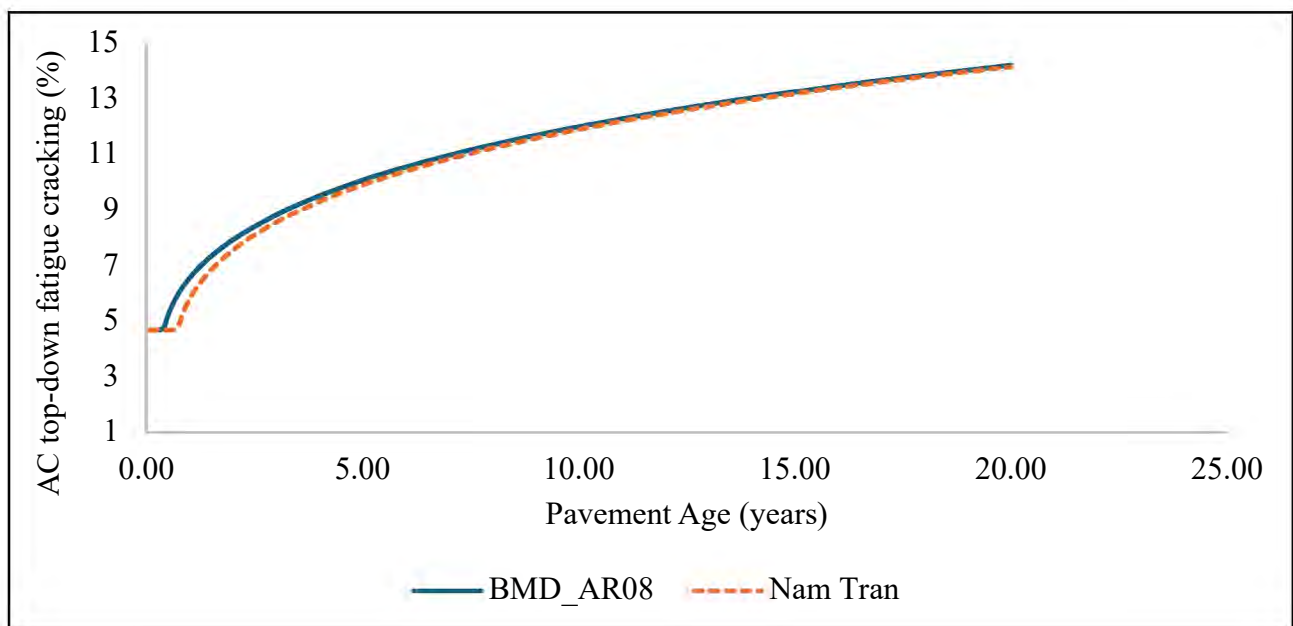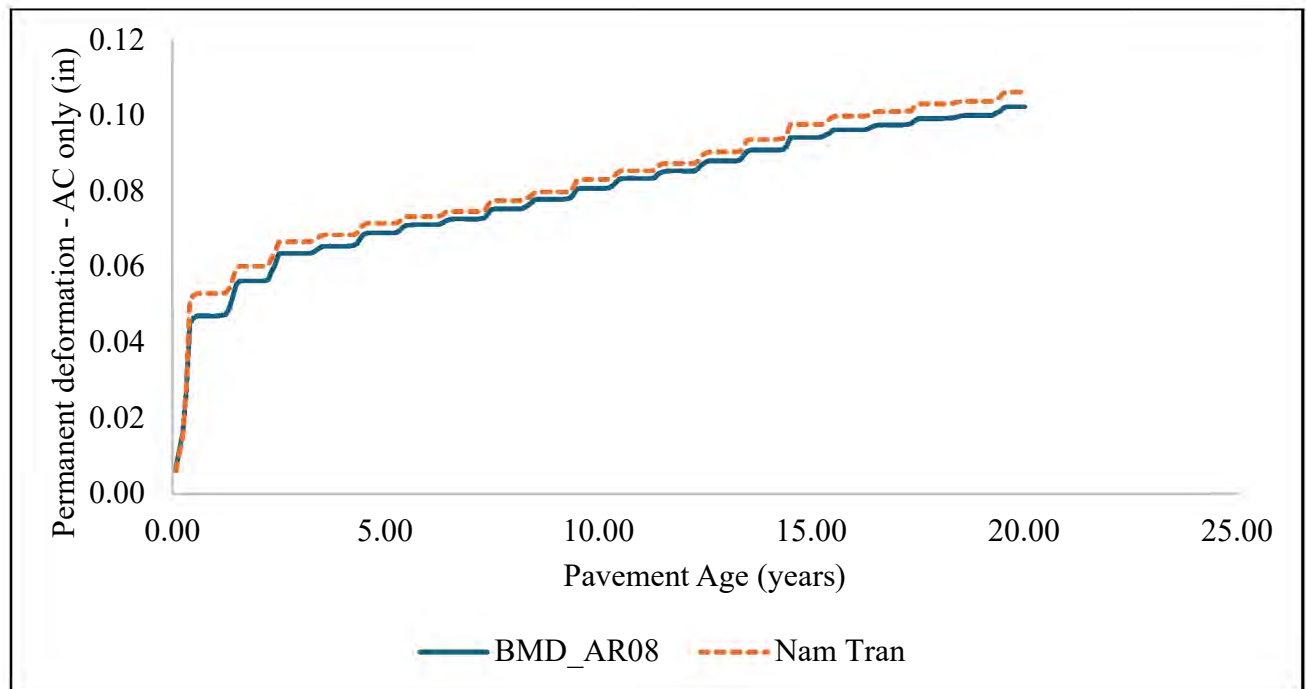**Figure 100: Comparison of Permanent deformation - AC only for BMD and Superpave mixture (Nam Tran) mixtures at I-555 section in BMD project AR08.**

Chapter 5. Life Cycle Cost Analysis

The life cycle cost analysis (LCCA) will follow the Federal Highway Administration's process of performing an LCCA (51). In this analysis, there are six steps: 1) establish alternate pavement design strategies, 2) determine the performance period, 3) estimate agency costs, 4) estimate user costs, 5) develop expenditure stream diagrams, and 6) calculate the net-present value. For this project, these six steps will be used, along with AASHTOWare Pavement-ME, to compare a Superpave mix to a BMD mix through AASHTOWare Pavement-ME.

Step 1 - Establish Alternative Pavement Design Strategies

The first step to an LCCA is to establish alternative pavement design strategies. This research will compare two maintenance treatments: a standard Superpave mix (from Dr. Nam Tran's work) to a Balanced Mix Design mix. The Balanced Mix Design (AR08) had an optimal asphalt binder content of 6.0%, and it was assumed that this was an increase of 0.5% over the Superpave mix, which was set at 5.5%. This will allow for a comparison of a BMD mixture with a standard Superpave mixture.

Step 2 – Determine the Performance Period

The second step to an LCCA analysis is to determine the performance period. According to **Figures 95-100** above, the IRI, top-down fatigue cracking, bottom-up fatigue cracking, total deformation, and asphalt mixture deformation all remain below the threshold after twenty years. However, the thermal cracking of the Superpave mixture reached the threshold after 5 years, while the BMD did not reach the threshold after 20 years. Therefore, it is assumed that the standard Superpave mixture will need a 2-inch mill and fill every five years, and the BMD will need the first mill and fill at 20 years. This assumes that the CT_{Index} values are optimal at 20 years. Therefore, a performance period of 20 years is assumed.

Step 3 – Estimate Agency Costs

The third step to an LCCA analysis is to estimate the agency costs. According to ARDOT's weighted average prices from 2024, the cost of a surface course aggregate for a 12.5 mm NMAS aggregate and the PG70-22 is as follows:

- MA IN ACHM SURFACE (1/2") = $112.42/ton

- AB(PG70-22) ACHM SURFACE (1/2") = $531.06/ton

- COLD MILLING ASPHALT PVMT. = 4.09/yd^2

Using these three costs, **Table 95** summarizes the cost of two inches of each mix.

Table 95. Agency Costs

Mixture	% Mineral Aggregate	% Asphalt Binder	Cost of Mineral Aggregate ($)	Cost Asphalt Binder ($)	Total Cost ($)
Superpave	94.5	5.5	112.42/ton	531.06/ton	135.45/ton
BMD	94.0	6.0	112.42/ton	531.06/ton	137.54/ton

Using these costs, the cost of a 2-inch surface layer for the Superpave mix would be $14.58/yd^2:

- Total = $135.45/ton = $0.07/lb

- Assuming a density of 143.5 lbs/ft3, cost/ ft3 = $9.72/ ft3

- Assuming a thickness of 2.0-inch, $9.72/ft3 = $87.47/yd2-ft = $7.29/yd2-in = $14.58/yd^2

Similarly, the cost of a 2-inch surface layer for the BMD mix would be $14.58/yd^2:

- Total = $137.54/ton = $0.07/lb

- Assuming a density of 143.5 lbs/ft^3, cost/ ft^3 = $9.87/ ft^3

- Assuming a thickness of 2.0-inch, $9.87/ft^3 = $88.86/yd^2-ft = $7.40/yd^2-in = $14.80/yd^2

Step 4 – Estimate User Costs

The fourth step to an LCCA analysis is to estimate the user costs. For this example, it is assumed that the user costs will be equal between the two treatments. In any LCCA, if any costs are equal, they do not need to be considered (51).

Step 5 - Develop an Expenditure Stream Diagram

The fifth step to an LCCA analysis is to develop an expenditure stream diagram. This is simply a graphical representation of the cost of the roadway over time. **Figure 101** shows the

expenditure stream for a Superpave overlay (every five years) and a BMD overlay (every 20 years).
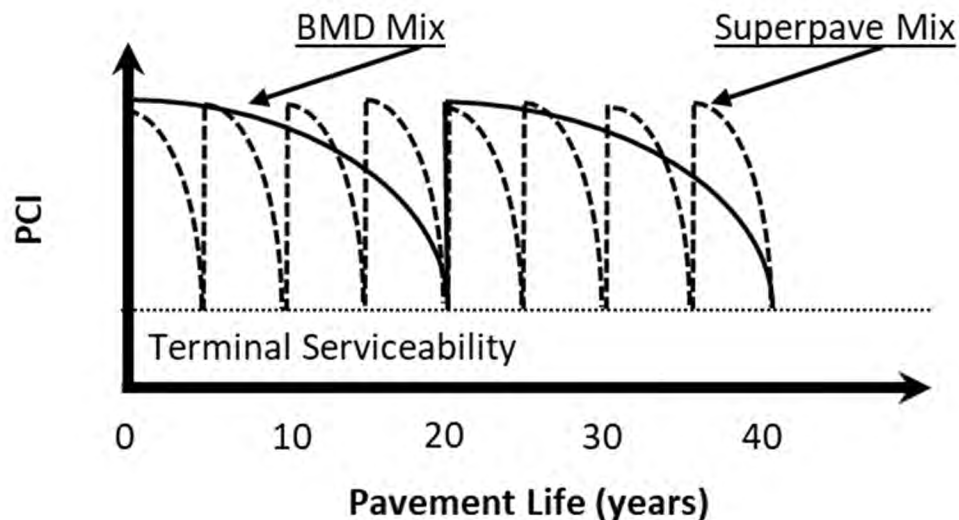

Figure 101: Expenditure streams for BMD mix (solid line) and Superpave mix (dashed line)

Step 6 - Calculate the Net Present Value

The sixth step to an LCCA analysis is to calculate the net-present value (NPV). The NPV is calculated by taking the initial cost and adding the future cost of each maintenance treatment. The future cost of each maintenance treatment is brought back to the present value at a 4% interest rate. Using the I-555 data, the project was 24,902.10 feet long. With four, 12-foot-wide lanes, this is a total of 11,067.60 yd^2. Using the costs from Step 3, including the cost of milling the pavement for each mill and fill (Years 5, 10, 15, and 20 for the Superpave mix; Year 20 for the BMD mix), it would cost $679,724.30 to maintain the Superpave mix road for 20 years, while it would cost $259,215.90 to maintain the BMD mix road for 20 years. Finally, it is worth noting that the user cost for each mill and fill operation was considered equal in this analysis. However, the Superpave mix would require four mill and fills, whereas the BMD mix would only require one. Therefore, in addition to the calculated agency cost savings, there would be additional cost savings due to user costs if included in the analysis. Regardless, adding the extra 0.5% asphalt binder would save approximately 61% for the four-mile stretch of I-555 going through Jonesboro.

162

References

1. Cominsky, R. J., Huber, G. A., Kennedy, T. W., & Anderson, M. (1994). The Superpave mix design manual for new construction and overlays (Issue SHRP-A-407). Strategic Highway Research Program. Washington, DC.

2. Tran, N. H., Yin, F., Leiva, F., Rodezno, C., Huber, G., & Pine, W. (2022). Volumetric Mix Design Adjustments for Improving ACHM Durability. *Transportation Research Record*, *2676*(7), 445-455.

3. Prowell, Brian D., Brown, E Ray. (2007). Superpave Mix Design: Verifying Gyration levels in the N_{design} Table. *National Cooperative Highway Research Program*, NCHRP Report 573.

4. Feng, B., Wang, H., Li, S., Ji, K., Li, L., & Xiong, R. (2022). The durability of ACHM with the action of salt erosion: A review. *Construction and Building Materials*, *315*, 125749.

5. Aschenbrener, T., Brown, E., Tran, N. H., & Blankenship, P. B. (2020). Demonstration project for enhanced durability of asphalt pavements through increased in-place pavement density.

6. Nicholls, J. C., McHale, M. J., & Griffiths, R. D. (2008). *Best practice guide for durability of asphalt pavements*. Berkshire, UK: Transport Research Laboratory.

7. Tran, N., P. A., Huber, G., Leiva, F., & Pine, B. (2019). Mix Design Strategies for Improving ACHM Performance NCAT Report 19-08. *National Center for Asphalt Technology, Auburn, Al. Tran, N., Yin, F., Leiva, F., Rodezno, C., Huber, G., and Pine, B., Adjustments to the Superpave Volumetric Mixture Design Procedure for Selecting Optimum Asphalt Content. Final Report of NCHRP*, 20-07.

8. Aguiar-Moya, J. P., Prozzi, J. A., & Tahmoressi, M. (2007). Optimum number of Superpave gyrations based on project requirements. *Transportation Research Record*, *2001*(1), 84–92.

9. Diefenderfer, S. D., Bowers, B. F., & McGhee, K. K. (2018). Impact of gyration reduction and design specification changes on volumetric properties of Virginia dense-graded ACHM. *Transportation Research Record*, *2672*(28), 143–153.

10. Watson, D. E., Moore, J., Heartsill, J., Jared, D., & Wu, P. (2008). Verification of Superpave number of design gyration compaction levels for Georgia. *Transportation Research Record*, *2057*(1), 75–82.

11. AASHTO. (2022). Standard Specification for Superpave Volumetric Mix Designs. Designation M 323-22 (2022). *American Association of State Highway and Transportation Officials. Washington, DC*

12. Levels, G. C. (2010). Superpave Mix Design and Gyratory Compaction Levels. *Technical Brief, FHWA-HIF-11-031, Federal Highway Administration*.

13. West, R., Rodezno, C., Leiva, F., & Yin, F. (2018). Development of a framework for balanced mix design. *Project NCHRP*, 20-07.

14. Coree, B. and Hislop, W.P., 2000. A laboratory investigation into the effects of aggregate-related factors of critical VMA in asphalt paving mixtures (No. IDOT TR-415). Iowa State University. Center for Transportation Research and Education.

15. Hajj, E. Y., Sebaaly, P. E., West, R., Morian, N., & Loria, L. (2012). Recommendations for the characterization of RAP aggregate properties using traditional testing and mixture volumetrics. *Road materials and pavement design*, *13*(sup1), 209-233.

16. Othman, O., Underwood, B. S., Habbouche, J., Boz, I., & Diefenderfer, S. D. (2024). Assessment of Conventional and Engineered Surface ACHM Through Empirical and Fundamental Performance Tests. *Transportation Research Record*, 03611981241234915.

17. Bittner, J., Hajj, E.Y., Aschenbrener, T., Gopisetti, P. and Rockwood, H., 2023. Northeast Peer Exchange on Balanced Mix Design (BMD): Outcomes Summary (No. FHWA-HIF-23-042). United States. Federal Highway Administration. Office of Preconstruction, Construction, and Pavements.

18. Bittner, J., Hajj, E.Y., Aschenbrener, T., Gopisetti, P. and Rockwood, H., 2023. North Central Peer Exchange on Balanced Mix Design (BMD): Outcomes Summary (No. FHWA-HIF-23-032). United States. Federal Highway Administration. Office of Preconstruction, Construction, and Pavements.

19. Bittner, J., Hajj, E.Y., Aschenbrener, T., Gopisetti, P. and Rockwood, H., 2023. Southeast Peer Exchange on Balanced Mix Design (BMD): Outcomes Summary (No. FHWA-HIF-23-031). United States. Federal Highway Administration. Office of Preconstruction, Construction, and Pavements

20. AASHTO. (2020). Standard Practice for Balanced Design of ACHM. Designation PP-105 (2020). *American Association of State Highway and Transportation Officials*. Washington, DC.

21. Hall, K. D., Castillo-Camarena, E., Braham, A. F., Parnell, N., & Richey, A. (2022). *Performance-based ACHM design (PBD) for Arkansas* (No. TRC1802). Arkansas. Department of Transportation. Transportation Research Committee.

22. Habbouche, J., Boz, I., & Diefenderfer, S. D. (2022). Validation of performance-based specifications for surface ACHM in Virginia. *Transportation Research Record*, *2676*(5), 277-296.

23. ARDOT. (2019). Test Method for Determining Rutting Susceptibility Using a Loaded Wheel Tester (LWT). Designation 480-07. Manual of field sampling and testing procedures. Arkansas Department of Transportation. Little Rock, AR.

24. ASTM. (2019). Standard Test Method for Determination of Cracking Tolerance Index of ACHM Using the Indirect Tensile Cracking Test at Intermediate Temperature. Designation D8225-19. *ASTM International,* West Conshohocken, PA.

25. AASHTO. (2022). Standard Method of Test for Determining the Dynamic Modulus and Flow Number for ACHM Using the ACHM Performance Tester (AMPT) (2022). Designation T 378 (2022). *American Association of State Highway and Transportation Officials*. Washington, DC.

26. AASHTO. (2022). Standard Method of Test for Determining the Fracture Potential of ACHM Using the Illinois Flexibility Index Test (I-FIT). Designation T 393 (2022). *American Association of State Highway and Transportation Officials*. Washington, DC.

27. AASHTO. (2023). Standard Method of Test for Hamburg Wheel-Track Testing of Compacted ACHM. Designation T 324 (2023). *American Association of State Highway and Transportation Officials*. Washington, DC.

28. AASHTO. (2022). Standard Method of Test for Resistance of Compacted ACHM to Moisture-Induced Damage. Designation T 283 (2022). *American Association of State Highway and Transportation Officials*. Washington, DC.

29. AASHTO. (2022). Standard Practice for Superpave Volumetric Design for ACHM. Designation R 35 (2022). *American Association of State Highway and Transportation Officials*. Washington, DC.

30. Prowell, Brian D., Brown, E Ray. (2007). Superpave Mix Design: Verifying Gyration levels in the N_{design} Table. *National Cooperative Highway Research Program*, NCHRP Report 573.

31. Diefenderfer, S. D., Bowers, B. F., & McGhee, K. K. (2018). Impact of gyration reduction and design specification changes on volumetric properties of Virginia dense-graded ACHM. Transportation Research Record, 2672(28), 143-153.

32. Watson, D. E., Moore, J., Heartsill, J., Jared, D., & Wu, P. (2008). Verification of Superpave number of design gyration compaction levels for Georgia. Transportation Research Record, 2057(1), 75-82.

33. Katicha, S. W., & Flintsch, G. W. (2016). Improving Mixture Durability Through Design Gyrations, Air Voids, and Binder Content (No. VTRC 16-R17). Virginia Transportation Research Council.

34. Baker, J. L. (2022). Initial Exploration of Reduced Gyrations for Arkansas Asphalt Mix Designs, master's thesis, University of Arkansas.

35. ARDOT. (2019). Manual of Field Sampling and Testing Procedures. Materials Division, *Arkansas Department of Transportation*. Little Rock, AR.

36. AASHTO. (2023). Standard Method of Test for Theoretical Maximum Specific Gravity (G_{mm}) and Density of ACHM. Designation T 209 (2023). *American Association of State Highway and Transportation Officials*. Washington, DC.

37. AASHTO. (2022). Standard Method of Test for Preparing and Determining the Density of ACHM Specimens by means of the Superpave Gyratory Compactor. Designation T 312 (2022). *American Association of State Highway and Transportation Officials*. Washington, DC.

38. AASHTO. (2023). Standard Method of Test for Bulk Specific Gravity (G_{mb}) and Density of Compacted ACHM Using Automatic Vacuum Sealing Method. Designation T 331 (2023). *American Association of State Highway and Transportation Officials*. Washington, DC.

39. Chen, J., Huang, B., & Shu, X. (2013). Air-void distribution analysis of ACHM using discrete element method. *Journal of materials in civil engineering*, *25*(10), 1375-1385.

40. Polaczyk, P., Shu, X., Gong, H., & Huang, B. (2019). Influence of aggregates angularity on the locking point of ACHM. *Road Materials and Pavement Design*, *20*(sup1), S183-S195.

41. Polaczyk, P., Ma, Y., Xiao, R., Hu, W., Jiang, X., & Huang, B. (2021). Characterization of aggregate interlocking in hot mix asphalt by mechanistic performance tests. *Road Materials and Pavement Design*, *22*(sup1), S498-S513.

42. Pouranian, M. R., & Haddock, J. E. (2021). A new framework for understanding aggregate structure in ACHM. *International Journal of Pavement Engineering*, *22*(9), 1090-1106.

43. AASHTO. (2002). Standard Practice for Mixture Conditioning of Hot Mix Asphalt. Designation R 30 (2002). *American Association of State Highways and Transportation Officials*. Washington, DC.

44. AASHTO. (2023). Standard Practice for Reducing Samples of ACHM to Testing Size. Designation R 47 (2023). *American Association of State Highway and Transportation Officials*. Washington, DC.

45. ARDOT. (2019). Test Method for Determining Rutting Susceptibility Using a Loaded Wheel Tester (LWT). Designation 480-07. Manual of field sampling and testing procedures. *Arkansas Department of Transportation*. Little Rock, AR.

46. AASHTO. (2022). Standard Practice for Laboratory Conditioning of ACHM. Designation R 30 (2022). *American Association of State Highways and Transportation Officials*. Washington, DC.

47. Johnson, E., Johnson, G., Dai, S., Linell, D., McGraw, J., & Watson, M. (2010). *Incorporation of recycled asphalt shingles in hot-mixed asphalt pavement mixtures* (No. MN/RC 2010-08).

48. Mogawer, W., Bennert, T., Daniel, J. S., Bonaquist, R., Austerman, A., & Booshehrian, A. (2012). Performance characteristics of plant produced high RAP mixtures. *Road Materials and Pavement Design*, *13*(sup1), 183-208.

49. Xiao, F., Putman, B., & Amirkhanian, S. (2015). Plant and laboratory compaction effects on performance properties of plant-foamed ACHM containing RAP. *Journal of Materials in Civil Engineering*, *27*(9), 04014240.

50. Mc Daniel, R.S., Soleymani, H., and Shah, A., 2002. Use of reclaimed asphalt pavement (RAP) under Superpave specifications: a regional polled fund study. West Lafayette, IN: Purdue University.

51. Texas Department of Transportation (TxDOT), TEX-242-F: Test procedure for Hamburg Wheel-Tracking Test, 2014. https://ftp.dot.state.tx.us/pub/txdot-info/cst/TMS/200-F_series/pdfs/bit242.pdf.

52. Oklahoma Department of Transportation. (2014). Method of test for Hamburg rut testing of compacted hot-mix asphalt (HMA). OHD L-55, http://www.odot.org/materials/pdfs-ohdl/ohdl55.pdf

53. Mohammad, L. N., Kim, M., & Challa, H. (2016). *Development of performance-based specifications for Louisiana ACHM* (No. FHWA/LA. 14/558). Louisiana. Department of Transportation and Development.

54. Tran, N. H. (2005). *Characterizing and predicting dynamic modulus of hot-mix asphalt for mechanistic-empirical design guide*. University of Arkansas, Fayetteville.

55. Pierce, L. MG., & McGovern, G. (2014). *Implementation of the AASHTO Mechanistic-empirical pavement design guide and software*. Transportation Research Board.

56. Tiwari, A., Ansari, M. T., Cook, A., Hedden, J., Ogundipe, T., Ortlieb, J., Nunez, T., Roy, A., Turben, T., & Braham, A. (2025). Comparative life-cycle cost analysis of flexible and rigid pavement: a case study of four Arkansas roadway sections. *The International Journal of Pavement Engineering*, *26*(1), Article 2489044.https://doi.org/10.1080/10298436.2025.2489044